Satellite Based Exploration of land-use dynamics, drought susceptibility, and land suitability in central highlands of Ethiopia

Implication to Sustainability

By Moges Yohannes

Advisor Engdawork Assefa (PhD)

Addis Ababa University

July, 2021

Addis Ababa, Ethiopia

SATELLITE BASED EXPLORATION OF LAND-USE DYNAMICS, DROUGHT SUSCEPTIBILITY, AND LAND SUITABILITY IN CENTRAL HIGHLANDS OF ETHIOPIA

IMPLICATION TO SUSTAINABILITY

BY

MOGES YOHANNES

A Thesis Submitted to

College of Development Studies, Center for Environment and Development

Presented in Partial Fulfillment of the Requirements for the Degree of Master of Arts in Development (Environment and Sustainable Development)

Addis Ababa University

Addis Ababa, Ethiopia

July 2021

DECLARATION

I hereby declare that this thesis titled **Satellite Based Exploration of Land-use Dynamics, Drought Susceptibility, and Land Suitability in Central Highlands of Ethiopia** Submitted to Addis Ababa University College of Development Studies, Center for Environment and Development for the award of the degree of master of arts is a record of original and independent research work done by me under the supervision and guidance of Engdawork Assefa (PhD) has not been submitted for the award of any other degree or diploma or fellowship or any other similar title to any candidate of this or any other university/institution. And that all sources of materials used for the study are accordingly acknowledged.

Declared by

Name Moges Yohannes

Signature

Date 16/09/2021

Addis Ababa University

School of Graduate Studies

This is to certify that the thesis prepared by **Moges Yohannes** entitled **Satellite Based Exploration of Land-use Dynamics, Drought Susceptibility, and Land Suitability in Central Highlands of Ethiopia** Implication to Sustainability submitted in partial fulfillment of the requirements for the Degree of Environment and Sustainable Development complies with the regulations of Addis Ababa University and meets the accepted standards with respect to originality and quality.

Signed by the Examining Committee:

Advisor Engdawork Assefa (PhD) Signature ____ Date 16.09.21

Internal Examiner Shimeles Damene(PhD) Signature ____ Date 16/9/2021

External Examiner Asmamaw Legass(PhD) Signature ____ Date 16/9/21

Curiginal

Document Information

Analyzed document	Moges_ plagiarism check b.docx (D109961667)
Submitted	6/30/2021 5:02:00 PM
Submitted by	
Submitter email	engdawork.assefa@aau.edu.et
Similarity	13%
Analysis address	engdawork.assefa.aauni@analysis.urkund.com

Sources included in the report

SA **University of Addis Ababa / Moges_ plagiarism check.docx**
Document Moges_ plagiarism check.docx (D109786245)
Submitted by: engdawork.assefa@aau.edu.et
Receiver: engdawork.assefa.aauni@analysis.urkund.com
5

Curiginal

Entire Document

1. CHAPTER ONE: INTRODUCTION

1.1. Background of the Study

The biophysical cover of Earth's surface is in a state of continuous modification at local, national, and global scales. Amid these land cover changes, land degradation, and periodic droughts are at an alarming level these days – besides climate change. The ever-growing human population and the associated high demands for resources are putting increasing pressure on socio-ecological systems. These systems link humans, and the natural environment in an interdependent mannerCITATION Ang19 \m Wub20 \l 1033 (Angessa, Lemma, & Yeshitela, 2019; Damtea, Kim, & Im, 2020). The advent and advancement of remote sensing technologies in the last few decades have played a critical role in understanding these intertwined systems. Satellite systems and the newly emerging Unmanned Aerial vehicles are enabling environmental monitoring tasks of (i) land-cover mapping, (ii) vegetation state, phenology, and health, (iii) precision farming, (iv) crop monitoring, (v) atmospheric observations, (vi) disaster mapping, (vii) soil erosion, (viii) change detection at larger and smaller spatial scales respectively CITATION Man18 \l 1033 (Manfreda, Helman, Su, & Toth, 2018).

Unsustainable use of land resources results in the decline of land quality, and quantityCITATION Ewn21 \l 1033 (Ewnetu, Simane, Teferi, & Zaitchik, 2021). It also resulted in high soil erosion, decreased crop production, decreased productivity, and deterioration of soil quality CITATION Mos21 \l 1033 (Mostafiz, Noguchi, & Ahmed, 2021). One of how sustainability challenges are addressed includes an understanding of land-use change and land-use systems. Land systems constitute complex, adaptive, ecological systems shaped by different actors, and demands that act upon; land, technologies, institutions, and societal practices CITATION Mey18 \l 1033 (Meyfroidt, Chowdhury, & Garrett, 2018). Remote sensing and GIS methods are effective, and convenient ways for assisting agricultural land-use planning, and policymaking and spatial planning is commended to be the center of research, and policy development CITATION Mos21 \l 1033 (Mostafiz, Noguchi, & Ahmed, 2021). Recent advanced in UAV technology could back the well established satellite technology based earth monitoring tasks CITATION Man18 \l 1033 (Manfreda, Helman, Su, & Toth, 2018). Mapping land-cover change helps to analyze the magnitude, intensity, and direction of landscape changes. Since the first aerial photograph, taken from a balloon in 1858, and the Landsat satellite was launched in 1972, information extraction of the physical environment has improved significantly. Traditionally, it was mapped through costly, and time-consuming direct field survey methods. With the emergence of very advanced earth science monitoring methods, now it is measured, and quantitated with relatively lesser efforts. More specifically, Lan-use/ Land-cover (LULC) is the most widely applied earth observation application areaCITATION Ber15 \m Wub20 \l 1033 (Bewket, Gessesse, & Bräuning, 2015; Damtea, Kim, & Im, 2020). Droughts pose significant water, and food security concerns worldwideCITATION Kou15 \l 1033 (Kouchak, Farahmad, Melton, Teixeira, & Anderson, 2015). It is among the threats and core challenges to sustainable development in Africa CITATION Afr07 \l 1033 (UNESC, 2007). Droughts can have a devastating effect on the supply of water, crop production, and livestock rearing. Drought-prone area identification is fundamental to increase food security, better manage risks, and efficient food-aid delivery. Droughts along with floods accounts for 80% of life, and 70% of economic losses among the natural hazards in Sub-Saharan Africa. The droughts of the 1980s, and 90s in Africa affected several countries, and outrageous famine emergencies have occurred. The 1984 drought for instance took the lives of over 1 million people, and 1.5 million livestock population in Ethiopia CITATION Oro11 \l 1033 (Rojas, Vrieling, & Rembold, 2011). The more recent drought events occurred in 2002, 2011 and 2015 - times where Ethiopia's resilience has improved significantly from that of 30 years before CITATION hum21 \l 1033 (Centre for humandata, 2021). World Meteorological Organization categorizes drought indicators and indices into meteorology, soil moisture, hydrology, remote sensing, composite (modeled). Commonly used meteorological indicators such as Aridity Anomaly Index (AAI), Standardized Precipitation Index (SPI), Palmer Drought Severity Index (PDSI), and Weighted Anomaly Standardized Precipitation (WASP) requires adequate temperature, precipitation, and associated inputs for calculation CITATION WMO16 \l 1033 \m Far20 (WMO & GWP, 2016; Faridatul & Ahmed, 2020). In practice, these are limited by the scarcity of reliable rainfall data. The rainfall stations are mostly situated in large spatial gaps, so rainfall measurements usually are replaced by atmospheric circulation models or satellite imageries. Even other international meteorological sources contain errors and show deviations in African countries. To fill the gap, remote sensing vegetation abundance methods are increasingly being used as optional methods of providing information on droughts CITATION Jan04 \l 1033 (Artiola, Pepper, & Brusseau, 2004). Vegetation classification, corresponding with drought indices, has been a research topic of interest for quite a long time in the remote sensing scientific community. Multiple methods have been developed in this respect, and studies mostly focused on composition surveys, and classifications using the low, and medium spatial resolution satellite data sourcesCITATION

2/42

Acknowledgment

Glory be to God who is at work in us according to his purpose and good pleasure. He is the sole provider and the one who transforms difficulties into opportunities.

I want to sincerely appreciate the continuous motivation, follow-up, guidance, and most importantly his friendly and sympathetic approach of my advisor Engdawork Assefa (Ph.D.). If not for him, I couldn’t assume finalizing such a large task in the shortest possible time. Tesfa Debebe, my newly wedded bride and the love of my life, you have spared the most romantically obsessive year and essential resources for me to finalize this work. I love you to the moon and back. I would like to thank everyone in my family, especially Easaw Alemayehu for his encouragement, motivation, and insightful comments, Mindaye Yohannes and Debebe Lemma, for promptly sharing their resources in a critical moment.

This thesis may not happen if MoA staff particularly Meeraph did not allow me to access the UAS data as an input for this thesis. I'd also like to thank both GII and ESRI for providing an ArcGIS Pro license. The facilities and enabling environment of Addis Ababa University premises are worth mentioned to be appreciated.

Let this work be dedicated to Kebebush Atebo and the late Yohannes Ergicho, my beloved parents, for their many years of caring, support, and motivation in my life.

Abstract

Land use land cover is dynamically changing in Ethiopia, with far-reaching implications on recurrent droughts and land suitability status. The central highlands in particular are recognized for a unique precipitation pattern, intensive cultivation, periodic droughts, and land degradation. The study intends to use satellites (mainly Landsat) to map land-use dynamics, drought susceptibility, and agricultural suitability and comparative analysis in Basona Werana district (Woreda). The land use land cover seemed to be dominated by cultivated land with approximately 74.34 percent (3/4th) of the area in 2021. Non-dominant LULC types share the rest 25.66% in the following percentage. Shrub and Bush (15.37%), Forests (5.2%), Built-up and settlement (2.87%), Wetlands (1.22%), and water bodies, pasture land, and bare land collectively account for 1% of the area. While cultivated land, grassland, shrubland, built-up and settlement areas, and water bodies have had rising land cover change trends over the last 32 years, forests, bare land, and wetlands have witnessed a decreasing trend. The Vegetation Condition Index (VCI) and Normalized Difference Drought Index (NDDI), among other indices, were used to estimate historical and non-temporal droughts respectively. While VCI estimated that extreme drought conditions affected 30.18%, 7.34%, 22.55%, and 1.77% of the area in 1989, 2000, 2010, and 2021 respectively, NDDI estimated it to be 35.91%, 40.58, 39.23, and 53.87% in those same years. To see the real context of cropland suitability constraints such as elevation, slope, soil type, Soil Adjusted Vegetation Index (SAVI), Normalized Difference Water Index (NDWI), and river proximity were weighted by various degrees of influence. The result demonstrates 5.35% of the area is highly suitable, 49.9% is moderately suitable, 28.72% is marginally suitable, 13.46% is less suitable and 2.56% is not suitable for agriculture. In this particular study, UAV imagery was particularly useful for ground-truthing satellite-based classification. It does, however, have inherent limitations when it comes to addressing standardized drought indices and land suitability evaluations. Choosing the path of sustainable development would provide a long-term solution to Basona Werana's drought susceptibility. In agrarian areas like Ethiopia, LULC and drought conditions must be closely monitored.

Key Words: UAS, satellite images, land-use dynamics, drought susceptibility, agricultural suitability, VCI, NDDI, ground-truthing, Ethiopia

Contents

Acknowledgment v

Abstract vi

Abbreviations x

List of Tables xi

List of Figures xii

List of Appendices xiv

1. CHAPTER ONE: INTRODUCTION 1

1.1. Background of the Study 1

1.2. Problem Statement 3

1.3. Objectives 5

1.4. Research Questions 5

1.5. Significance of the Study 5

1.6. Scope of the Study 6

1.7. Limitations of the Study 7

1.8. Organization of the Thesis 8

2. CHAPTER TWO: LITERATURE REVIEW 9

2.1. Basic Concepts 9

2.1.1. Land Cover, and Land-use Dynamics 9

2.1.2. Drought 9

2.1.3. Sustainability, and Sustainable Development 9

2.2. Empirical Studies 10

2.3.1. LULC Dynamics in Ethiopia 10

2.3.2. Studies on Drought Monitoring 11

2.3.3. Studies on Land Suitability 12

2.3. Remote Sensing Technologies 12

2.4. Change Detection 16

2.5. Vegetation Indices, and Drought Assessment 16

2.5.1. Satellite-Based Vegetation Indices 17

2.5.2. Visible Range (UAS Suited) Vegetation Indices 20

2.5.3. Advanced Drought Indices 22

2.6. Conceptual Framework 24

3. CHAPTER THREE: MATERIALS AND METHODS 25

3.1. Description of the Study Area 25

3.2. Data Sources 29

3.3. Data Processing and Analysis 32

3.3.1. Sampling Method 33

3.3.2. Image Classification Methods 33

3.3.3. Vegetation and Drought Mapping Methods 35

3.3.4. Land Suitability Analysis through GIS Overlay 36

3.3.5. Accuracy Assessment, and Data Validation 36

3.4. Analytical Framework 37

4. CHAPTER FOUR: RESULTS AND DISCUSSION 38

4.1. Results 38

4.1.1. Classification Accuracy Assessment 38

4.1.2. UAS Based Accuracy Assessment 39

4.1.3. Land Use Land Cover Dynamics 44

4.1.4. Land-cover Change Trends 46

4.1.5. Vegetation Indices based Biomass Monitoring 49

4.1.6. Relationship of LULC and Vegetation Indices... 55

4.1.7. Drought Susceptibility Mapping.. 56

4.1.8. UAS Based Biomass Assessment 62

4.1.9. Land Suitability Analysis... 63

4.2. Discussion 70

4.2.1. LULC Changes 70

4.2.2. Drought Susceptibility 73

4.2.3. Land Suitability and Sustainable Development... 75

4.2.4. Remotely Sensed Data for Sustainable Development 77

5. CHAPTER FIVE: CONCLUSION AND RECOMMENDATION 79

5.1. Conclusion 79

5.2. Recommendation 81

References... 83

Appendices.. 92

Abbreviations

ALOS	Advanced Land Observing Satellite
ARARI	Amhara Agricultural Research Institute
ARVI	Atmospheric Antivegetation Index
ASPRS	American Society of Photogrammetry, and Remote Sensing
CCD	Charge Coupled Devise
CMOS	Complementary Metal Oxide Semiconductor
DEM	Digital Elevation Model
EMA	Ethiopian Mapping Agency
EVI	Environmental/Enhanced Vegetation Index
GII	Geospatial Information Institute
GSD	Ground Sample Distance
GWP	Global Water Partnership
IDMP	Integrated Drought Management Programme
LiDAR	Light Detection, and Ranging
LST	Land Surface Temperature
MoA	Ministry of Agriculture
MSI	Multi Spectral Instrument
NDDI	Normalized Difference Drought Index
NDWI	Normalized Difference Woisture Index
NDVI	Normalized Difference Vegetation Index
RDVI	Renormalized Difference Vegetation Index
REILA	Responsible, and Innovative Land Administration
RVI	Ration Vegetation Index
SARVI	Soil, and Atmospherically Resistant Vegetation Index
SAVI	Soil Adjusted Vegetation Index
SLMP	Sustainable Land Management Project
SOOAC	Standardized Object-Oriented Automatic Classification
SPOT	Satellite Pour l'Observation de la Terre (French)
SSO	Sun Synchronous Orbit
SVM	Support Vector Machine

TGI	Triangular Greenness Index
TM	Thematic Mapper
UAV/S	Unmanned Aerial Vehicles/ Systems
VARI	Visible Atmospheric Resistant Index
VCI	Vegetation Condition Index
VI	Vegetation Index
WLRC	Water, and Land Resource Centre
WMO	World Meteorological Organization

List of Tables

Table 1: Landsat bands characteristics 13

Table 2: Data Sources (Images) 30

Table 3: UAV Mounted Camera Information 30

Table 4: Comparison of Landsat, Sentinel 2A, and UAS images of the same area around Wayou Kebele, Basona Worana District 32

Table 5: Features of imageries used in the research 32

Table 6: Description of Various Land Use Land Cover Types applied 34

Table 7: Software applications used to conduct the study 35

Table 8: Classification Accuracy Assessment Error Matrix for 2021 LULC classification......... 38

Table 9: LULC results of 1989, 2000, 2010, and 2021 45

Table 10: The Percent Increase/ Decrease of LULC classes in Basoa Werana Woreda 47

Table 11: Relationship between LULC and NDVI.. 55

Table 12: VCI Table for 1989, 2000, 2010 and 2021 57

Table 13: NDDI based drought approximations for Basona Werana (1989 - 2021) 58

Table 14: Areas affected by drought (in percent) using NDDI values for 8 selected years 60

Table 15: Correlation between drought severity levels of 8 years VCI and NDDI values with respective precipitation amounts ... 60

Table 16: Soil Types and their ecosystem services compared ... 64

Table 17: Constraints for land suitability analysis ... 64

Table 18: Cropland Suitability Assessment results ... 66

List of Figures

Figure 1: Flow Chart of Conceptual Framework ... 24

Figure 2: Location Map of Basona Worana Woreda ... 25

Figure 3: Topography Map of Basona Werana Wärädа ... 26

Figure 4: Annual Precipitation of Basona Werana (24 Yrs. Average) ... 27

Figure 5: Wayou Kebele, Basona Worana Woreda. Picture by Thomas Dubois) ... 27

Figure 6: Soil Types (Basona Werana Woreda) ... 28

Figure 7: UAS block (Wayou Kebele) ... 31

Figure 8: Flow Chart of Analytical Framework ... 37

Figure 9: UAS Based Validation - Scenario 1 ... 40

Figure 10: A graph showing Wayou Kebele UAS block LULC Status in 2020 ... 40

Figure 11: Distribution of Accuracy Assessment Points inside UAS Block for Scenario II Accuracy Assessment ... 42

Figure 12: UAS Based Accuracy Assessment - Scenario 3 ... 43

Figure 13: 2021 Land-use Land-cover Status of Basona Werana Woreda ... 44

Figure 14: Bar chart of LULC 2021 ... 44

Figure 15: Land-use Dynamics in Basona Werana Woreda (1989 - 2021) ... 45

Figure 16: A bar graph of LULC in Basona Werana (%) ... 46

Figure 17: Zonal Change Map (1989 -2021) 48

Figure 18: Graphical representation of the LULC Changes 49

Figure 19: NDVI Values of 1989, 2000, 2010, and 2021 of Basona Werana 50

Figure 20: Comparison of Six Vegetation Indices (2010 and 2021) 52

Figure 21: Vegetation Indices by Range of Values Min. Max. (1989 -2021........ 53

Figure 22: NDVI and other vegetation indices correlation........ 54

Figure 23: Line Chart of Vegetation Indices correlation 54

Figure 24: Scatter plot Matrix of six vegetation indices........ 55

Figure 25: VCI Map for four historical years 1989, 2000, 2010, and 2021 56

Figure 26: A stacked bar of VCI for 1989, 2000, 2010 and 2021 57

Figure 27: A stacked bar of VCI for 2018 - 2021........ 58

Figure 28: A Normalized Difference Drought Index (NDDI) Map for Eight Historical Years ... 59

Figure 29: Normalized Difference Drought Index for selected years (1984 – 2021 59

Figure 30: Correlation of VCI and NDDI severity degrees with precipitation........ 61

Figure 31: Visible Atmospheric Resistance Index (VARI) using UAV Imagery 62

Figure 32: Map of constraints for suitability assessment........ 66

Figure 33: Agricultural Suitability Map of Basona Werana 68

Figure 34: A stacked bar of Agricultural Suitability Rank by Kebeles 69

Figure 35: Agricultural suitability map across Kebeles........ 70

Figure 36: Typical Settlement Patterns in Basona Werana 73

Figure 37: Shrub, and bush alongside agricultural areas on the northern tip of Basona Werana Woreda (GE courtesy) 76

Figure 38: Dibut Kebele terracing practices 76

List of Appendices

Appendix 1: Description of UAV flight at Wayou Kebele.. 92

Appendix 2: Confusion Matrix of 1989 classification.. 92

Appendix 3: Confusion Matrix of 2000 classification.. 92

Appendix 4: Confusion matrix of 2010 classification 93

Appendix 5: VARI model [Landsat 4 to 7] Erdas Imagine® 93

Appendix 6: Freq. Dist. of Agricultural Suitability via 300m equal interval samples 94

Appendix 7: VCI calculated for 2018, 2019, 2020 and 2021 using those year's minimum and maximum 95

Appendix 8: The precipitation data used in correlation of VCI and NDDI in section 4.1.5.3 95

1. CHAPTER ONE: INTRODUCTION

1.1. Background of the Study

The biophysical cover of Earth's surface is in a state of continuous modification at local, national, and global scales. Amid these land cover changes, land degradation, and periodic droughts are at an alarming level these days – besides climate change. The ever-growing human population and the associated high demands for resources are putting increasing pressure on socio-ecological systems. These systems link humans, and the natural environment in an interdependent manner (Angessa, Lemma, & Yeshitela, 2019; Damtea, Kim, & Im, 2020). The advent and advancement of remote sensing technologies in the last few decades have played a critical role in understanding these intertwined systems. Satellite systems and the newly emerging Unmanned Aerial vehicles are enabling environmental monitoring tasks of (i) land-cover mapping, (ii) vegetation state, phenology, and health, (iii) precision farming, (iv) crop monitoring, (v) atmospheric observations, (vi) disaster mapping, (vii) soil erosion, (viii) change detection at larger and smaller spatial scales respectively (Manfreda, Helman, Su, & Toth, 2018).

Unsustainable use of land resources results in the decline of land quality, and quantity (Ewnetu, Simane, Teferi, & Zaitchik, 2021). It also caused significant soil erosion, decreased crop production, decreased productivity, and deterioration of soil quality (Mostafiz, Noguchi, & Ahmed, 2021). One of how sustainability challenges are addressed includes an understanding of land-use change and land-use systems. Land systems constitute complex, adaptive, ecological systems shaped by different actors, and demands that act upon; land, technologies, institutions, and societal practices (Meyfroidt, Chowdhury, & Garrett, 2018). Remote sensing and GIS methods are effective, and convenient ways for assisting agricultural land-use planning, and policymaking and spatial planning are commended to be the center of research, and policy development (Mostafiz, Noguchi, & Ahmed, 2021). Recent advances in UAV technology could back the already well-established satellite technology-based earth monitoring tasks (Manfreda, Helman, Su, & Toth, 2018).

Mapping land-cover change helps to analyze the magnitude, intensity, and direction of landscape changes. Since the first aerial photograph, taken from a balloon in 1858, and the Landsat satellite was launched in 1972, information extraction of the physical environment has improved significantly. Traditionally, it was mapped through costly, and time-consuming direct field survey methods. With the emergence of very advanced earth science monitoring methods, now it is measured, and quantitated with relatively lesser efforts. More specifically, Lan-use/ Land-cover (LULC) is the most widely applied earth observation application area (Bewket, Gessesse, & Bräuning, 2015; Damtea, Kim, & Im, 2020).

Droughts pose significant water, and food security concerns worldwide (Kouchak, Farahmad, Melton, Teixeira, & Anderson, 2015). It is among the threats and core challenges to sustainable development in Africa (UNESC, 2007). Droughts can have a devastating effect on the supply of water, crop production, and livestock rearing. Drought-prone area identification is fundamental to increase food security, better manage risks, and efficient food-aid delivery. Droughts along with floods account for 80% of life, and 70% of economic losses among the natural hazards in Sub-Saharan Africa. The droughts of the 1980s and 1990s in Africa affected several countries, and outrageous famine emergencies have occurred. The 1984 drought for instance took the lives of over 1 million people, and 1.5 million livestock population in Ethiopia (Rojas, Vrieling, & Rembold, 2011). The more recent drought events occurred in 2002, 2011, and 2015 - times where Ethiopia's resilience has improved significantly from that of 30 years before (Centre for humandata, 2021).

World Meteorological Organization categorizes drought indicators and indices into meteorology, soil moisture, hydrology, remote sensing, composite (modeled). Commonly used meteorological indicators such as Aridity Anomaly Index (AAI), Standardized Precipitation Index (SPI), Palmer Drought Severity Index (PDSI), and Weighted Anomaly Standardized Precipitation (WASP) requires adequate temperature, precipitation, and associated inputs for calculation (WMO & GWP, 2016; Faridatul & Ahmed, 2020). In practice, these are limited by the scarcity of reliable rainfall data. The rainfall stations are mostly situated in large spatial gaps, so rainfall measurements usually are replaced by atmospheric circulation models or satellite imageries. Even other international meteorological sources contain errors and show deviations in African countries. To fill the gap, remote sensing vegetation abundance methods are increasingly being used as optional methods of providing information on droughts (Artiola, Pepper, & Brusseau, 2004).

The growing interest in how Unmanned Aerial Vehicles (UAVs) for different applications, have increased in the past 30 years, and particularly expanded rapidly in the last decade (Manfreda, Helman, Su, & Toth, 2018). The increased availability of these drones in recent years, the related technological advancements, and their analytical capability enabled the integration of multispectral, hyperspectral, thermal, Synthetic Aperture Radar (SAR), and Light Detection, and Ranging (LiDAR) sensing. Remote sensing of UAVs (RS UAV) emerged along with advancements in robotics, computer vision, and sensor miniaturization (Colomina & Molina, 2014).

Ethiopia, often named as 'the roof of Africa', has an estimated 490,000 km^2 area covered by highlands. It accounts for around 44% of the total areal coverage of the country i.e., nearly half of the total highland areas of the entire African continent (Ayele, 2009). In an era where UAV mapping methods are rapidly evolving, a mountainous country such as Ethiopia, where ground-truthing of satellite measurements is a tough task, necessitates additional research that synergizes the use of satellites and UAVs. In this regard, this study has presented the case of the Basona Werana district (or locally called Woreda), in the central highlands of Ethiopia. Because of the ever-increasing human and animal population, the Woreda has inherited the current ecological deterioration in this area (Tizale, 2007).

1.2. Problem Statement

Environmental processes are variable spatially and need a high spatial, and temporal resolution for deeper understanding. In practice scientifically describing the effects of land-use changes, its association with agricultural suitability, and drought prevalence is a challenging task (Manfreda, Helman, Su, & Toth, 2018). Maps can simplify such challenges by offering simplified solutions through integrating statistical, and spatial environmental variables. Decisions about such environmental issues require maps that have a known accuracy (Bewket, Gessesse, & Bräuning, 2015).

Central highlands, a segment of this 11% of the country's portion, and the larger Amhara regional state share a lot of similar characteristics as a whole. The area is known for erratic rainfall, high population density, high degree of land degradation, high poverty rate, and malnutrition. Nearly one out of five households cover their food requirements from their agricultural production for three months (Ayalew, et al., 2012). Basona Werana Woreda, in central highlands, has been known for intensive agricultural practices and good productivity, and perhaps self-sufficient. Nonetheless, climate change effects affected the food security status of the Woreda significantly (Ayele, 2009). The recurrent drought of every eight to ten years, which affects most of the country, also affects this district (Liou & Mehabie, 2019).

Several Ethiopian researchers used freely available satellite images for land-use land cover mapping, natural resource monitoring, and NDVI based biomass classification. The central highland watershed of Lake Wanchi is studied by (Angessa, Lemma, & Yeshitela, 2019), while a similar study for the Chemoga watershed is carried by (Damtea, Kim, & Im, 2020). The Land-cover changes alongside the temperature variability in Addis Ababa and its satellite towns are studied by (G/Michael, 2021). Forest degradation, and biomass change in Harenna Buluk District, Bale Zone has been analyzed by (Dinku, 2017) using Landsat, and Sentinel-2A images. A comprehensive study for the whole Woreda on LULC, drought, and agricultural suitability is not available.

One of the major gaps in similar domestic literary works is the use of a single or few droughts and/or biomass estimation indices in their analysis. Another identified gap is the underutilization of UAV/Satellite synergy in the published literature. Few or no adequate literature reviews analyze UAV and satellite synergies across the academic community. For instance, (Emilien, Thomas, & Thomas, 2021) discovered 19 and 39 related publications published in 2008 and 2019, respectively. Few fields, such as ecology, and agriculture have been quite involved. Because of its early stages of developmental status as an optional earth observation method, a combined workflow hasn't been fully established. Each platform, with its sensor types, has its advantages, and limitations (Abdullah, Gholoum, & Abbas, 2018; Zhao, Wu, & Wang, 2020).

The sustainability challenges, which have been briefly discussed above, are exemplified by actual drought conditions, resulting in famine, deteriorating suitability of land for crop production and associated degradation, malnutrition, which are also represented by some parts of Basona Werana. The dietary requirements are greatly affected. This steady decline in food security status, in which people are unable to meet their daily dietary needs, forces people to use their resources in an unsustainable manner, putting their resilience capacity into question. While land, the primary resource, is used in an unsustainable manner, ecosystem services and agricultural yields decrease as a result.

1.3. Objectives

1.3.1. General Objective

The thesis explores the dynamics in LULC, drought vulnerability, and agricultural suitability in Basona Werana and their implications for sustainable development.

1.3.2. Specific Objectives

The thesis aims to

i. Explore the land-use dynamics of Basona Werana
ii. Map the temporal changes in drought susceptibility of Basona Werana through standardized vegetation index mapping methods
iii. Analyze the land suitability of Basona Werana for crop production

1.4. Research Questions

i. What are the historical and contemporary land-use dynamics status of the Basona Werana district?
ii. How does the drought susceptibility of Basona Werana can be quantified and shown using standardized vegetation index mapping methods?
iii. What is the land suitability status of Basona Werana for crop production currently?

1.5. Significance of the Study

This thesis is part of the requirement to obtain an MA in Environment, and Sustainable Development from the College of Development Studies at Addis Ababa University. The researcher's effort in finding related literature indicates the existence of quite a substantial number of articles, and publications available in the satellite-based land-use land-cover analysis in Ethiopia. In almost every part of the region, some studies attempt to link the dynamic nature of land-uses with the socio-economic condition of that particular area.

Among the major outputs of this paper is the LULC classification, change analysis, and its integration with UAVs for training sample collection, and validation or "ground-truthing". It addresses the gaps of high cost, and time taking satellite classification accuracy assessments and presenting a possible solution for accuracy assessment particularly in the highland dominated areas of Ethiopia. By doing so, this thesis aims at adding a sample study for the greater "satellite-UAV synergy" a newly emerging study theme area in the earth observation – environment academia endeavors (Emilien, Thomas, & Thomas, 2021; Zhao, Wu, & Wang, 2020).

The thesis also contributes to the environmental assessment of that Woreda by visualizing the natural resources, and land covers, and analyze the possible reasons for the food insecurity status, and agricultural product losses in the last couple of years. The land suitability and drought susceptibility maps are fittingly adjusted for the lowest administrative structure, the Kebeles for reducing obscurity of getting adequate information.

The findings of this study as well as the plenty of map-based visualizations, and their statistical accounts will facilitate the decision-making process of local administrative experts in Basona Werana Woreda as well as nearby areas. It also embarks on other researchers elsewhere to test the validity of this method to accurately examine their satellite-based land-cover classifications.

Policymakers these days highly require remote sensing and GIS-based tools, and research works for their future planning, and decision making. This study by far provides input for land-use planning in North Shoa areas, particularly Basona Werana Woreda. It can be used for extrapolating the tools, methods, analysis, and information extraction to other parts of the country as well as anywhere else in the world. It also assists policymakers and development practitioners to develop policies that are better aligned with climate change variables, and assists to combat drought, enhance climate resilience, and reducing food security concerns in the surrounding.

1.6. Scope of the Study

Spatially speaking, the land-cover dynamics portion, drought assessment, and land suitability for crop production covered the whole area of Basona Werana Woreda, in the North Shoa Zone of Amhara regional state. But a comparison with the UAV data appeared to be limited to a specific Kebele in the Woreda known as Wayou. The UAV covered an area of 1000 ha which is taken during the rainy season of 2020.

The thesis is mainly focused on the general land cover of the study area, drought status and susceptibility, and land suitability for agriculture. Other profound environmental concerns such as soil erosion, degradation, and flooding are not the central devotion of this study.

Temporally speaking, the past 32-year period - to be exact has been purposively used in almost every part of the study. Nonetheless, the year1984 is added later to effectively compare the drought conditions with the historical year of deadly drought in Ethiopia. The satellite images are mainly captured in the Winter season, where there is a high possibility of obtaining cloud-free images. So, except for NDDI comparisons, the seasonal changes in drought situations are not fully embraced in this thesis. To fill this gap, monthly rainfall data for 24 years has been applied.

The thesis has focused on a particular type of drought i.e., agricultural drought based on soil moisture deficits, and vegetation health. So, it doesn't include other meteorological data for drought vulnerability analysis. A methodological argument for this is provided in the literature review, and materials and methods chapters. The land suitability analysis for crop production is exclusively based on the widely employed GIS-RS procedures and pragmatic pieces of literature and not based on an in-depth agricultural acquaintance or experience.

1.7. Limitations of the Study

Among the major limitations of optical satellite images is their frequent failure to collect cloud-free imagery during rainy seasons. Due to this, a proper comparison with the UAV images, which are taken during the rainy season, of similar temporal resolution has been hampered. The coverage of satellite-based mapped areas vs. UAS-based mapped areas has a huge difference in their spatial coverage. This affected the side-by-side comparison of land-use land-cover changes and vegetation coverage. Some LULC classes, which exist in the larger block, also had a fewer or no representation in this smaller UAS-captured area.

All types of agricultural lands (cultivated or uncultivated) are in general considered as cultivated lands. So, it should be understood as this class refers generally to agricultural lands. The categorical classification of crop types in the land cover classification is beyond the scope of this study. This is due to the lack of sufficient ground-truthing data from the agricultural bureau of the Woreda, and the researcher's financial constraint for a detailed survey on the ground.

1.8. Organization of the Thesis

The thesis includes five chapters and is organized with respective themes accordingly. Chapter 1 presented the background of scientific trends in remote sensing techniques in using multiple source imageries. It also indicated the land-use land-cover conditions in Ethiopian highlands and the importance of the thesis. The chapter also includes the problem statement, the objectives, and the research questions, the significance of the study, and many more.

Chapter two – the literature review – mainly presents the application of remote sensing methods for land-use land-cover, drought vulnerability as well as agricultural suitability. In its preliminary portion, introduces the reader to the basic concepts. The theoretical review indicated few theories that are more relevant to the point of discussion of the thesis. The detailed explanations for comparing satellite-based vs. UAV platforms are an integral part of the chapter. While explaining that, several standardized vegetation indices, and their prone, and cons, as well as their particular application areas, are briefly indicated. Image classification, and accuracy assessment techniques in remote sensing are presented, and the widely used methods are discussed, which particularly go along with this study.

Chapter three clarifies the methodological essence of the research work. It introduces the readers to the description of the study area; its agro-climatic zones, topography, soil, population, and general land use. The chapter also defines the input data types, their descriptions, how they are processed in a GIS environment, and validated for their accuracy. It ends by depicting the validation techniques and providing an analytical framework for the whole study.

Chapter Four presented the results, and findings of the entire paper along with discussions. It discusses how these findings are comparable to other literature. These include the LULC mapping, land-cover change trends, biomass, and drought mapping, UAS based biomass mapping, and accuracy assessments.

Chapter Five embraces a brief account of the general conclusions made based on thorough exploration, assessment and discussions conveyed out of the input data and data processing. Based on these conclusions few timely and relevant recommendations have been forwarded.

2. CHAPTER TWO: LITERATURE REVIEW

2.1. Basic Concepts

2.1.1. Land Cover, and Land-use Dynamics

Land-cover is originally used to define the vegetation’s status, such as grassland or forestry. But broadly it also comprises built-up and settlements, soil types, and water bodies. The land cover has been modified by human beings for thousands of years. It’s mainly for livelihood activities such as fuel, fiber and the intensity of the change is enhanced to an alarming level in recent times. In a larger sense the population growth, overgrazing, unsustainably managed tourism, misuse of different resources are also the cause of land-cover change (Dinku, 2017; Bai, et al., 2017).

2.1.2. Drought

Drought is defined as an extended period of rainfall deficit relative to the statistical multi-year averages for that region. Droughts adversely affect agriculture and food security, livelihood security (WMO & GWP, 2016). Droughts can be broadly classified into four categories including meteorological (precipitation deficits), agricultural (soil moisture deficits), hydrological (runoff, groundwater, water storage deficit), socioeconomic (including water supply, demand, and social response) (Kouchak, Farahmad, Melton, Teixeira, & Anderson, 2015).

2.1.3. Sustainability, and Sustainable Development

Sustainability, initially came to public attention after the Brundtland Report of 1987. Since then, it has shifted in a different direction. It encapsulates development (the socio-economic development, ecological constraints), needs (redistribution, and quality of life), and future generations (long-term resource use). The triple bottom line concept is an essential term; i.e., the balance between three pillars of sustainability. These are environmental sustainability, social sustainability, and economic sustainability (Klarin, 2018). In the context of environmental management, sustainable development is defined as "expanding what nature offers to the maximum and keeping that expansion indefinitely without environmental interruption, to make the most of human well-being, security, and adaptability" (Barrow, 2006).

In the year 2015, the United Nations proposed a 15-year comprehensive strategy called – Sustainable Development Goals, a total of 17 goals with associated 169 target indicators were pledged by world leaders. This is a very holistic document that tried to include many sectors, apart from economic-centered goals. Economic development is also aimed to be sustained, inclusive, and incorporate sustainable economic growth (UN, 2015). Goal 11 states "Make cities, and human settlements inclusive, safe, resilient, and sustainable" (UN, 2015). Goal 15, on the other hand, states: Protect, restore, and promote sustainable use of terrestrial ecosystems, sustainably manage forests, combat desertification, and halt, and reverse land degradation, and halt biodiversity loss.

2.2. Empirical Studies

2.3.1. LULC Dynamics in Ethiopia

Ethiopia has experienced rapid land-cover changes since the mid-20th century (Damtea, Kim, & Im, 2020). The cost of these LULC changes in Ethiopia have an estimated loss of ecosystem value of $4.3 billion per year, an amount of more than $3 billion from neighboring Kenya (Gebreselassie, et al., 2016; Mulinge, et al., 2016). Ethiopia's forest coverage of 40% at the beginning of the 20th century has reduced to 2.36% in 2000. Later evidence showed that the forest cover has recovered to 12% (Ewnetu, Simane, Teferi, & Zaitchik, 2021). The Environment Forest and Climate Change Commission of Ethiopia has publicly announced through (EBC, 2021) a 17.2% national forest cover at the eve of a summer tree planting season of 5 billion, which is initiated particularly by the prime minister in the year 2019.

An interesting study conducted by (Worku, Mekonnen, Yitaferu, & Cerdà, 2021) in the northwest highland of Ethiopia used a supervised classification method to classify land use. The result of the study indicated the expansion of plantation forestry and a decreasing trend of grazing land among the total seven dominant land-use land-cover classes. A series of studies in this regard have indicated that natural forests have shown a downward trend, while intentionally planted forests; mainly the eucalyptus (*Eucalyptus chamadulenis, and Eucalyptus globulus*) plantation has shown an increase (Worku, Mekonnen, Yitaferu, & Cerdà, 2021).

The sustainability of forests is at the center of land-use analysis across various literature. Forest is the presence of trees with a land cover of more than half a hectare. According to a recently published report of (FAO and UNEP, 2020), the global forest cover is just 4.06 billion hectares, i.e., 31 percent of the world's total area or approximately half-hectare per person.

While (Dinku, 2017) applied remote sensing methods for monitoring forest degradation, deforestation, and biomass estimation in the Harenna Buluk District of Bale Ethiopia, a ten-year gap time-series Landsat images of 20 years have been used. The advanced satellite images helped in monitoring forest cover and the degradation process of habitats. The Biomass has been quantitated using NDVI, and land-use land-cover analysis. Some 15 years back, the LULC of Basona Werana Woreda indicated by (Ayele, 2009) proportions the area for cultivated land i.e., 47.3% followed by grazing land 13.1%, Forest, Shrub, and bushland together accounts 8.5%, and others (including wasteland) accounts for 31.1% of the total area.

2.3.2. Studies on Drought Monitoring

Growing interest to predict people's vulnerability to drought and other climate change hazards began in the late 1990s and augmented onwards (Barrow, 2006). A coarse resolution MODIS-based NDVI values are most commonly used in drought assessments so far.

A MODIS NDVI time-series data is applied to study the drought conditions for the whole of Kenya by (Klisch & Atzberger, 2016). Another study by (Pahar, Paembonan, & Soma, 2021) applied Normalized Difference Latent Heat Index (NDLI) based drought assessment in Indonesia. A drought vulnerability mapping for northwestern Bangladesh is conducted by (Hoque, Biswarjeet, & Ahmed, 2020) using a multi-criteria-based approach. The study identified four types of drought types namely meteorological, hydrological, agricultural, and socio-economical. Using these four types of droughts, a total of 16 variables were weighted to identify which areas are said to be vulnerable to drought in various degrees.

A notable study of the Spatio-temporal distribution of drought is conducted by (Liou & Mehabie, 2019) from the period 2001 to 2018 for the entire Ethiopia. A 16-day monthly average MODIS Tera dataset of 18 years was used and the whole country is represented by 250m and 1km spatial resolution for NDVI and LST. A comparative study of Landsat-NDVI with MODIS-NDVI in Jordan for Barley has indicated that the previously mentioned one is much better in detecting drought conditions (Al-Bakri, et al., 2016). Another investigation of MODIS and NDWI comparison for five years in the united states is conducted by (Gu, Brown, Verdin, & Wardlow, 2007). Their outcomes indicate, during summer seasons average NDVI and NDWI values were lower as far as <0.5 and <0.3 respectively for the study area. Among the two indices, NDWI values declined more in response to drought than NDVI, indicating that it is a more drought-responsive metric.

2.3.3. Studies on Land Suitability

Spatial multi-criteria analysis (MCA) is considerably in use recently to integrate diverse metrics that are obtained through different measurement techniques and not easy to compare to each other. It's used for themes of studies such as agricultural land suitability (Mostafiz, Noguchi, & Ahmed, 2021), surface irrigation (Nigussie, Moges, Michael, & Steenhuis, 2019), and land degradation (Ewnetu, Simane, Teferi, & Zaitchik, 2021). The concept of fuzzy logic in environmental science is another known statistical method (Sinshaw, et al., 2021). AHP method is a semi-target and multicriteria method from various alternatives at unique scales used for decision making.

A multi-criteria decision-based weighted analysis of agricultural land suitability is conducted by (Mostafiz, Noguchi, & Ahmed, 2021). They used criteria (elevation, slope, several soil vegetation indices) to assess the most suitable lands into a degree of highly, moderately, marginally suitable. Soil erosion susceptibility is mapped by (Sinshaw, et al., 2021) for the upper blue Nile area through fuzzy logic and AHP methods by considering rainfall, land use, slope, soil, aspect, SPI, river proximity, and curvature.

A recent study conducted by (Alemayehu, et al., 2020) used three global atmospheric circulation models to study the climate change effects on the land suitability of Ethiopia for alfalfa production. Using the multi-criteria evaluation method biophysical, climate, and topographic factors were employed to assess the land suitability of the entire country.

2.3. Remote Sensing Technologies

2.3.1. Satellite Remote Sensing

According to the ASPRS, remote sensing is "the measurement or acquisition of information about some property of an object or phenomenon by a recording device that is not in physical or intimate contact with the object or phenomenon under study". Remote sensing is also understood as a tool or a technique similar to mathematics. It provides fundamental scientific data of x, y location, z elevation or depth, biomass, temperature, moisture content, etc. (Jenson, 2015).

Remote sensing has the advantage of attaining a time series of consistent, and comparable data, which is cost-efficient (Xue & Su, 2017). With the use of high-resolution spectral instruments, the number of bands is increasing, while the bandwidth is becoming narrower. Recently vegetation mapping using near-surface multispectral, hyperspectral, or Lidar imaging from manned or unmanned aircraft is trending (Sharma, Hara, & Hirayama, 2017).

Table 1: Landsat bands characteristics

Landsat 4, 5, and 7 Bands	**Characteristics**
Band 1 (Blue) 0.45-0.52 µm	Increased penetration of waterbodies, supports analysis of land use, soil, and vegetation characteristics
Band 2 (Green) 0.52-0.6 µm	Reacts to the green reflectance of healthy vegetation
Band 3 (Red) 0.63-0.69 µm	Useful for vegetation discrimination, soil-boundary, and geological boundary delineations
Band 4 (Near-infrared) 0.76-0.90 µm	Responsive to the amount of vegetation biomass and/or leaf area present, useful for crop identification, and helps to emphasize soil/crop, and land/water contrasts
Band 5 (Mid Infrared) 1.55-1.75 µm	Sensitive to the amount of water in plants, and helps in crop drought studies, and plant vigor investigations
Band 6 (Thermal Infrared) 10.4 – 12.5 µm	Useful for geothermal activity detection, thermal inertia mapping for geologic investigations, vegetation classification, and stress analysis, soil moisture studies.
Band 7 (Mid-Infrared) 2.08-2.35	Helps to discriminate geologic rock formations, effective for identifying zones of hydrothermal alteration in rocks

Adapted from (Barrow, 2006) page 194

The more recent Copernicus Programme, an earth observation program of the European Space Agency (ESA), has Sentinel satellite families. Sentinel-1 family has the Multi-Spectral Instrument (MSI), with a relatively high-resolution optical instrument that has similar spectral characteristics to SPOT, and Landsat. Sentinel 2A launched on 23 June 2015, and Sentinel-2B launched on 7

March 2017. It improved the spatial resolution of Landsat by 3 times with more spectral bands and greater temporal resolution. The multispectral instrument of Sentinel has 13 spectral bands, at different spatial resolutions. This includes four visible, and near infra-red bands at 10m resolution, roughly equivalent with TM bands, and six near IR bands, and shortwave IR bands at 20m spatial resolution (Flood, 2017).

The surface reflectance of Landsat and Sentinel-2 is compared in six test sites in Europe, reported Root Mean Square error values of 0.03 reflectance units, and proves that the systems are well set up. However, these two products were created using different surface reflectance transformation algorithms (Flood, 2017).

WorldView-2 and -3 (Digital Globe) were the first high-resolution satellites offered for commercial purposes. It provides eight spectral sensors; visible to near-infrared range (Xue & Su, 2017). CubeSat platform, even though it is commercial, presents a promising technology operating in the visible to near-infrared regions with high spatial, and temporal resolution (Manfreda, Helman, Su, & Toth, 2018). While MODIS and AVHRR are considered low resolution, Landsat, Sentinel, HJ, and GF have been categorized as medium resolution satellites (Zhao, et al., 2019). After the launch, and successful operation of SPOT-5, IKONOS, QuickBird, and EROS, China deployed Beijing-1, Cartosat-1, and 2, ALOS/PRISM, ROCCAT-2, and JOMPSAT-2 between 2004, and 2008 (Li, Chen, Baltsavias, & Aplin, 2008).

In the past few years, there is an increasing interest in hyperspectral imaging sensors. They are comparatively expensive than multispectral sensors but offer a greater potential for quantitative soil vegetation, and crop studies. Their focus is on the VIS-NIR (near-infrared) portion of the spectrum and offers high radiometric accuracy (Manfreda, Helman, Su, & Toth, 2018).

2.3.2. Unmanned Aerial Vehicles (Systems)

Unmanned Aerial Vehicles are air vehicles and accompanying equipment that are remotely piloted or fly autonomously and do not carry a human operator. Unmanned Aerial Systems (UAS), Unmanned Aerial Vehicles (UAV), Remotely Piloted Aircraft Systems (RPAS), and drones are all terms used to describe UAV (ITA, UDC, 2021). Although UAVs don’t require pilots, they are not necessarily autonomous. They are remotely controlled from the ground through real-time command-and-control links (Li, Chen, Baltsavias, & Aplin, 2008).

Generally, a longer flying time is achieved by fixed-wing systems, which also demands lighter payloads. On the other hand, battery-powered multirotor UAVs with higher spatial, and temporal resolution, allows plant water status sensing for irrigation scheduling, and evapotranspiration modeling (Xue & Su, 2017).

UAV data collection improves time, and cost efficiency than ground-based surveys (Solazzo, Sankey, Sankey, & Munson, 2018), and it also improves operational flexibility, better spatial resolution, and enhanced classification results when compared to satellite sensors. This is why UAVs are great options in fillings the gaps in remote locations where existing data is limited (De Giglio et al., 2017).

UAV platform, with low altitude flight, allows collection of data in cloudy or hazy conditions that otherwise couldn't be obtained using satellite or aircraft. This is evident when metrological data of daily revisits are compared. There is a 20% possibility of obtaining a usable image with optical satellite image, while with UAVs it is 45% to 70%. These capabilities of UAV and sensor technologies stimulated an explosion of interest among researchers who monitors rainy regions (Manfreda, Helman, Su, & Toth, 2018).

Some of the factors associated with choosing UAS imagery are derived from the initial investment, the processing software, storage capacity, fieldwork costs. On the other hand, there exists - operational, processing, and retrieval limitations associated with it (Manfreda, Helman, Su, & Toth, 2018). It ranges from the blurring of images, due to the forward motion of the UAV, orthorectification issues due to geometric distortion associated with inadequate image overlaps. Even though UAV images have a greater advantage in obtaining ground vegetation types, they are limited to cover larger areas.

UAS, on the other hand, can play an important role in the explanation, validation, and completion of satellite data. The explanation role is materialized while satellite observations cover larger areas but have a coarse resolution ineffective for interpretation, UAV fills this gap. It also plays a validation role of ground-truthing, or "drone truth". UAV data can replace in-situ observations for applications where objects are identified, such as plant cover, water bodies, or urban areas. In non-parametric supervised learning methods, such as random forest, UA systems can play a role in providing "ground truth". But, as the area becomes larger their heavy logistical requirement makes their usability a bit illogical (Emilien, Thomas, & Thomas, 2021).

UAVs are strongly recommended by scholars like (Gray, et al., 2018) over field-based assessments, while field-based assessments are still an important tool for accuracy assessments, whenever it is possible to undertake. This is due to the UAVs increased ability of sampling validation points of a larger part of study areas, while requiring less time, and less interruption on the area of interest. It is strongly argued that UAS-based training and validation enables a larger sample, and training size within a fixed budget (Gray, et al., 2018). UAS images, with a properly rectified structure from motion processing, enables <0.05m spatial errors. The limitations of UAVs for accuracy assessment include the startup costs, shadows, and haze might visually prevent for determining water depth or vegetation type (Gray, et al., 2018).

UAV systems cannot compete with satellite platforms in terms of spatial coverage. For larger areas, the costs of acquisition, georeferencing, and orthorectification costs of UAV acquired images impact negatively (Manfreda, Helman, Su, & Toth, 2018). Comparing the three platforms, UAS, Aircraft, and Satellite, (Matese, et al., 2015) concluded that UAS is a cost-effective solution for areas less than 20 ha. The quantitative analysis of UAS-based NDVI maps of 5 ha field costs up to 400 €. The same area with commercial satellite products may cost 30% more (Matese, et al., 2015).

2.4. Change Detection

LULC change detection and analysis assists in clarifying the extent of the change between periods and helps in categorizing these changes to make valuable decisions (Berihun, et al., 2019).

The percentage change between two periods is calculated as:

$$Percentage\ Change\ (\%) = \frac{(A_2 - A_1)}{(A_1)} \times 100 \quad (1)$$

Where A_1 is the area in year 1, whereas A_2 is the area in year 2 of that class (Thonfeld, Steinbach, Muro, & Kirimi, 2020).

2.5. Vegetation Indices, and Drought Assessment

Many areas used for agricultural production are not well instrumented to provide ground-based observations for precipitation, near-surface temperature, atmospheric water vapor, etc. It is due to this limited availability of these observations that makes satellite imagery-based vegetation indices become more applicable solutions in the estimation of drought ecosystem impacts – including vegetation health, and growth (Kouchak, Farahmad, Melton, Teixeira, & Anderson, 2015).

The quantitative assessment of vegetation condition is generally based on the spectral signature of vegetation greenness i.e., expressed in the red, and near-infrared regions of the electromagnetic spectrum (Kouchak, Farahmad, Melton, Teixeira, & Anderson, 2015). A vegetation index combines or filters multiple spectral data sets into a single value for each point on an image. Mostly, it is expressed as in a mathematical form, and the output i.e., the index is assigned specific color ramps and visualized as the false-color image of a particular field (McKinnon & Hoff, 2017).

According to World Meteorological Organization, drought can be monitored and can be early warned in three methods. These are i. using a single indicator (index), ii. Using multiple indicators (indices) and iii. Using composite (hybrid) indicators. In the past scientists used to employ a single indicator for the limited availability of data and time. Now, multiple indicators have been established due to the strong global interest (WMO & GWP, 2016).

2.5.1. Satellite-Based Vegetation Indices

Remote sensing of the growth and dynamics of terrestrial vegetation is insightful for applications ranging from agriculture to urban infrastructure planning. Vegetation information from remotely sensed images is inferred by differences, and changes of the green leaves from plants' spectral characteristics (Xue & Su, 2017). Until recently, there was no uniform mathematical expression for vegetation indices because of their complexity in spectral range, and combination, instrumentation, platforms, and resolutions. However, in general, vegetation indexing is accomplished by obtaining electromagnetic wave reflectance information from canopies via passive sensors (Xue & Su, 2017).

Remote sensing of vegetation mainly uses the following reflectance regions;

i. The ultraviolet region (UV), goes from 10 – 380nm
ii. The visible region (blue, green, red); blue (0.45 - 0.495 μm), green (0.495 - 0.570 μm), and red (0.620 - 0.750 μm)
iii. The near-infrared, and mid-infrared bands (0.850 μm – 1.7 μm)

The surface of leaves of a fully grown green plant without biotic or abiotic stress has an emissivity rate of 0.97, and 0.98. On the other hand, dry plant's emissivity ranges from 0.88 to 0.94. The indices extracted from the spectral ranges of near, and infrared regions could provide information for growth, water content, pigments, sugar, and carbohydrate content, protein content, and aromatics, among others (Arkebauer, 2005; Xue & Su, 2017).

The thermal infrared region (8-14 μm), within the blackbody radiation law, allows interpretation of emissivity linking to the plant's temperature. Indices calculated from this spectral region are essential to assess stomata dynamics that regulate the transpiration rate of plants. They are used to indicate plant water status, and estimation of abiotic/biotic stress levels (Prashar & Jones, 2016).

Many studies have limited their vegetation indices interpretation to individual light spectra bands or a group of single bands for data analysis. Most often, researchers combine the near-infrared (0.7 – 1.1 μm), and red (0.6 – 0.7 μm) bands in various ways. Though its application to heterogeneous canopies, such as horticultural plantations, makes the distinction very difficult (Xue & Su, 2017).

Some of the most common vegetation indices are listed here;

i. Normalized Difference Vegetation Index (NDVI) is among the most popular, and widely applied vegetation indices (Kouchak, Farahmad, Melton, Teixeira, & Anderson, 2015). It is seemingly based on the work by Tarpley et al., and Kogan from the National Oceanic, and Atmospheric Administration (NOAA) of the US. NDVI is highly related to LAI (leaf area index), and the photosynthetic activity of green vegetation. It is a normalization procedure where the resulting values range between 0, and 1, depicting an arid area as it is closer to 0 and more vegetated as it approaches a value of 1. Negative values indicate the presence of water, clouds, or snow (Artiola, Pepper, & Brusseau, 2004; Xue & Su, 2017).

$$NDVI = \frac{(\rho_{NIR} - \rho_{RED})}{(\rho_{NIR} + \rho_{RED})} \tag{2}$$

NDVI is very much sensitive to green vegetation responses, even for lightly vegetated areas. Many studies compare it with the Leaf Area Index (LAI), where LAI is defined as the area of single-sided leaves per area of soil (Hazaymeh & Hassan, 2016). NDVI has limitations to include the effects of soil humidity, and surface anisotropy (Artiola, Pepper, & Brusseau, 2004). It is said to be the most widely used vegetation index in Ethiopian remote sensing-based works of literature (Dinku, 2017; G/Michael, 2021).

ii. Renormalized Difference Vegetation Index (RDVI): is developed based on the derivation of NDVI. It calculates the deviation between NIR, and R wavelengths, alongside NDVI, and highlights the health of vegetation. It doesn't consider the effects of soil, and sun angles in the calculation (Barati, Rayegani, Saati, Sharif, & Narsi, 2011).

$$RDVI = \frac{(R_{NIR} - R_{RED})}{\sqrt{R_{NIR} + R_{RED}})} \tag{3}$$

iii. Transformed Normalized Difference Vegetation Index (TNDVI)

TNDVI is proposed by Tunker, 1979. This index is robust for biomass and vegetation cover estimation (Tahir, et. al., 2018).

$$TNDVI = SQRT\left(\frac{\rho_{NIR} - \rho_{RED}}{\rho_{NIR} + \rho_{RED}}\right) + 0.5 \tag{4}$$

iv. Soil Adjusted Vegetation Index (SAVI)

The highly applied NDVI values have been provided to estimate phenological patterns of the Earth's vegetated surface. However, the empirically derived NDVI values can be unstable, varying with soil color, and moisture conditions, atmospheric conditions, and dead materials on the soil. So, SAVI incorporates a soil background and/or atmospheric adjustment factor (Barrow, 2006).

$$SAVI = \frac{(\rho_{NIR} - \rho_{R})}{(\rho_{NIR} + \rho_{R} + L)} (1 + L) \tag{5}$$

Where L is a canopy background adjustment factor that accounts for differential red, and NIR extinction through the canopy. L is dependent upon the proportional vegetation cover, and density. For very sparse vegetation (bare soils), L will be one, whereas zero in densely vegetated areas (Barrow, 2006).

v. Soil, and Atmospherically Resistant Vegetation Index (SARVI)

Huete and Liu (1994) created SARVI by combining the L function from SAVI and the blue-band normalization from ARVI. It takes into account both soil and atmospheric noise.

$$SARVI = \frac{(\rho_{NIR} - \rho_{RB})}{(\rho_{NIR} + \rho_{RB} + L)} \quad (6)$$

vi. Modified Soil Adjusted Vegetation Index (MSAVI)

Wiegand and Richardson proposed it in the year 1977 to replace the L factor in the equation (*6*) and expressed as the following. It is widely used for soil and drought monitoring (Xue & Su, 2017).

$$MSAVI = \frac{1}{2}[2R_{NIR} + 1 - \sqrt{(2R_{NIR} + 1) - 8\,(R_{NIR} - R_{RED})}] \quad (7)$$

Other vegetation indices include Enhanced Vegetation Index (EVI), Advanced Vegetation Index (AVI), Optimized Soil-Adjusted Vegetation Index (OSAVI), and Atmospheric Antivegetation Index (ARVI) (Xue & Su, 2017). Remote sensing by far is limited in observing, monitoring quantifying carbon, and nitrogen cycles that have huge influences on natural vegetation, and ecosystem services (Kouchak, Farahmad, Melton, Teixeira, & Anderson, 2015).

2.5.2. Visible Range (UAS Suited) Vegetation Indices

Most, but not all, of the vegetation indices, require near-infrared (NIR) wavelength data. Since most low-cost drones do not contain a camera that supports ranges beyond the R, G, B (true color), and scientists have been working to produce indices that can provide other indices approximate or comparative to the well-known ones. In doing so, indices that utilize RGB data can minimize the data acquisition cost. Some camera companies try to replace the NIR with among the RGB channels. A good example is 'agribotix', which used a filter that blocks the red light while passing NIR, to obtain NIR from the red channel (McKinnon & Hoff, 2017; Costa, Nunes, & Ampatzidis, 2020).

i. **Visible Atmospheric Resistant Index (VARI)**; is developed at the University of Nebraska, seeking a method to predict vegetation fraction (VF), and leaf area index (LAI) (McKinnon & Hoff, 2017). It only uses visible (RGB) imagery to calculate the crop index (Costa, Nunes, & Ampatzidis, 2020). The addition of the blue band is to reduce the effect of the atmosphere (Eng, Ismail, Hashim, & Baharum, 2019).

$$VARI = \frac{R_{GREEN} - R_{RED}}{(R_{GREEN} + R_{RED} - R_{BLUE})} \tag{8}$$

ii. **Triangular Greenness Index (TGI)**; has been created to estimate leaf chlorophyll, and indirectly plant nitrogen content, using RGB images (McKinnon & Hoff, 2017).

$$TGI = R_{GREEN} - 0.39 * R_{RED} - 0.61 * R_{BLUE} \tag{9}$$

However, the proposed vegetation indices have limitations. The visible atmospheric resistant index (VARI), the reflectance from the green vegetated surface is not so high, and the reflectivity difference level among the visible channels is not as desirable. The triangular greenness Index (TGI), which uses a triangle in the spectral features of the chlorophyll region was developed and tested. But it did acquire the status of 'reliable general-purpose crop health indicator' (Costa, Nunes, & Ampatzidis, 2020).

iii. vNDVI

Another study was conducted using the three crop types (citrus, grapes, and sugarcane) a formula for vNDVI is calculated by using red, green, and blue values along with NDVI values (Costa, Nunes, & Ampatzidis, 2020).

$$vNDVI = 0.5268 * (red^{-0.12942} * green^{0.3389} * blue^{-0.3118}) \tag{10}$$

It showed a comparable result with the most widely used NDVI calculation. This proposed method for only RGB cameras accurately predicted NDVI values (using multispectral cameras). To evaluate the accuracy of the vNDVI method, an evaluation matrix was used: coefficient of determination (R2), mean absolute error (MAE), and mean percentage error (MPE).

Error = Absolute (NDVI – nNDVI)/ NDVI

A study conducted by agribotix (McKinnon & Hoff, 2017) tested VARI, and TGBI indices for corn, wheat, tomatoes, and rice while (Costa, Nunes, & Ampatzidis, 2020) tested for citrus, grapes, and sugarcane. Besides comparable results to show general trends in vegetation health, the result showed that it is not a reliable recommended method.

2.5.3. Advanced Drought Indices

Although vegetation indices such as NDVI are frequently used for drought estimates on their own, further advanced indices employ these indices to transform them into agreed-upon drought status mapping. Agricultural droughts begin with rainfall deficits, which leads to a lack of soil moisture, an increase in land surface temperature, and, eventually, a halt in vegetation growth (Kumar, et al., 2020).

i. **Precipitation Condition Index (PCI)** is an indirect method to estimate precipitation using rainfall estimates of sources such as (CHIRPS, 2021). Its values range between 0 and 1, from undesirable to optimum, based on precipitation estimates. When a flooding condition occurs the value becomes close to 1 (Kumar, et al., 2020).

$$\mathrm{PCI} = \frac{(\mathrm{CHIRPS_i} - \mathrm{CHIRPS_{min}})}{(\mathrm{CHIRPS_{max}} + \mathrm{CHIRPS_{min}})} \tag{11}$$

where $\mathrm{CHIRPS_i}$ designates the value of a specific pixel in the month of i, $\mathrm{CHIRPS_{max}}$ and $\mathrm{CHIRPS_{min}}$ show the highest and lowest CHIRPS values of similar periods.

ii. Vegetation Condition Index (VCI) is another commonly applied drought monitoring index. It helps to compare current NDVI values with historical values of the same seasons. The vegetation condition index is developed to detect the intensity, duration, and impact of drought (Jayawardhana & Chathurange, 2020). It is previously tested in Iran (Shahabfar, Ghulam, & Eitzinger, 2012), Kenya (Klisch & Atzberger, 2016), Ethiopia (Liou & Mehabie, 2019), and Bangladesh (Faridatul & Ahmed, 2020). It is calculated as follows.

$$\mathrm{VCI} = \frac{(\mathrm{NDVI_i} - \mathrm{NDVI_{min}})}{(\mathrm{NDVI_{max}} + \mathrm{NDVI_{min}})} \tag{12}$$

where, $\mathrm{NDVI_i}$ indicates the value of a specific pixel in that particular month of i, $\mathrm{NDVI_{max}}$ and $\mathrm{NDVI_{min}}$ shows the historically highest and lowest NDVI values of similar periods (Faridatul & Ahmed, 2020).

iii. **Normalized Difference Water Index (NDWI)** is a moisture-related index of satellite-derived index that makes use of short wave infrared (SWIR) bands to detect changes in water content and spongy mesophyll in vegetation canopies (Taloor, Manhas, & Kothyari, 2021). SWIR absorbs water better than the NIR region. Therefore, the crop with higher water content has higher NDWI values whereas stressed vegetation has negative or lesser NDWI values (Jayawardhana & Chathurange, 2020). Mainly because of its sensitivity to vegetation aridity and drooping, it's sometimes considered as a better indicator of drought conditions than NDVI (Gu, Brown, Verdin, & Wardlow, 2007).

$$NDWI = \frac{(\rho_{NIR} - \rho_{SWIR})}{(\rho_{NIR} + \rho_{SWIR})} \tag{13}$$

iv. **Normalized Difference Drought Index (NDDI)** is generated by using NDVI and NDWI values using the following equation (Gu, Brown, Verdin, & Wardlow, 2007). NDDI is among the non-temporal drought indices because it is calculated using one-time observation of the particular bands (Jayawardhana & Chathurange, 2020).

$$\mathrm{NDDI} = \frac{(\mathrm{NDVI} - \mathrm{NDWI})}{(\mathrm{NDVI} + \mathrm{NDWI})} \tag{14}$$

v. **Normalized Difference Latent Heat Index (NDLI)** is a recently developed index to quantify latent heat and indirectly assess the photosynthetic needs of plants.

The amount of energy absorbed/ released when a substance changes in phase from one to another state without changing its temperature is referred to as latent heat flux (Le, Chien, & Liou, 2019). The appearance of water content in materials is an essential component to estimate latent heat flux and phase change of the water process.

$$\mathrm{NDLI} = \frac{(\mathrm{GREEN} - \mathrm{RED})}{(\mathrm{GREEN} + \mathrm{RED} + \mathrm{SWIR})} \tag{15}$$

The green band represents the chlorophyll content in the vegetation and water, red band indicates absorption of pigmentation, where healthy vegetation has strong pigmentation absorption. SWIR band is sensitive to water content, both in vegetation and in soil. NDLI values range between -1 and +1, where positive values indicate areas with satisfactory water content with latent heat (Pahar, Paembonan, & Soma, 2021).

When the soil moisture is dried due to lack of rain or sufficient drainage, the upper surface of the soil will dry out and latent heat flux will be controlled by water availability. This leads the values to be close to zero or sometimes even negative (Le, Chien, & Liou, 2019).

2.6. Conceptual Framework

The conceptual framework of this thesis depicts the fundamental connections between the thesis's major components. It illustrates the temporal components of land use dynamics and drought mapping, as well as the elements that most influences suitability for cropland. At a glance, the generic overview of data processing inputs, processes, and outputs is comprised.

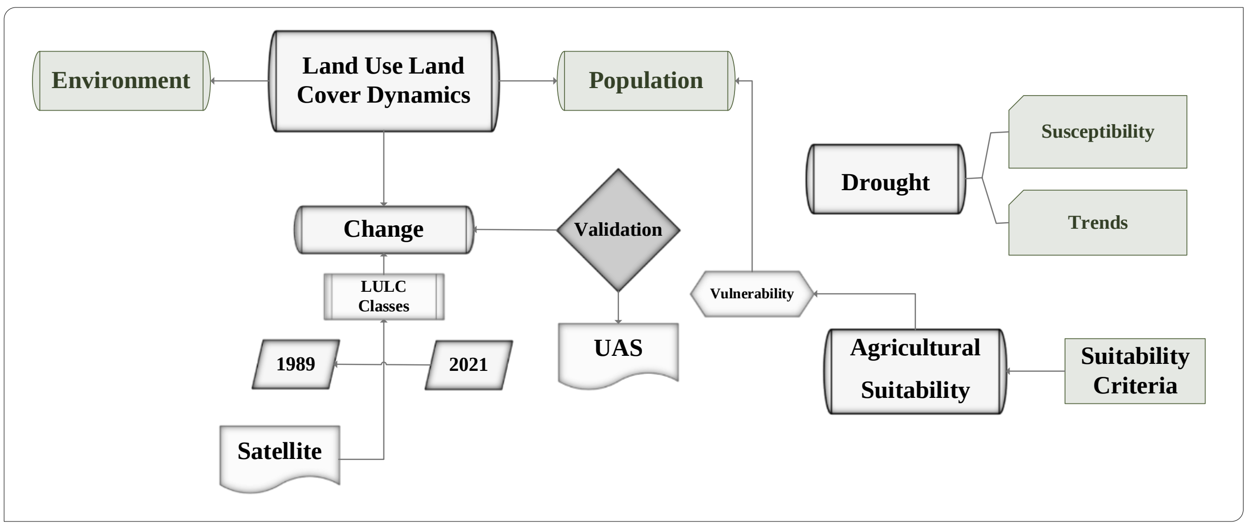

Figure 1: Flow Chart of Conceptual Framework

3. CHAPTER THREE: MATERIALS AND METHODS

3.1. Description of the Study Area

3.1.1. Location

Basona Werana Woreda is located between 9°27'48.08''N - 10°0'29.29''N, and 39°15'35''E, and 39°44'19''E. It was formerly named DebreBerhan Zuria (Greater DebreBerhan). The Woreda is among the 10 Woredas of North Shoa Zone in Amhara National Regional State. The total area of the Woreda covers 1,399 square kilometers, i.e., approximately two times the size of Addis Ababa (Ayele, 2009). The Woreda is mainly delineated by natural features such as banks of rivers.

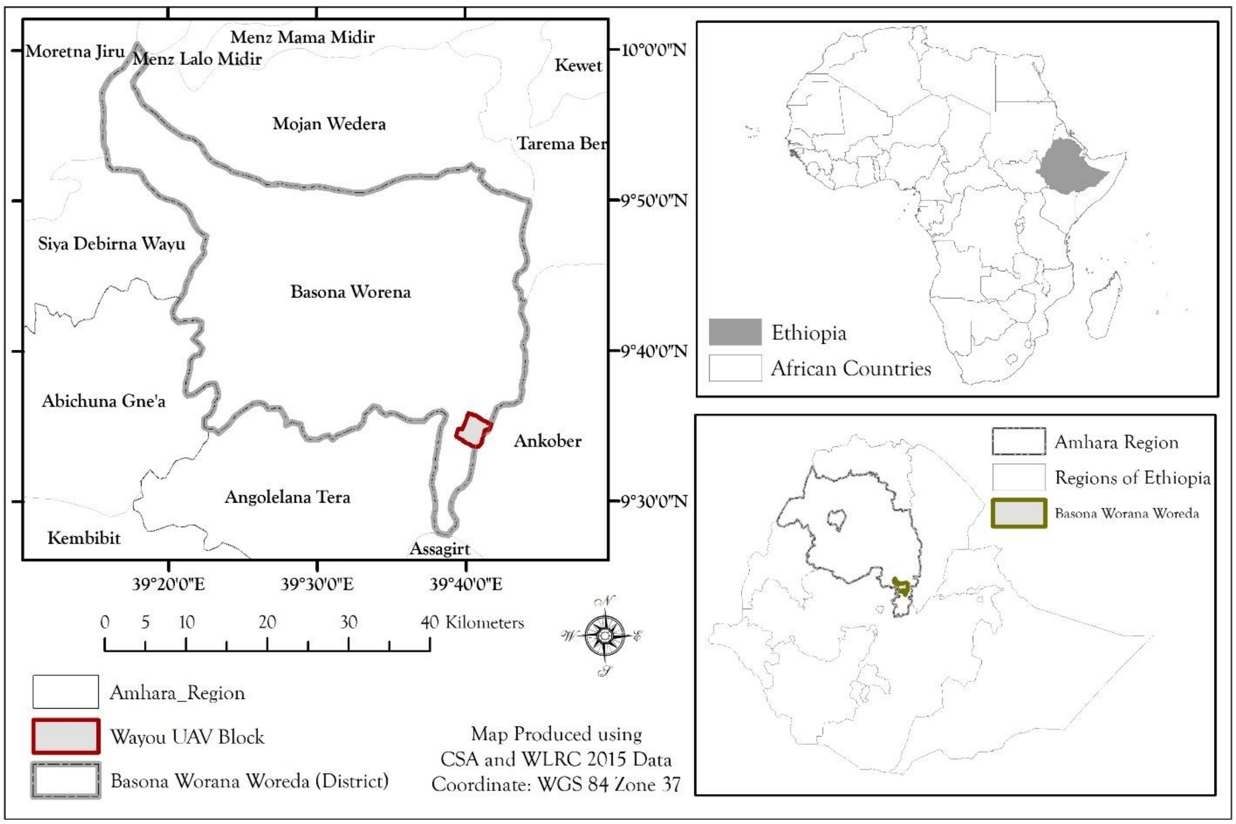

Figure 2: Location Map of Basona Worana Woreda

For several GIS, and Remote Sensing based studies, some researchers such as (Angessa, Lemma, & Yeshitela, 2019), (Damtea, Kim, & Im, 2020) use watersheds to delineate the study area, others like (Dinku, 2017) use local administrative districts for similar purposes. The researcher chooses the latter method, and the most recent administrative boundary served as a delineating extent.

3.1.2. Topography and Drainage

The shoan plateau, also called central highlands, covers at least 11% of the area of the country, bounded by the rift valley in the east, and southeast, by Abay gorge in the north, and northwest, and the Omo gorge in the south, and west. Basona Werana Woreda is situated among this highland-dominated area (Mekonnen, Gebremedhin, Assefa, & Moreda, 2019).

The altitude of the Woreda ranges from 1554 to 3660m (WLRC, 2014). Most of the Woreda has rugged topography, and it's by far unlikely to find larger areas with flat topography. Because of the topography, the rivers flow mostly from a southeastern direction to a northwestern direction in a similar fashion.

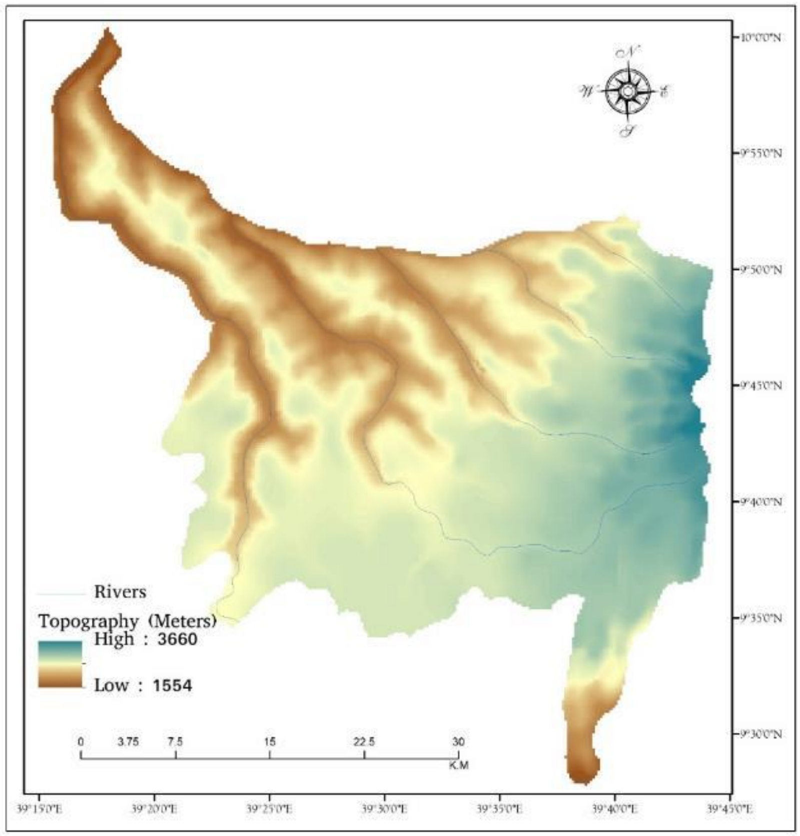

Figure 3: Topography Map of Basona Werana Wäräda

This district is located at the eastern tip of the Abbay basin, where the Awash River basin continues to shower the rest of the zones in this Woreda. The Abbay basin completely encloses more than one-fifth of the Woreda. According to the hydrological mapping of (WLRC, 2014), only the southernmost tip of Basona Werana, including Wayou, Dobele, and Dibut Kebeles, is part of the Awash watershed.

3.1.3. Climate

The agro-climatic characteristics in Basona Worana Woreda are designated as moderate to cool sub-moist mid-highland. Annual rainfall varies from 467 mm to 1068 mm with 874 mm long-term average (Ayele, 2009). The researcher's GIS-based rainfall estimates from 1984-2021 using (CHIRPS, 2021) approximate rainfall dataset ranges between 309mm and 1308mm with an average of 947 mm long term average. Among this 20% falls during the non-rainy season, while 80% falls during rainy seasons.

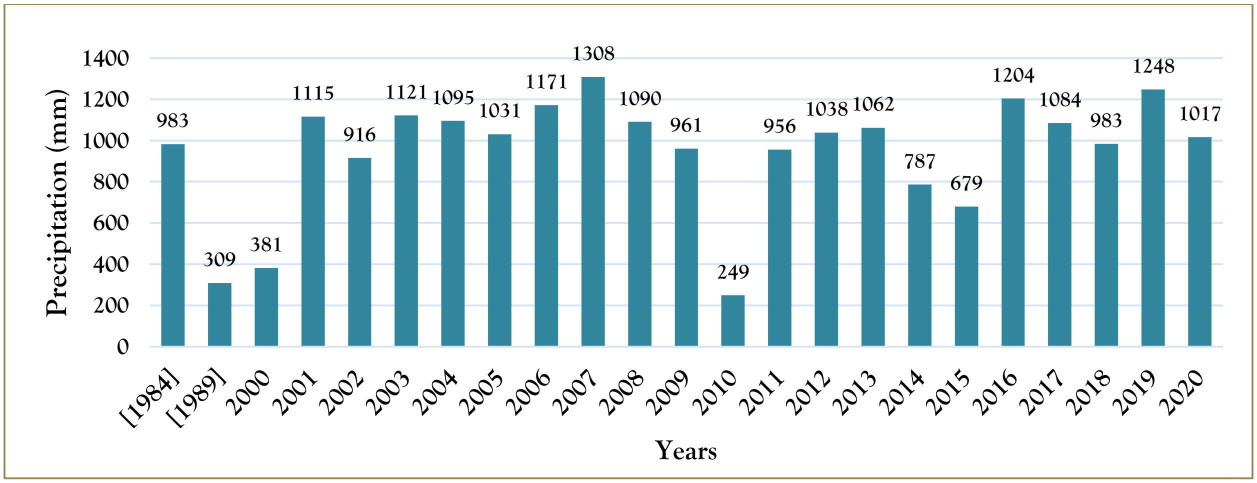

Figure 4: Annual Precipitation of Basona Werana (24 Yrs. Average)

The two rainy seasons are the short rains of Belg (February to April) and the long rain of Meher (June to October). While the Woreda mostly receives monomodal rain, some parts receive bi-modal rainfall. These rainfalls occur from June through September, and the short rainfalls from February to May (Tizale, 2007; Ayele, 2009). The researcher prepared the following bar chart using imagery-based (CHIRPS, 2021) monthly precipitation data for 24 years.

Figure 5: Wayou Kebele, Basona Worana Woreda. Picture by Thomas Dubois)

For the most part, the Woreda is hilly or mountainous along with some plains. The study site is part of the central Ethiopian highlands. Central highlands have an altitude range between 1,500 to 3,500 m.a.s.l.

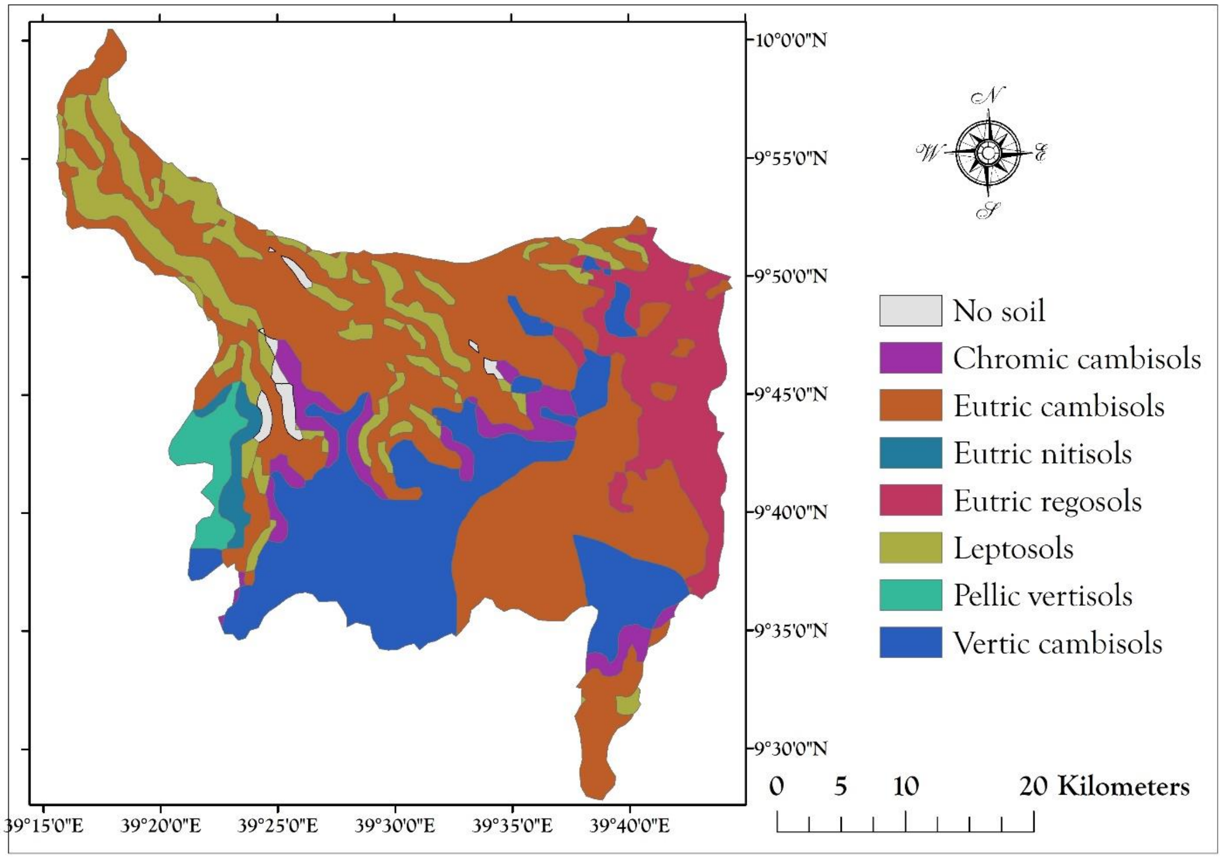

Figure 6: Soil Types (Basona Werana Woreda)

According to the most widely used ethiogis based (WLRC, 2014) data major soil types include vertic cambisols, eutric cambisols, eutric regosols and leptosols. The agro-ecological zones range from *dega*, *woyina dega, and wurch*. These ecological zones share 50%, 48%, and 2% of the total area of the Woreda respectively. Most of the Woreda is part of the Abay river basin. Only the southeastern parts, where Wayou kebele is located, are part of the Awash river basin (Tizale, 2007; Fiker, 2020; Hana, 2019; Ayele, 2009).

In recent years, the demand for short matured, and drought-tolerant improved crop varieties are increasing. The Woreda has a considerable cattle and poultry population. The dominant forest species include *Croton macrostachyus* (Bisana), *Podocarpus falcatus* (Zigba), *Cordia africano*

(Wanza), *Grevillea robusta*, *Rhammus prinoides* (Gesho), *Eucalyptus* (Bahirzaf), and *Junipers* (Tigabie, Legesse, Chanyalew, Getachew, & Wondale, 2018).

3.1.4. Population

Basona Werana Woreda has a population of 140,386 according to the (CSA, 2017) national census, and a recent population projection made by (Qotera.org, 2021) claims the Woreda to have 149,728 people in 2021. Rural areas in this particular district are home to approximately 95% of the total population. North Shoa Zone, which includes this Woreda, has a total population of 2,300,951 people with a total area of 15,955 km^2. According to the *Woreda* administration, Wayou Kebele, the study area, has a population of 4,547. According to the Woreda office of agriculture, Basona Werana Woreda has 31,110 total households. In the years 2019-20 Ethiopian budget year around 1,252 households have received food aids from the government. Their livelihood is highly attached to natural resources, where farming and charcoal are the major sources of income. The major growing crops include teff, wheat, barley, faba bean, and field pea (Ayele, 2009; CSA, 2017; Fiker, 2020).

3.1.5. Rationale for selection of Study Area

Basona Werana district has been selected as a study site from the central highlands of Ethiopia based on the following pragmatic reasons.

- The geographic diversity of the agro-ecological setting in the Woreda representing the central highlands of Ethiopia which is also known as the Shoan plateau
- The convenience of available data for GIS-RS based assessment
- The researcher's engagement in the UAV based mapping test project deliberated by the MoA as an associate of the Geospatial Information Institute technical team
- The prior photogrammetry, remote sensing, and GIS-related experience and a motivation to apply these skills in the development endeavor

3.2. Data Sources

The researcher had a field visit and systematic observation of the area during the acquisition of the UAV data. Secondary data sources are cited from relevant books, articles, international journals, reports, thesis papers, and government offices. The previous year's crop data for Basona Werana is obtained from the North Shoa office of Agriculture. A long time series of precipitation data is acquired and adjusted to the area of interest from the Climate Hazards Group InfraRed Precipitation with Station data, African monthly data available at (CHIRPS, 2021).

Landsat is the only operational medium spatial resolution satellite that provides long-term data for the last 45 years (Thonfeld, Steinbach, Muro, & Kirimi, 2020). For spatial analysis, the following data sources are used. Landsat images were obtained from USGS https://earthexplorer.usgs.gov/, and Sentinel 2A images were obtained from https://scihub.copernicus.eu.

Time series Landsat 7, 4, and 5 with 30m spatial resolution used for change detection, and classification purposes. Sentinel 2A imagery with B, G, R, NIR, IR, MIR spectral bands of 10m, and 20m spatial resolution have also been used in the classification for comparison, and training sample collection. These have been accessed and downloaded from earth explorer, and the ESA Sentinel Data Hub respectively. These satellite images were chosen for their minimal cloud cover as well as temporal proximity to each other.

Table 2: Data Sources (Images)

No.	Image	Sensor	Acquisition Date	Path/Row	Sp. Res.	Purpose	No. of Bands
1	Landsat	LT05	1989-01-29	168/53	30m	Multiuse	8
2	Landsat	L7_ETM	2000-02-05	168/53	30m	Multiuse	8
3	Landsat	LE07	2010-01-15	168/53	30m	Multiuse	8
4	Landsat	LC08	2021-01-05	168/53	30m	Multiuse	8
5	Landsat	LC08	2018-01-13	168/53	30m	Drought Map	8
6	Landsat	LC08	2019-01-16	168/53	30m	Drought Map	8
7	Landsat	LC08	2020-01-19	168/53	30m	Drought Map	8
8	UAS IMG	Sony	2020-07	-	0.08m	Assessment	3
9	Sentinel	2A	2020-10-26	-	10m	Comparison	12
10	Sentinel	2A	2021-03-29	-	10m	Comparison	12

The UAV images were captured by the planning, coordination, and execution the Ministry of Agriculture Sustainable Land Management Program (SLMP) to test an optional method for cadastral surveying, from the previously used method of aerial photography. The author of this study is also part of the collaborative team representing GII (Thomas & Meeraph, 2020).

Table 3: UAV Mounted Camera Information

Camera Name	Sony

Camera Model	DSC-RX1RM2
Focal Length	33.6177 mm
Pixel Size	4.52
Dimensions	7952*5304 pixels
Principal Center	0.016787 -0.218162 mm

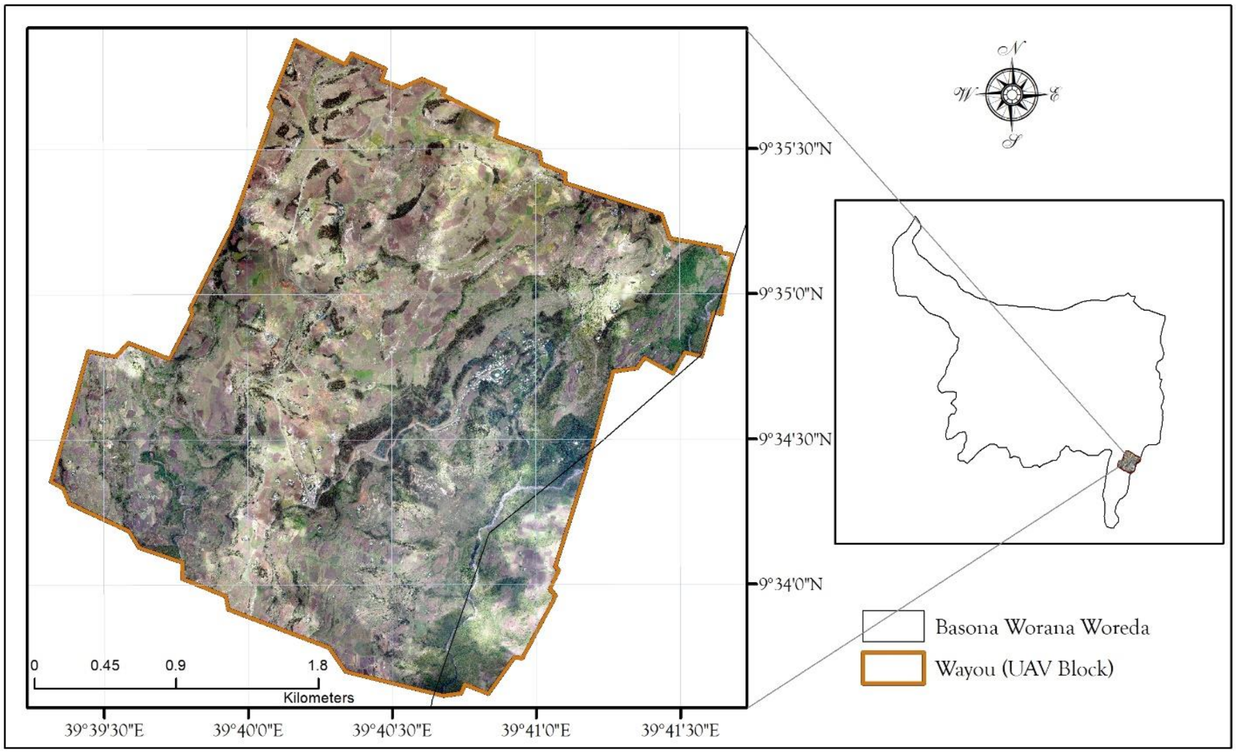

Figure 7: UAS block (Wayou Kebele)

UAV imagery of 420 images acquired with 8cm Ground Sample Distance (GSD), its photogrammetrically produced DTM of 0.35m grid and orthomosaic of 0.16m spatial resolution. It was captured on July 2020 in the mid-day. The time of the day the image is captured is relatively ideal for getting an ideal image in high relief, and tall vegetation areas (Thomas & Meeraph, 2020). It is recommended that mid-day flights are ideal in such areas with hilly mountains. Weather effects and strong winds can prevent smaller UAV platforms from appropriately operating even in ideal daytime conditions (Gray, et al., 2018). After a series of tests, this trip was completed successfully with clear images.

		
Landsat 8 Imagery	Sentinel 2A Imagery	UAV Imagery
30 meters	10 meters	0.08 meters

Table 4: Comparison of Landsat, Sentinel 2A, and UAS images of the same area around Wayou Kebele, Basona Worana District

The UAV-based imagery covered a part of Basona Worana Woreda – a small area which is called Wayou kebele. The 419 individual JPEG true color UAV-based images, which are used in this study, covers 10 km^2 or 1000 hectares. To get enough overlap, a forward overlap of 80, and a side lap of 75 are used for the UAS block. Other details are available in Appendix 1: Description of UAV flight at Wayou Kebele.

3.3. Data Processing and Analysis

All images used the UTM Zone 37 within the WGS 84 datum. Before actual processing, image-enhancing, and noise-reduction techniques were applied for the Landsat images.

Table 5: Features of imageries used in the research

Features	**Descriptions**
Spectral	Blue, Green, Red, Near-infrared, Shortwave-infrared
Spectral Indices	NDVI, TNDVI, SAVI, VARI, VNDVI, RDVI
Topographic	Slope, altitude, aspect
Drought Indices	NDWI, NDLI

The use of ground control points can effectively mitigate the errors induced by the UAV system's inferior GPS quality (Solazzo, Sankey, Sankey, & Munson, 2018). A total of 8 control points and 4 checkpoints were used to meet the required accuracy.

The principal component analysis is applied to satellite images for easier image analysis further tasks. The satellite imagery has been clipped using the currently operational Woreda administrative boundary. The UAV image had a black background besides the main area of interest area, where the software considers it as data. It's clipped out of the main area, and ready for further analysis.

3.3.1. Sampling Method

A 10-11 years' gap is applied to satellite images of 1989, 2000, 2010, and 2021 to show a detailed account of the historical land-use/ land-cover of the Woreda. This is based on the availability of the data, and the long list of works, such as (Dinku, 2017; G/Michael, 2021) that use similar classification period gaps. The satellite imageries from 1984, 2018, 2019, and 2020 were additionally used in drought mapping to reflect Ethiopia's historically driest the year 1984 as well as current vegetation conditions.

As a general "rule of thumb", the minimum sample size for training samples for each LULC class, necessary for 85 and 90% accuracy requires 20, and 30 samples. To achieve a satisfactory result 50 samples per land-use class is required (Bewket, Gessesse, & Bräuning, 2015). For error estimation, any sample size less than 50 will be unsatisfactory. If it is indeed collected though, the area should not be larger than 4,000 km^2 and has less than 12 land-use classes (Lillesand, Kiefer, & Chaipman, 2008). A stratified random sampling scheme is used from each land-use land-cover unit, as recommended by (Bewket, Gessesse, & Bräuning, 2015).

As it's applied by (Worku, Mekonnen, Yitaferu, & Cerdà, 2021) Google Earth Pro is also used to support the signature collection process in areas where other sources couldn't ascertain the classes. The rich imagery data of the consecutive year's archives of Google earth couldn't be assumed as naïve, and inappropriate all the time in times where verifications at each stage are desired.

3.3.2. Image Classification Methods

Image classification is important to convert image data into thematic data. There are different classification methods, and related algorithms in the life cycle of remote sensing (Genemo, 2012; Sharma, Hara, & Hirayama, 2017; Dinku, 2017). Image Classification approaches are classified as supervised, and unsupervised (the most widely applied broad classification); parametric, and non-parametric, hard, and soft (fuzzy) classification, or per-pixel, sub-pixel, and pre-field (Damtea, Kim, & Im, 2020).

The study dominantly uses a quantitative approach to analyze the spatial attributes from a time series satellite imagery and comparing the results with a relatively smaller UAS based block. Eight main land-use classes have been identified in the study area.

Table 6: Description of Various Land Use Land Cover Types applied

LULC Class	Description	Image
Forest	Tree-covered areas having a closed canopy. This encompasses both natural and planted forests.	
Cultivated Land	Areas cultivated by Teff, Barley, Wheat, Faba bean, Field pea, Lentil, Chickpea, etc.	
Grassland	Areas covered with permanent grass and used as communal grazing land.	
Shrub and Bush	Areas covered with bushes, shrubs and scattered trees, and grasses.	
Built-Up and Settlement	Areas occupied by rural or urban houses, buildings, and industrial uses	
Bare land	Areas that have been cleared of all vegetation, including bare rocks.	
Waterbody	Areas covered by water either by a lake or a river	
Wetland	Marshy areas with grasses as the dominant vegetation. They can be found along with ponds and flood planes.	

The most widely used software packages of Erdas Imagine® and ArcGIS® along with ArcGIS Pro were used. These are also used by (Worku, Mekonnen, Yitaferu, & Cerdà, 2021; Bewket, Gessesse, & Bräuning, 2015; Damtea, Kim, & Im, 2020). ArcGIS® 10.8 is used for spatial analysis, geostatistical analysis, and mapping, Erdas Imagine® is used for image processing, vegetation mapping, and change detection, whereas ArcGIS Pro® is used for some indices and further visualization purposes. The freely available QGIS was also tested for its classification results, but the results have become tricky and not employed at all. The UAS imageries were initially processed using Skyphoto and further verified by the researcher using UAS Master.

Table 7: Software applications used to conduct the study

Software	Purpose used	References
ArcGIS®	Image Classification, Geostatistical analysis, drought mapping, land suitability weighting, etc.	(Worku, Mekonnen, Yitaferu, & Cerdà, 2021; Thonfeld, Steinbach, Muro, & Kirimi, 2020; Angessa, Lemma, & Yeshitela, 2019; Mostafiz, Noguchi, & Ahmed, 2021)
Erdas Imagine®	Image Enhancement, Principal component analysis, Vegetation Mapping, change detection	(Worku, Mekonnen, Yitaferu, & Cerdà, 2021; Bewket, Gessesse, & Bräuning, 2015; Damtea, Kim, & Im, 2020; Genemo, 2012; Taloor, Manhas, & Kothyari, 2021)
ArcGIS Pro®	Correlation Graphs, RGB based vegetation indices, crosschecking of ArcGIS results	(Gray, et al., 2018)

A random forest classification algorithm, which is used in various literature (Solazzo, Sankey, Sankey, & Munson, 2018; Belgiu & Csililik, 2014; Sharma, Hara, & Hirayama, 2017; Thonfeld, Steinbach, Muro, & Kirimi, 2020) is employed for classification. It was chosen after a series of preliminary examinations, and comparisons with various algorithms including Maximum Likelihood, and Vector Machine classification for similar test areas.

3.3.3. Vegetation and Drought Mapping Methods

The vegetation indices are chosen and categorized based on the groupings used by (Barati, Rayegani, Saati, Sharif, & Narsi, 2011) in the following category lists.

- Conventional ratio, and differential indices NDVI
- Correlated, and Modified indices RDVI, TNDVI

- Soil Reflectance Adjusted Indices SAVI, MSAVI
- Visible range ratio, and difference index VARI
- Drought Assessing Indices VCI, NDDI

For computing vegetation indices NDVI, RDVI, SAVI, TNDVI Erdas Imagine® software is used. On the other hand, ArcGIS Pro® has been used to process MSAVI, VARI. To cross-check its accuracy, a specific model for VARI is established in Erdas Imagine® produced by ArcGIS Pro®. It's customized by the researcher using the spatial model editor in Erdas Imagine® and visualized in the appendix section 1. Similarly, indices created by Erdas Imagine® are crosschecked using ArcGIS 10.8.

3.3.4. Land Suitability Analysis through GIS Overlay

A weighted Overlay function of ArcGIS, which is an intersection of standardized and differently weighted layers, is used to generate the unified final land suitability maps. It overlays various criteria among with their percent of influence for the overall results. The scale value, similar to ranking, is specified by the evaluation scale setting. Constraints or criteria were used for the suitability analysis. These are elevation, slope, soil type, SAVI, NDWI, and river proximity. Elevation plays an important role in defining plant cover. It is also associated with changes in temperature, particularly in the highlands. In higher elevations, the complications in rainfall amounts and soil erosion are intensified (Mostafiz, Noguchi, & Ahmed, 2021).

3.3.5. Accuracy Assessment, and Data Validation

The problem of geographic inaccuracy has always been a concern for many researchers in various contexts (Kusumo, Reckien, & Verplanke, 2019). As (Lillesand, Kiefer, & Chaipman, 2008, p. 585) noted that "…a classification is not complete until the accuracy of the classification is determined". Accuracy assessment starts by defining the geographic extent of the study area from which the thematic layers are extracted (Bewket, Gessesse, & Bräuning, 2015).

Error matrix or confusion matrix or contingency table is the most appropriate validation tool for accuracy of remotely sensed data classification and error reporting. In line with this, univariate statistical measures of overall accuracy, user's accuracy, and producer's accuracy are by far the most well-established methods of classification accuracy assessment (Thonfeld, Steinbach, Muro, & Kirimi, 2020). Several pieces of research have included some or all of these accuracy verification methods for their classification results (Solazzo, Sankey, Sankey, & Munson, 2018; Gray, et al., 2018; Dinku, 2017; Genemo, 2012; Zhao, et al., 2019; Kusumo, Reckien, & Verplanke, 2019; Bewket, Gessesse, & Bräuning, 2015; Worku, Mekonnen, Yitaferu, & Cerdà, 2021; Damtea, Kim, & Im, 2020). These are applied in this thesis along with the Kappa Statistics. A detailed description of Kappa values is stated by (Angessa, Lemma, & Yeshitela, 2019) while sample size selection per class is discussed by (Lillesand, Kiefer, & Chaipman, 2008).

3.4. Analytical Framework

The analytical framework presents the following technical procedures for assessing land-use dynamics, drought susceptibility, and agricultural suitability.

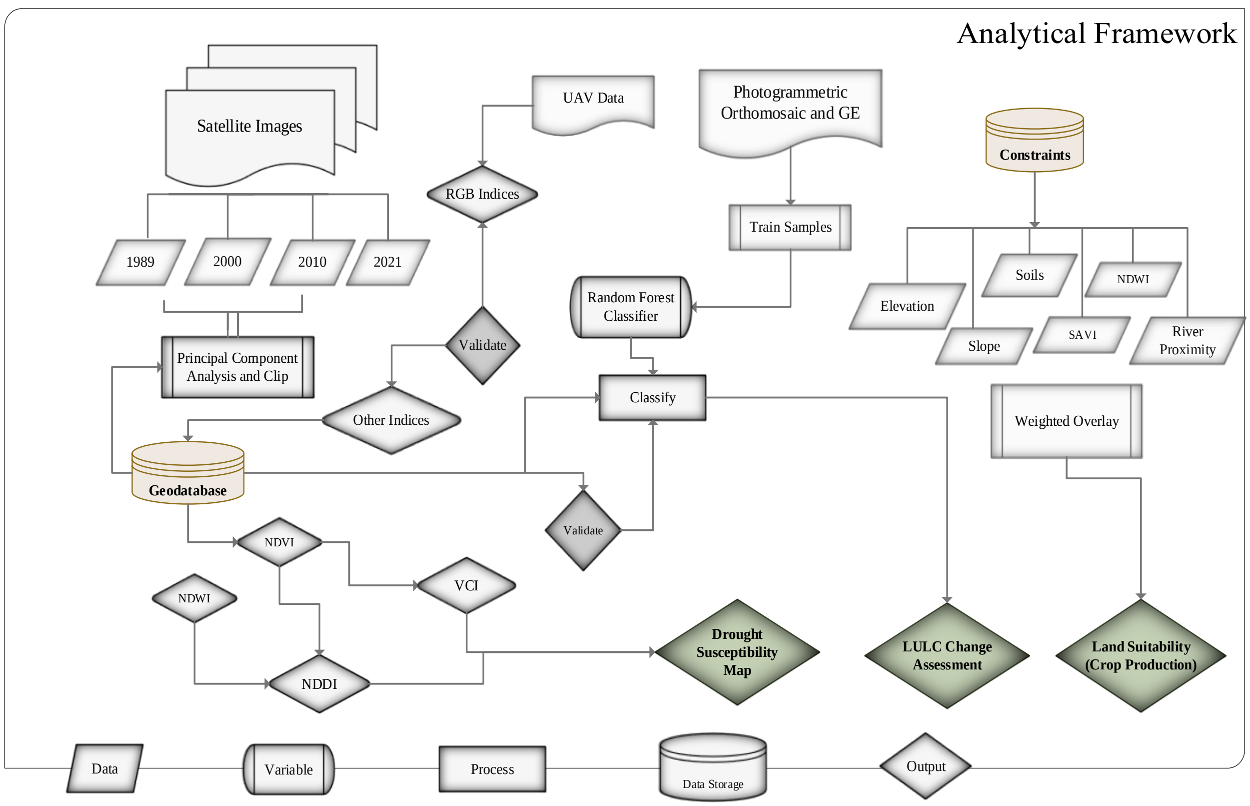

Figure 8: Flow Chart of Analytical Framework

4. CHAPTER FOUR: RESULTS AND DISCUSSION

4.1. Results

4.1.1. Classification Accuracy Assessment

The post-classification accuracy assessment has resulted in an overall accuracy of 86%, 84%, 79%, and 85% for the years 1989, 2000, 2010, and 2021 respectively. Their corresponding kappa statistics were 0.78, 0.77, 0.64, and 0.78 indicating a 'substantial agreement' based on (Angessa, Lemma, & Yeshitela, 2019). The producer's accuracy for Water land cover class in the year 2000 and grasslands for 2021 has been the lowest. The highest accuracy levels were achieved for grasslands in the years 2021.

The summarizes the results of the 2021 classification accuracy assessment using an error matrix.

Table 8: Classification Accuracy Assessment Error Matrix for 2021 LULC classification

Class	*For.*	*Cul.*	*Gra.*	*Shr.*	*Bul.*	*Bar.*	*Wat.*	*Wet.*	Total	User. Acc.
Forests	19	0	0	1	0	0	0	0	20	95%
Cultivated	2	246	0	17	1	3	2	1	272	90%
Grassland	0	1	5	2	0	0	0	2	10	50%
Shrub & Bush	3	4	0	64	1	0	0	0	72	89%
Built-up & Sett.	0	2	0	0	7	1	0	0	10	70%
Bare land	0	1	0	0	0	9	0	0	10	90%
Water body	0	3	0	2	0	0	5	0	10	50%
Wetlands	0	3	0	0	1	0	0	17	21	81%
Total	24	260	5	86	10	13	7	20	425	0
Prod. Acc.	79%	95%	100%	74%	70%	69%	71%	85%	0	**88%**

The kappa statistics result for 2021 appears to be 0.78. Based on the error matrix of 2021 the producer's accuracy for; Forests (79%), Cultivated land (95%), Grassland (100%), Shrub, and Bushes (74%), Built-up, and settlement (70%), Bare land (69%), Waterbody (71%), and Wetlands (85%). Their omission errors are obtained by deducting from 100% where bare land has the highest (31%), and grassland has the lowest – with no omission error. The user's accuracy, on the other hand, for; Forests (95%), Cultivated land (90%), Grassland (50%), Shrub, and Bushes (89%), Built-up, and settlement (70%), Bare land (90%), Waterbody (50%), and Wetlands (81%). The commission errors range from the lowest, forest 5%, and 50% for water bodies. The confusion occurred on the water body class because of the swift seasonal fluctuation of water-covered areas, and the reflectance value shifts on previously swampy areas to other types of similar land-cover classes. The confusion matrix for 1989, 2000, and 2010 are presented in the appendices section.

As recommended by (Gray, et al., 2018) a total of 50 or more samples per class, i.e., 425 points were collected and verified for their class accuracy using digital globe base maps, and aerial photos-based orthomosaics for accuracy assessment. In few instances, this verification is compromised with the digital globe data where there exist horizontal shifts compared to the mosaics in few areas.

The 1989, and 2000 data accuracy assessments are done using digital globe GE images. As the resolution of the 1989 image was course, there appears some ambiguity in the assessment. To reduce this gap, a comparison is made with the disparity brightness values of unsupervised classification.

4.1.2. UAS Based Accuracy Assessment

This piece of literature tries to validate satellite-based analysis through UAS based images. It is done for further cross-checking the conventional accuracy of the classification and vegetation indices. It should be understood as a supplementary assessment tool for classification accuracy. The UAS Based valuation is conducted for both Landsat LC08, and Sentinel 2A images (only used for this comparison) of the same area, i.e., Wayou kebele of Basona Werana Woreda in different scenarios.

Note: the discrepancy between scenarios 1, and 2 lies in the timing of the clipping, one is performed before classifying the input image, and the next is clipping the classified image itself.

4.1.2.1. Scenario I

Classification of Landsat LC08, and Sentinel S2A images that are clipped for Wayou block based on the training samples collected from the UAS image. Then a comparison is made with the classification i.e., already done for the entire study area (Baona Werana Woreda). The result revealed quite different results in the Landsat, and Sentinel Wayou clipped images when compared with the main Basona Werana classification block. A 10m spatial resolution Sentinel S2A image by far showed superior overall classification accuracy i.e., 71.5% and Kappa statistics of 0.54

indicating a 'moderate agreement'. The Landsat image, on the other hand, had an overall classification accuracy of 67.54% when compared with the actual mosaic.

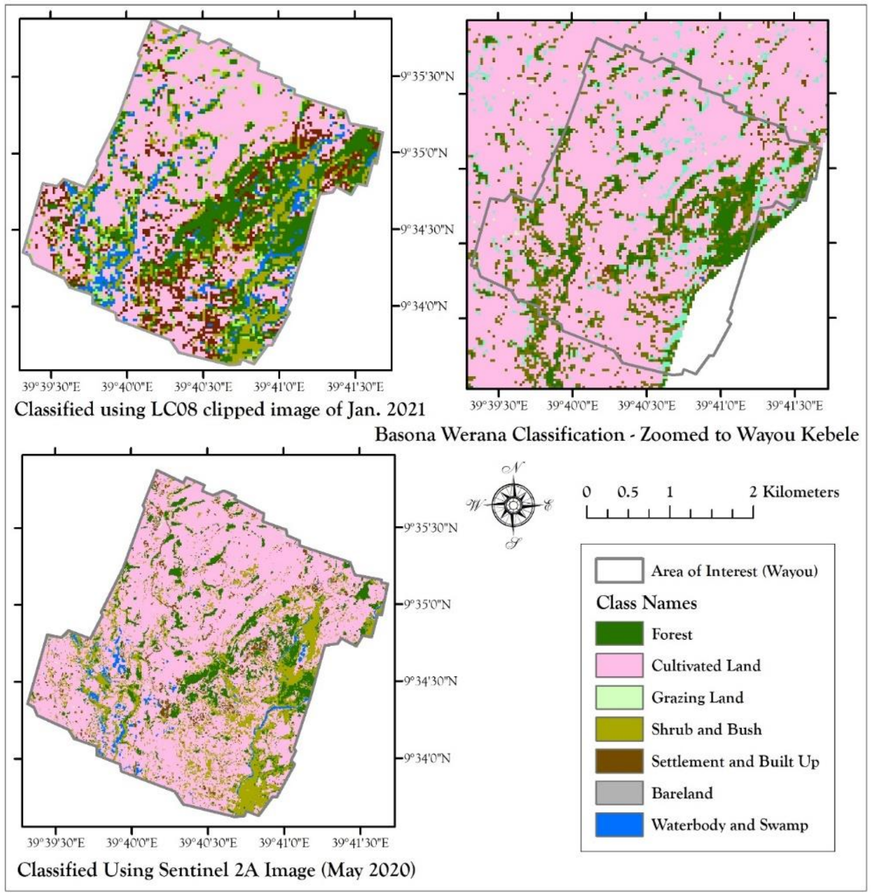

Figure 9: UAS Based Validation - Scenario 1

The Landsat 8 clipped image for Wayou doesn't produce valid, and satisfactory classification results in several instances. Its classification result doesn't contain the thematic attribute information that indicates the areal extents of delineated under each class category. One possible reason why the Sentinel 2A image produced a better result, in this case, is - its temporal proximity to the time of the UAS image taken i.e., May 2020 for the Sentinel 2A, and July 2020 for UAV image acquisition.

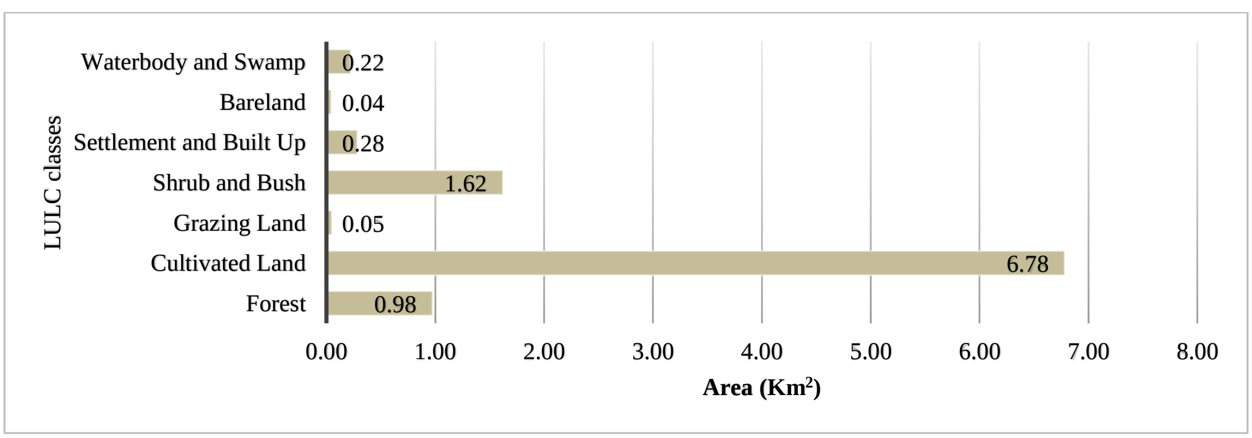

Figure 10: A graph showing Wayou Kebele UAS block LULC Status in 2020

Among the possible reasons are its continuous class changes, and non-generalizable spatial resolution available. It's also well noted that taking a training sample from a small (limited areal coverage) is by far disadvantageous to obtain a sufficient training sample as well as representing various types of land-uses for better classification.

4.1.2.2. Scenario II

Clipping from the classification raster data of 2021 of Basona Werana for Wayou UAS image covered area. Collecting accuracy assessment points from the clipped 2021 classification of Landsat image, and ground-truthing with the mosaic data of UAS image.

The clipped classification raster is used to create the accuracy assessment points. However, it has failed to obtain the necessary points with several attempts to apply different parameters. Thus, several tests were made to get sufficient points, and a total of 15,000 accuracy assessment points were generated. It uses a stratified random sampling using the whole Basona Werana classification raster data, and the points which lie inside the Wayou area of interest, a 9.3 km^2 area had 110 valid accuracy assessment points. These points have been assessed for their accuracy against the vividly perceptible mosaic image.

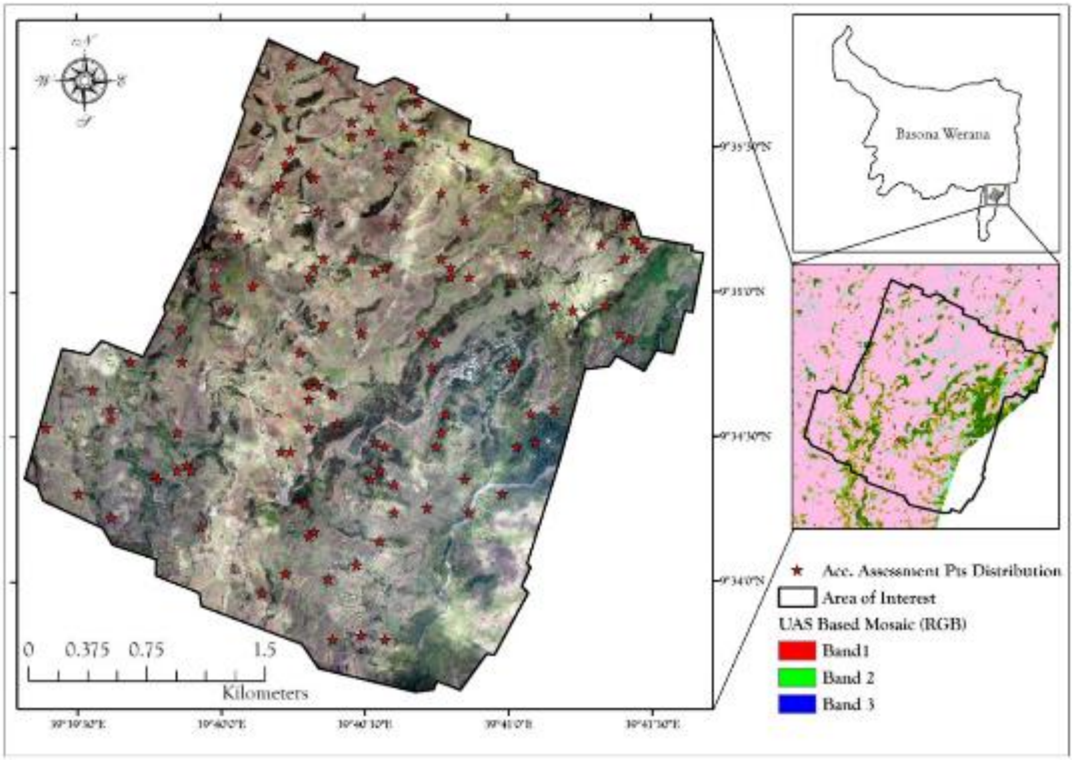

Figure 11: Distribution of Accuracy Assessment Points inside UAS Block for Scenario II Accuracy

The limitations of this assessment - minute LULC classes in Basona Werana Woreda such as small grasslands didn't fall into the coarse Satellite image haven't got a valid point to be checked and detected. Other LULC types got their share based on their proportional land coverage portions.

The result of scenario 2 UAS based accuracy assessment indicated an overall Accuracy and Kappa coefficient of 83% and 0.67 and the most widely existing land-use class, cropland, has a producer's accuracy of 100%, and a user's accuracy of 84.14%.

4.1.2.3. Scenario 3

The procedures used in this scenario include classifying the actual UAS based mosaic after resampling it to the spatial resolution of 1 meter. Then, resample the result of the 1m resolution classification result to the satellite image resolution (30m), and matching their results. For training the classifier in supervised classification, the same UAS image is used as an input.

The result wasn't satisfactory enough to test the accuracy of the satellite-based classification. The classification result has an overall accuracy of 65.85%, and a kappa coefficient of 0.55, which are below the expected accuracy level. It is based on 205 accuracy points clustered randomly across the block and checked along with the UAV high-resolution imagery. So, using this classification as a reference to check the accuracy of satellite-based classification doesn't qualify the minimum classification quality itself. Other non-dominant classes, other than cropland, are better represented by the UAS based classification.

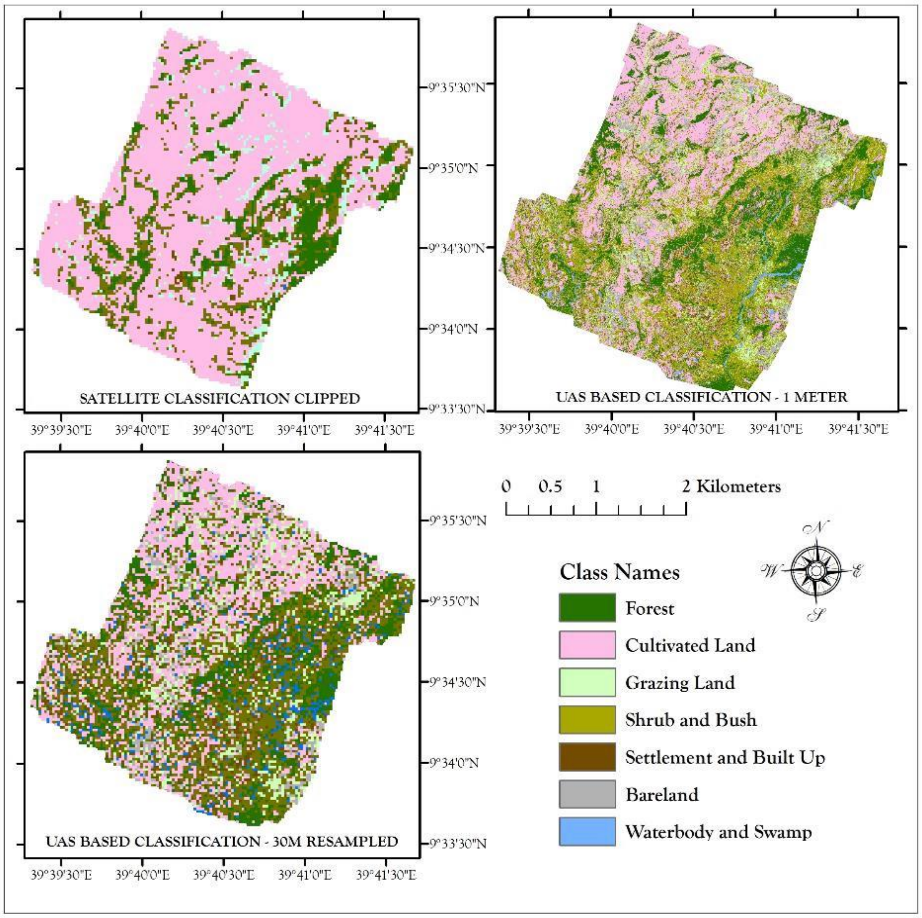

Figure 12: UAS Based Accuracy Assessment - Scenario 3

4.1.3. Land Use Land Cover Dynamics

The present LULC result entails that the dominant land-use type is by far cultivated land. It accounts for almost 3/4th of the total areal coverage of the Woreda with 74.34% of the total land cover. The rest 25.66 % of the area is shared with other 7 land-use classes namely - Shrub, and Bush (15.37%), Forests (5.2%), Built-up, and settlement (2.87%), Wetlands (1.22%), water body (0.68%), Grass or pasture land (0.30), and Bare land (0.005%). These land-use types approximately cover an area of 1,004.53 km^2, 207.78 km^2, 70.27 km^2, 38.8 km^2, 16.5 km^2, 9.26 km^2, 4.11 km^2, and 0.06 km^2 respectively.

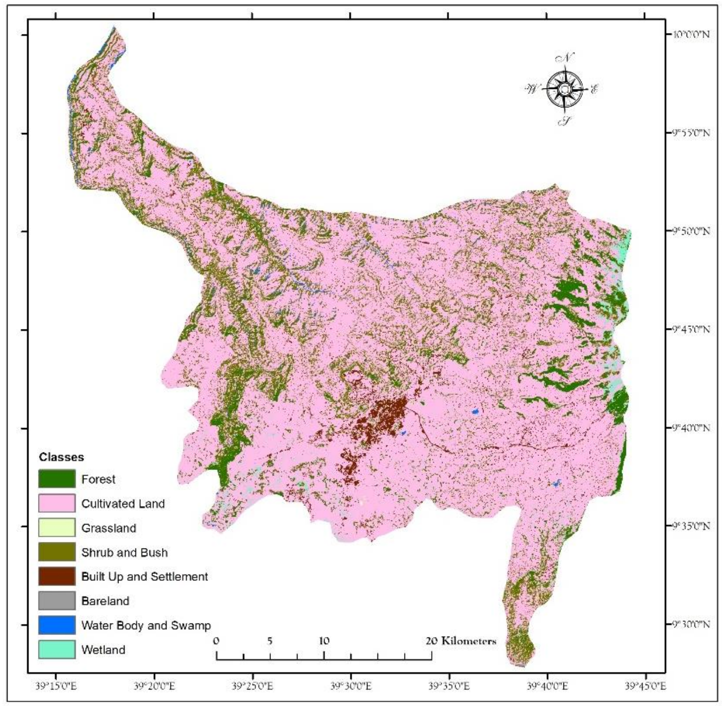

Figure 13: 2021 Land-use Land-cover Status of Basona Werana Woreda

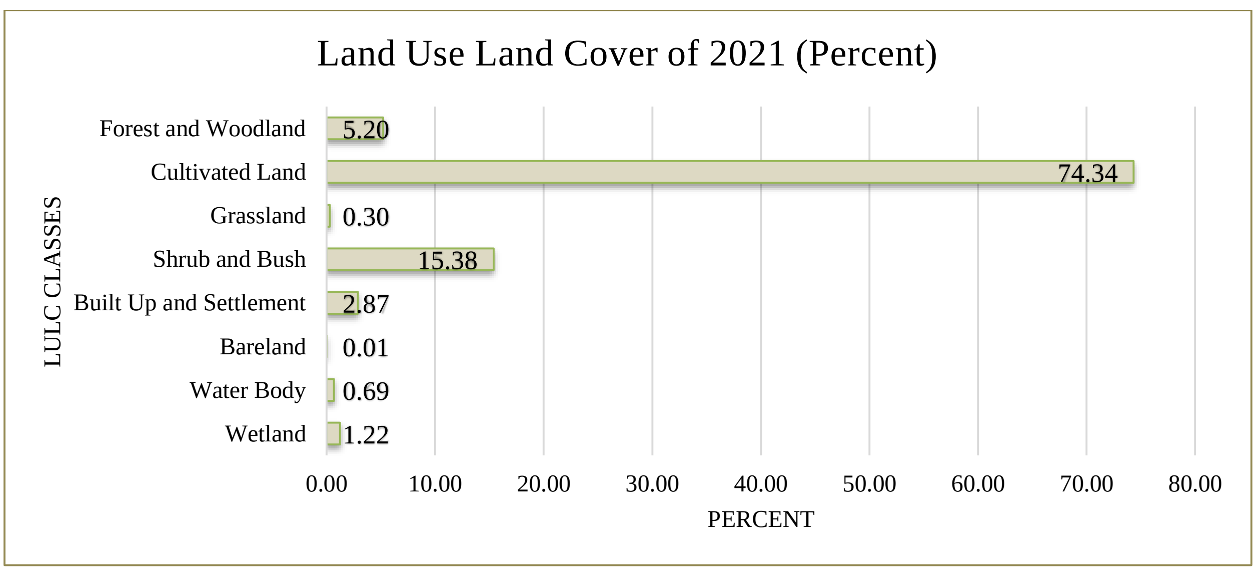

Figure 14: Bar chart of LULC 2021

The land-use dynamics in Basona Werana of the past 32 years, compared to 2021, are presented as follows.

The northwestern part of the Woreda has already been devoid of sufficient forest cover during the middle of the second half of the 20th century. It is evident in the 1989 land-use land-cover classification results. In the entire study period, a smaller portion of the land is covered with forests and plantations. The majority of the land has been intensively cultivated and has dominated the LULC of the entire district.

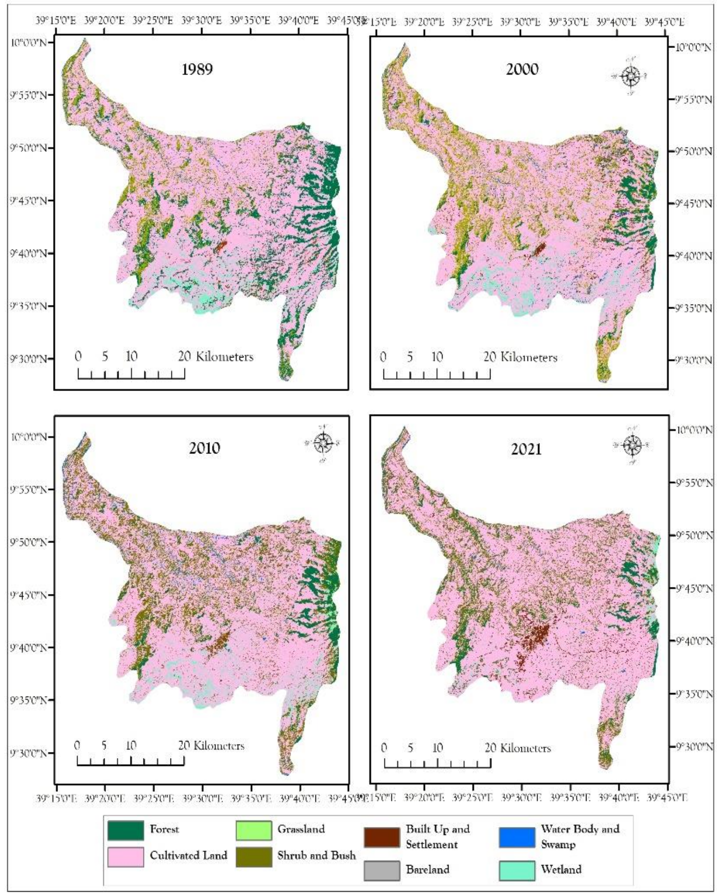

Figure 15: Land-use Dynamics in Basona Werana Woreda (1989 - 2021)

Table 9: LULC results of 1989, 2000, 2010, and 2021

	1989		2000		2010		2021	
Class Name	**Extent (km^2)**	**Share (%)**	**Extent (km^2)**	**Share (%)**	**Extent (km^2)**	**Share (%)**	**Extent (km^2)**	**Share (%)**
Forest	232.36	17.19	76.06	5.63	72.93	5.40	70.27	5.20
Cultivated Land	898.92	66.52	922.25	68.25	919.63	68.05	1004.54	74.34
Grassland	3.97	0.29	3.15	0.23	2.12	0.16	4.11	0.30
Shrub, and Bush	110.66	8.19	227.36	16.82	246.37	18.23	207.79	15.38
Built-up, and Settlement	26.11	1.93	27.70	2.05	26.51	1.96	38.80	2.87
Bare land	2.73	0.20	15.37	1.14	2.07	0.15	0.07	0.01
Water Body	5.81	0.43	30.80	2.28	16.75	1.24	9.26	0.69
Wetland	70.78	5.24	48.66	3.60	64.98	4.81	16.50	1.22
TOTAL	1351.35	100	1351.35	100	1351.35	100	1351.35	100

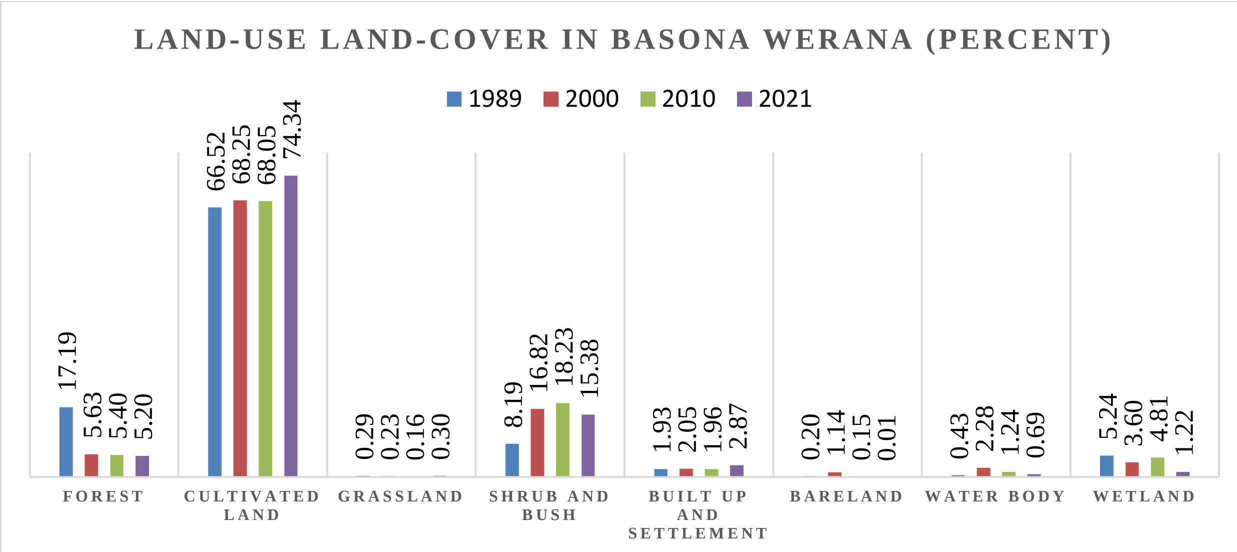

Figure 16: A bar graph of LULC in Basona Werana (%)

The major crops in the Woreda include Teff, Barley, Wheat, Faba bean, Field pea, Lentil, Chickpea which are inherently assumed as part of the LULC class 'cultivated land'. Sub-crop type classification is beyond the scope of this thesis. Nevertheless, based on the extrapolated information from (Meselu, 2019) agricultural data for the year 2016 Meher (autumn) production approximate values are calculated. Based on the presumption that similar crop types are planted - the total 1,004.53 km^2 area is perhaps shared for barley 291.82 km^2, Wheat 235.26 km^2, Faba bean 141.74 km^2, Teff 131.39 km^2, Field pea 94.43 km^2, lentil 54.85 $km^{2,}$ and chickpea 54.95 km^2.

4.1.4. Land-cover Change Trends

Utilizing equation (*1*) the land-cover changes are stated as follows. The past 3 decades have revealed that cultivated land has steadily increased and maintained a similar pace of 2.60%, -0.28%, and 9.23% every 10 years and an overall increase of 11.75%. Built-up and settlements increased by 6.08%, decreased by 4.27%, again increased by 46.35%, and an overall increment of 48.62% in the last 32 years. The biggest town in this Woreda, Debre Berhan, has the largest share of Built-up domains.

Over these years, the forest has shown a downward trend of 67.27%, 4.11%, and 3.64%, and a net of 69.76% over the study period. Wetlands have shown a decreasing trend of 31.25%, then an increase by 33.54%, and again a decrease of 74.6% resulting in a net decrement of 76.68%. Shrubs and Bushes have doubled (105.45%) in the 1990s, then increased by 8.36%, followed by a 15.66% decrease with an overall increase of 87.77% in 32 years.

Grassland has quite a small proportion among the other major LULC types. It has decreased by 20.59% and 32.95% in the first two study periods and increased by 94.34% with a net increase of 3.47% which is insignificant. Among the reasons for its smaller representation in the LULC is the characteristic appearance of shrubs and bushes classes that mostly also include grasses in between. Bare lands increased by 462.30%, decreased by 86.56%, and 96.69 in the second and third study periods to attain a net shrinkage of 97.5%. Water bodies, another insignificant class type, by far increased by 429.81% in the first study period, decreased by 45.63 and 44.70 to show a net increase of 59.29%.

A zonal change for the years 1989, and 2021 has been executed using Erdas Imagine® 2015 based on the LULC classification datasets. The results, as illustrated on Map 07, are set between 0 (no change) to 1 (complete change). Except for few places covered by forests, and shrubs, the Woreda has entirely seen some kind of LULC change.

Table 10: The Percent Increase/ Decrease of LULC classes in Basoa Werana Woreda

Land-use Land-cover Classes	Land-cover Change Quantity (Amidst each 10/11 study period)							
	(1989-2000)		(2000 -2010)		(2010-2021)		Net Period (1989-2021)	
	Change (km^2)	Percent	Change (km^2)	Percent	Change (km^2)	Percent	Change (km^2)	Percent
Forest	-156.30	-67.27	-3.13	-4.11	-2.66	-3.64	-162.09	-69.76
Cultivated Land	23.33	2.60	-2.62	-0.28	84.90	9.23	105.61	11.75
Grassland	-0.82	-20.59	-1.04	-32.95	2.00	94.34	0.14	3.47
Shrub, and Bush	116.70	105.45	19.01	8.36	-38.58	-15.66	97.13	87.77
Built-up & Settlement	1.59	6.08	-1.18	-4.27	12.29	46.35	12.69	48.62
Bare land	12.64	462.30	-13.30	-86.56	-2.00	-96.69	-2.66	-97.50
Water Body, & Swamp	24.99	429.81	-14.06	-45.63	-7.49	-44.70	3.45	59.29
Wetland	-22.12	-31.25	16.32	33.54	-48.48	-74.60	-54.27	-76.68

The Basodongora, Gudoberet, and Keyet Kebeles are among the least affected by the land-cover change. In terms of land cover types, the few spots of wetlands in Basodongora, and the forest premises in Gudoberet, and Keyet have largely been preserved. The blue shaded areas indicate the highest change values where DebreBerhan town is highlighted.

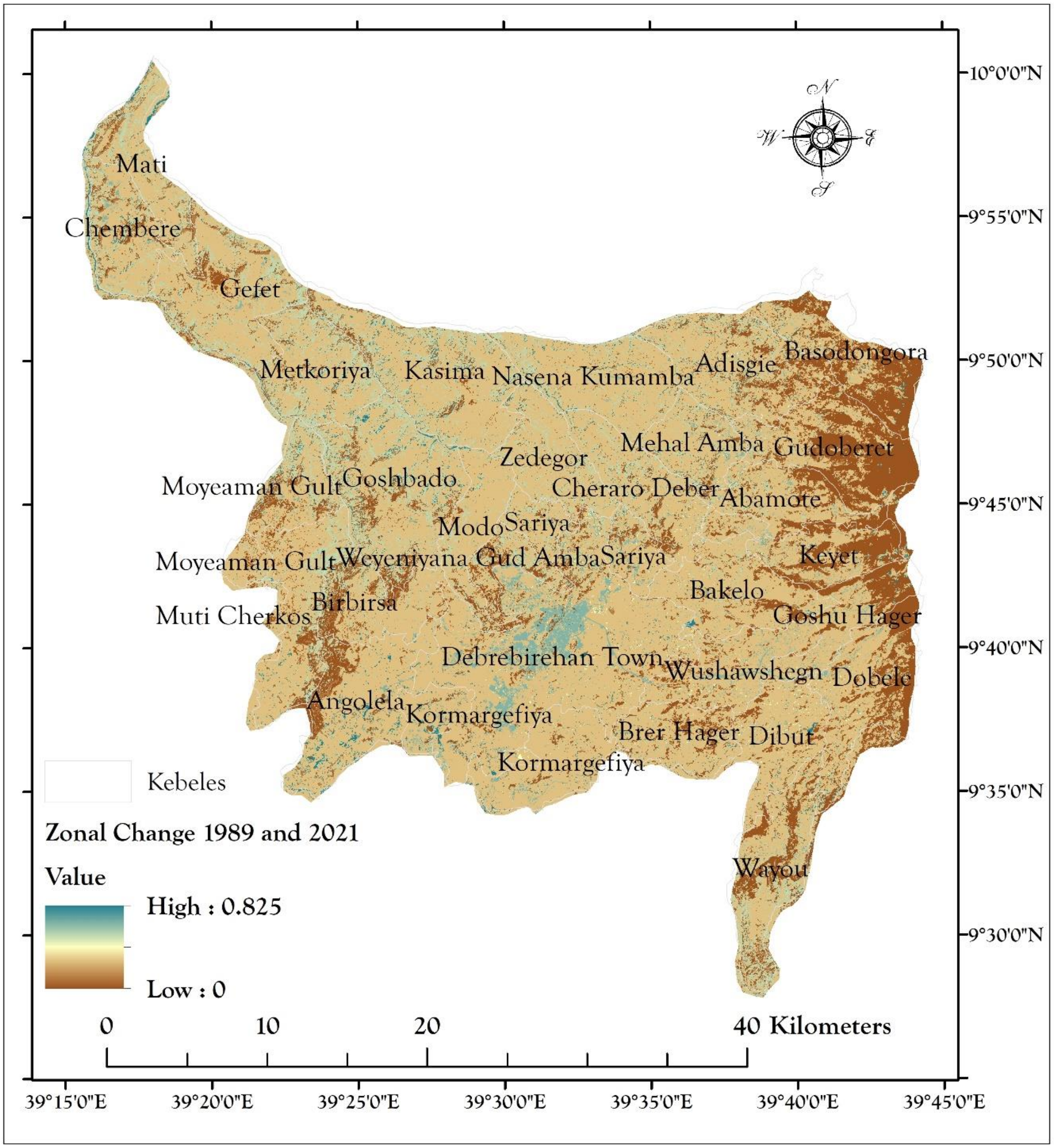

Figure 17: Zonal Change Map (1989 -2021)

Among the reasons for the smaller degree of land-cover change around few spots (highlighted in yellow) is attributed to steep slopes where agricultural activities are hardly realistic. This is true for few spots in the southwestern part of the Woreda such as Birbirsa, Angolela, and Muti Cherkos Kebeles. The forest cover and shrubs have been largely conserved over the years.

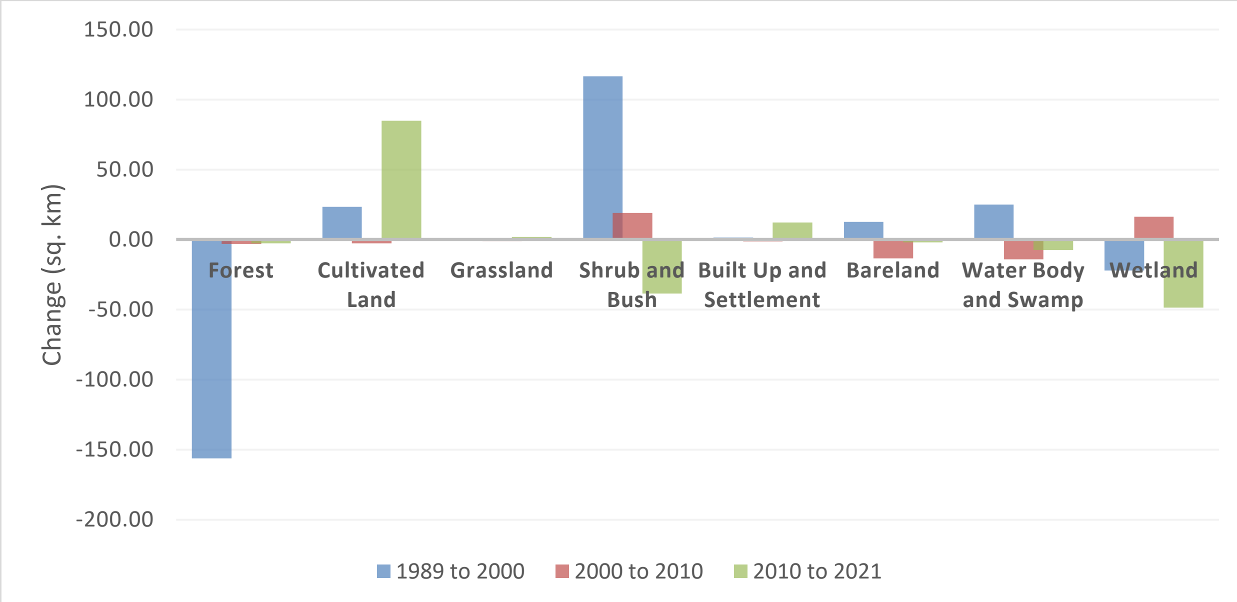

Figure 18: Graphical representation of the LULC Changes

4.1.5. Vegetation Indices based Biomass Monitoring

The classification results have already indicated that cultivated land is by far the largest land-use type, and forest cover is not more than 1/20th of the total area in this district. Further analysis of vegetation indices can add up to this by estimating the overall biomass using another remote sensing-based method i.e., vegetation index mapping.

The results of a few key vegetation indices, as well as their spatiotemporal distribution in Basona Werana Woreda, are shown below. Several vegetative parameters, such as leaf area, biomass, and physiological activities, are reflected by these indices. Most satellite-based vegetation indices are dependent upon the red, and near-infrared regions of the spectral ranges. As it's pointed out by (Barati, Rayegani, Saati, Sharif, & Narsi, 2011), for sparsely vegetated areas, like that of Basona Werana, vegetated areas reflect lesser amounts than that of sand and soils. This makes vegetation detection a bit difficult. This might be better detected by the indices such as – SAVI, and SARVI. For visualization of each vegetation index, a standard deviation stretch type is applied.

Comparing the range of NDVI values for the four years of the analysis indicates that 2010 has the highest of 1.98, and 1989, 2000, and 2021 have values of 1.16, 0.72, and 0.45 respectively. A high range value indicates a gap between arid areas, and vegetated areas within the same area of interest, and lower range values indicate a relatively similar vegetation coverage within the Woreda. All the four year's NDVI values indicated the existence of a high amount of biomass around the eastern tip of Basona Werana Woreda kebeles such as Basodongora, Gundoberet, Abamote, Keyet, Goshu Hager, and Dobele.

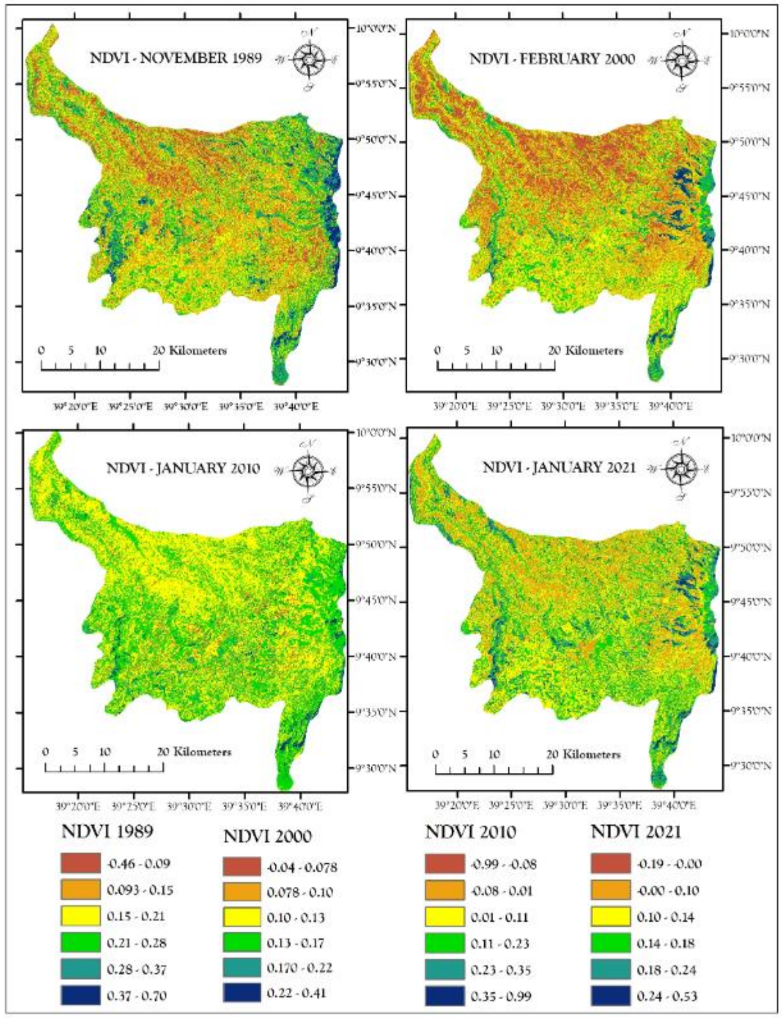

Figure 19: NDVI Values of 1989, 2000, 2010, and 2021 of Basona Werana

The 1989 NDVI values illustrate that parts of Goshbado, Muti Cherkos, Moyeaman Gult, and Wayou kebeles had high biomass coverage. Forest covers, based on the supervised classification, show a strong correlation with higher NDVI values. Goshbado is by far the kebele with has the highest ranges (high dry values, and high biomass). There is a high correlation in areas where water bodies exist with low NDVI values. This confirms the accurateness of the classification. Some of the lowest NDVI values were also recorded at the center of DebreBerhan Town.

The year 2000 is a year relatively with the better biomass cover among other years, indicated by the relatively good minimum value of -0.04. The NDVI values indicate high biomass values around some parts of Gudoberet, Abamote, and Keyet kebeles. Comparatively, the driest extents during this year's biomass estimation include parts of Kebeles which are found on the central, and northern Basona Werana Woreda including Nasena Kumamba, Kasima, and Zedegor.

In 2010 few agricultural lands in central, and eastern kebeles such as Mehal Amba, Cheraro Deber, and Abamote has some of the lowest NDVI values. The Built-up areas also show values less than zero, indicating very low or no biomass coverage. The shrublands in Modo, and Wayou has high biomass values in this year's vegetation index mapping. The eastern tip of Muti Cherkos kebele, where there is an elongated north-south chain of a forest, and shrublands, is among the areas which detected higher biomass values in 2000, and 2010.

For calculating SAVI, a 0.5 canopy adjustment factor (L), that differentiates red, and NIR, is applied for all images. This is the midway between the most densely vegetated areas (zero), and sparsely vegetated areas (one). Crop adjacent wetland areas, in the classification results, have shown higher NDVI values than their neighboring crop-covered areas.

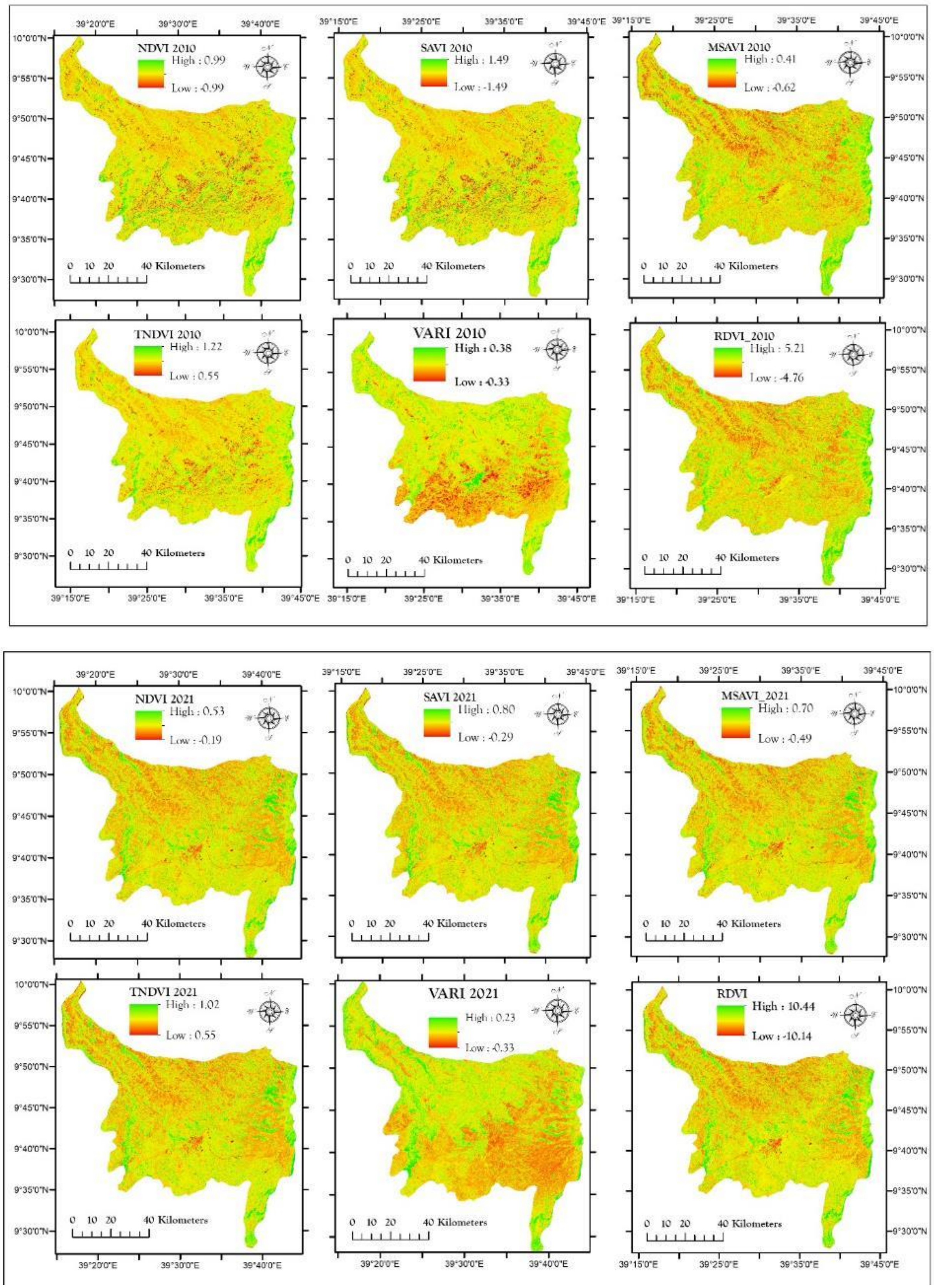

Figure 20: Comparison of Six Vegetation Indices (2010 and 2021)

The year 2010 has one of the lowest annual rainfall amounts, with 249 mm. As per that year's VARI, DebreBerhan has one of the highest biomass values in the entire Woreda. It is the place with some of the largest spots of urban establishments that exist. For comparison of vegetation indices obtained in a similar time of the year (January), 2010, and 2021 data is selected, and the same indices of 1989, and 2000 are included in the appendixes section for contrast.

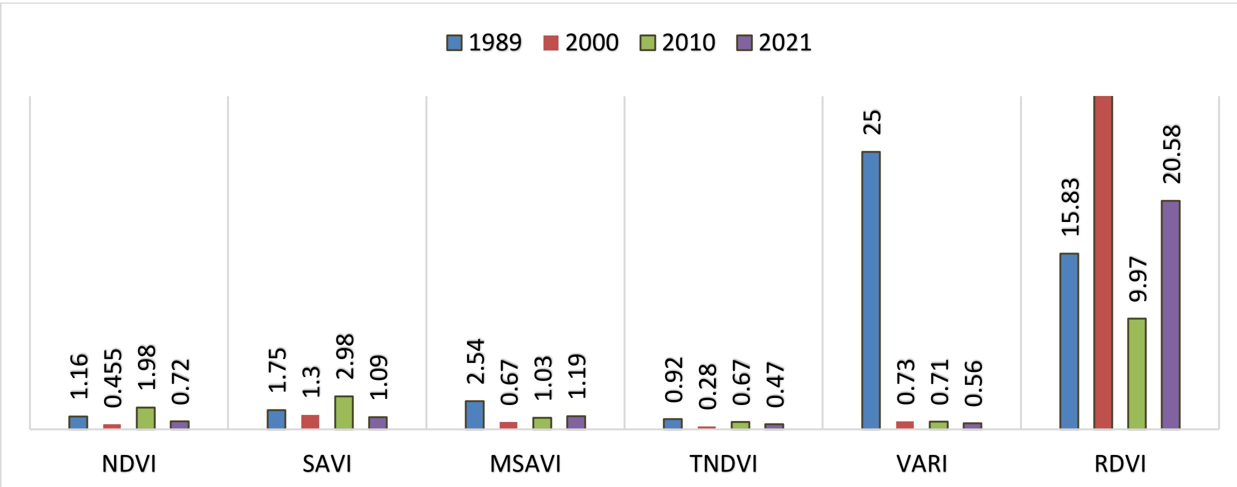

Figure 21: Vegetation Indices by Range of Values Min. Max. (1989 -2021

The vegetation mapping result shows RDVI, and VARI has the highest biomass range index values. **RDVI** is relatively the most sensitive index in detecting vegetation cover. This is based on the range of values from each year's values.

An equal distance (3k.m apart) points totaled 144 were generated across the entire area of interest, i.e., Basona Werana. The vegetation indices of 2021 were utilized to further analyze the relationship between NDVI and the other 5 vegetation indices. By applying the 'extract multi values to points' tool of ArcGIS® 10.8, 144 samples of the respective index values from each NDVI, SAVI, MSAVI, TNDVI, VARI and RDVI were collected. The output has been tabulated and presented in a scatterplot. SAVI, MSAVI, TNDVI, and to some degree RDVI has revealed a positive correlation with NDVI values. Distinctively VARI values don't indicate any positive or negative correlation with the NDVI values.

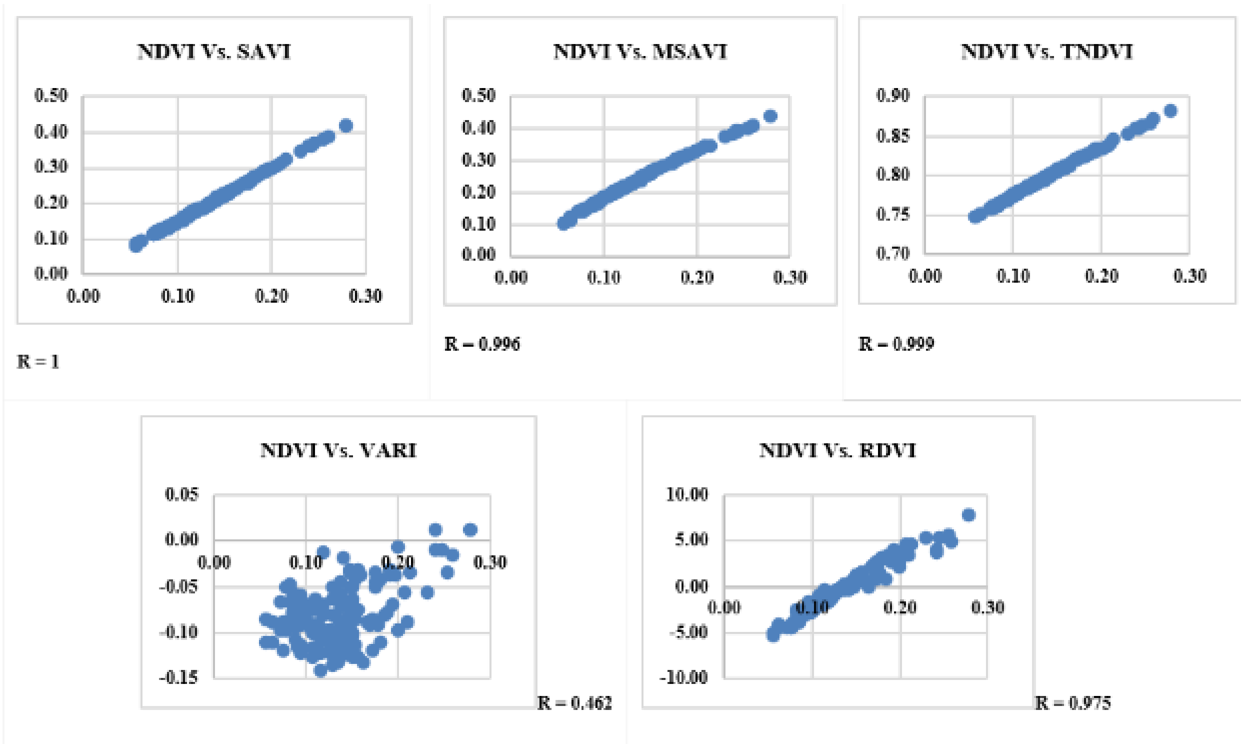

Figure 22: NDVI and other vegetation indices correlation

It reveals that SAVI and NDVI have a maximum correlation of 1, indicating that they are equally effective in distinguishing areas with higher biomass values. VARI, on the other hand, has the lowest correlation, implying a very uneven link with NDVI in detecting biomass cover across similar locations. In addition, a line chart depicting the relationship between five indices is used. The RDVI values were removed due to the index's distinct high-value ranges.

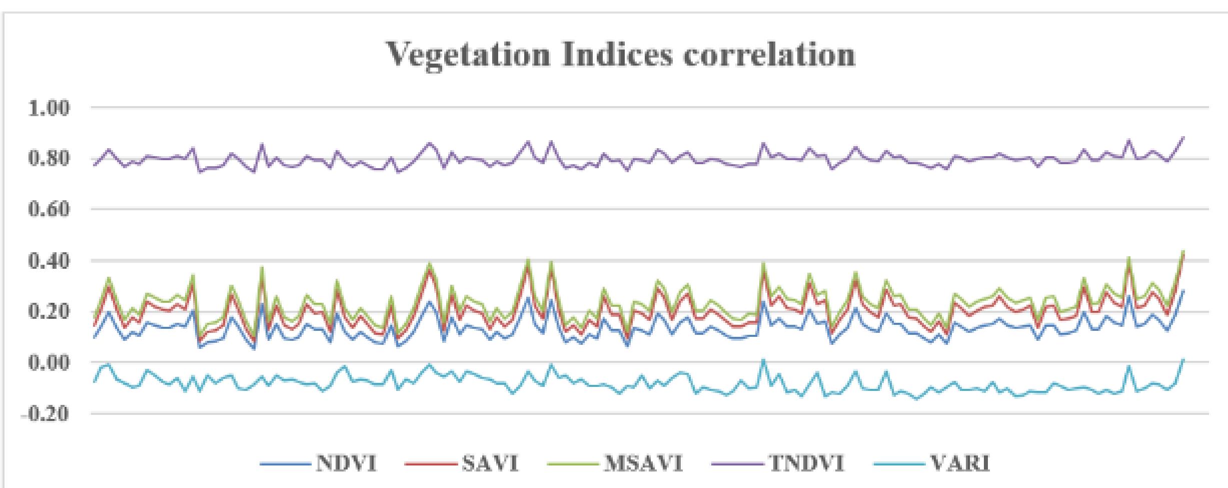

Figure 23: Line Chart of Vegetation Indices correlation

The relationship among each index is tabulated using a scatter plot matrix created by ArcGIS®. It correlates each index with the other five indices listed. For instance, the top left plot illustrates the positive correlation between SAVI with NDVI, while the bottom right plot indicates the very loose correlation between RDVI with VARI.

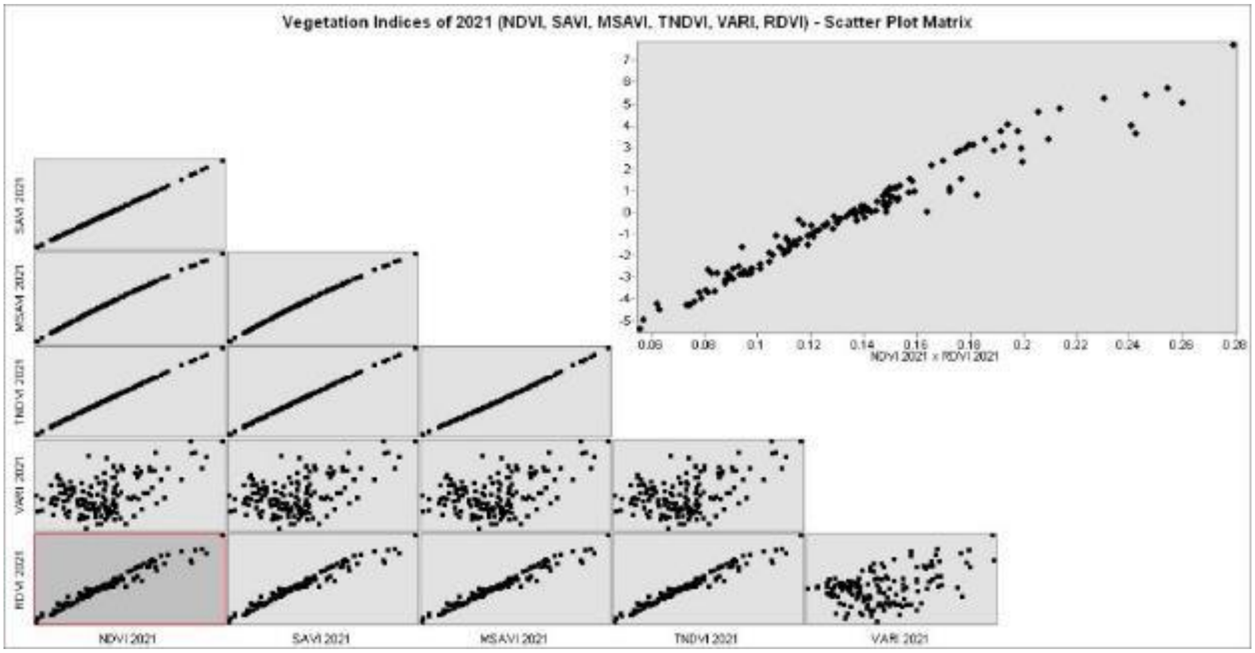

Figure 24: Scatter plot Matrix of six vegetation indices

4.1.6. Relationship of LULC and Vegetation Indices

To evaluate the land use land cover classes with the most widely used vegetation index NDVI, a cross-tabulation is supplemented.

Table 11: Relationship between LULC and NDVI

2021 Class Names	Area (Km2)	NDVI min	NDVI max	Range	NDVI Mean	NDVI Std.
Forest	70.2747	-0.01	0.54	0.55	0.21	0.08
Cultivated Land	1004.535	-0.06	0.40	0.47	0.13	0.04
Grassland	4.1103	0.08	0.27	0.18	0.14	0.02
Shrub and Bush	207.7893	0.01	0.45	0.44	0.17	0.04
Built Up and Settlement	38.8044	-0.08	0.30	0.38	0.11	0.03
Bare land	0.0684	0.05	0.14	0.09	0.08	0.01
Water Body and Swamp	9.261	-0.20	0.20	0.40	0.06	0.04
Wetland	16.5042	0.09	0.40	0.30	0.21	0.04

Compared to their mean NDVI values forest has the largest NDVI mean of 0.21 in 2021 followed by wetlands (0.21). Shrub and Bush (0.17), Grassland (0.14), Cultivated land (0.13) Built-up and settlement (0.11), Bare land (0.08), and Waterbody and Swamp (0.06).

4.1.7. Drought Susceptibility Mapping

After reviewing a long list of existing literature and testing most of the major remote sensing-based methods, the researcher chose the two most relevant indices for drought mapping in Basona Werana. The Vegetation Condition Index (VCI) and the Normalized Difference Drought Index (NDDI) were used to assess historical drought and non-temporal drought values in selected years.

4.1.5.1. Vegetation Condition Index (VCI) Based Drought Estimations

Vegetation Condition Index (VCI) is calculated for 1989, 2000, 2010, and 2021. Though it is unintended when selected, the years 1989, 2000, and 2010 have been relatively arid than other years in between these years. As a result, four additional years of net values have been used to get a clear picture. These years are 1984, 2018, 2019, and 2020.

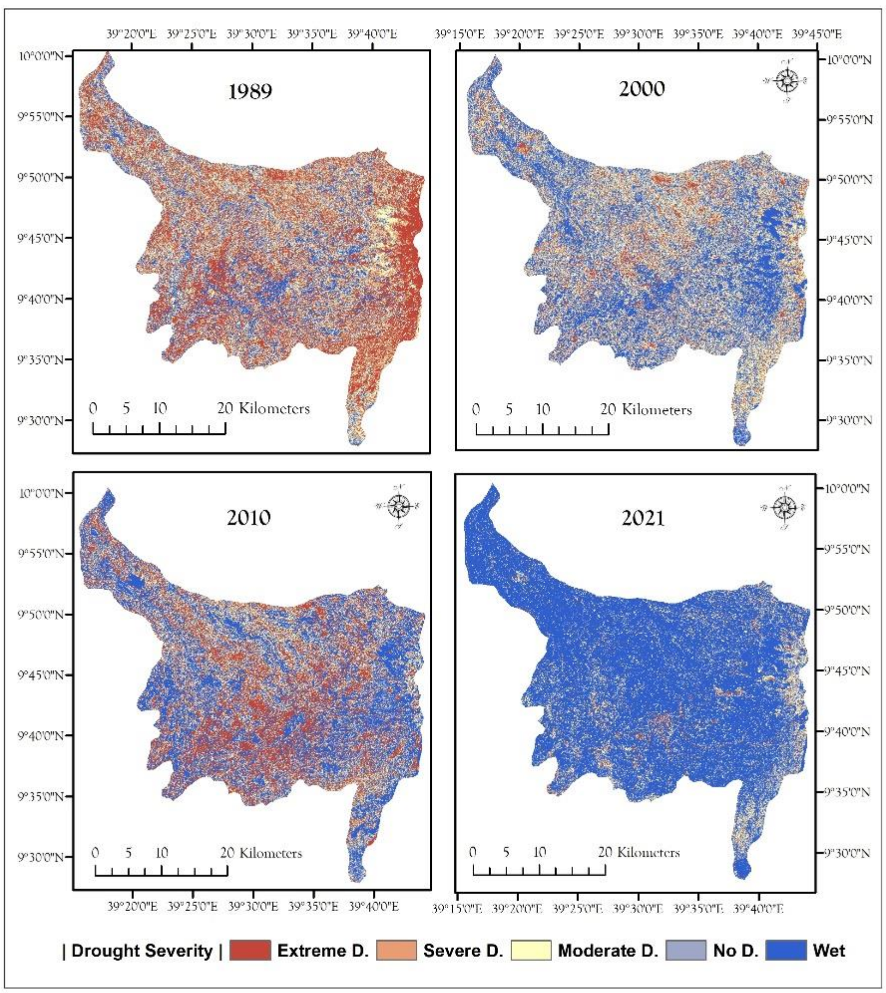

Figure 25: VCI Map for four historical years 1989, 2000, 2010, and 2021

Vegetation Condition Index (VCI) is computed to the historical images that are also used in the LULC change mapping. This is based on the minimum and maximum NDVI values of 1984, 1989, 2000, 2010, 2018, 2019, 2020, and 2021. The VCI map is produced based on equation (*12*) presented in the literature review section. The raster calculator is used to calculate VCI, while the Cell statistics tool is utilized to estimate the lowest and maximum NDVI values in the ArcGIS software environment.

Table 12: VCI Table for 1989, 2000, 2010 and 2021

VCI Severity Level	1989		2000		2010		2021	
	Ar.(km^2)	Percent	Ar.(km^2)	Percent	Ar.(km^2)	Percent	Ar.(km^2)	Percent
Extreme Drought (<10%)	407.82	30.18	99.18	7.34	304.71	22.55	23.87	1.77
Severe Drought (10%-20%)	249.33	18.45	156.44	11.58	115.41	8.54	35.52	2.63
Moderate Drought (20%-35%)	306.98	22.72	334.17	24.73	219.88	16.27	110.73	8.19
No Drought (35%-50%)	173.95	12.87	325.15	24.06	224.38	16.60	170.30	12.60
Wet (>50%)	213.28	15.78	436.42	32.29	486.99	36.04	1010.93	74.81

The result indicates that in 2021, 12.59% of the area has been affected by some degree of drought and 87.41% of the area has no drought or is more explicitly wet. Among these 4 years, extreme drought and severe drought were the highest in 1989 while the moderate drought was highest in the year 2000.

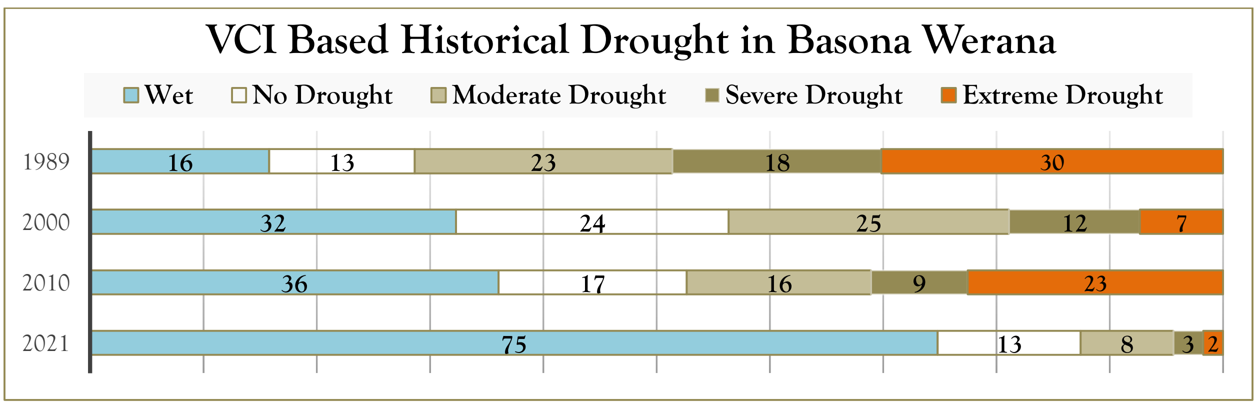

Figure 26: A stacked bar of VCI for 1989, 2000, 2010 and 2021

To minimize the assumption that 2021 is the wettest year, the comparison is made with the most recent 4 years. For the latest four consecutive years, 2018-2021 VCI is calculated using their minimum and maximum NDVI values. The outcomes indicate - extreme drought affected 59.97%, 12.15%, 9.79%, and 38.19% of the area in 2018, 2019, 2020, and 2021 respectively. While 18.47%, 68.42%, 75.21%, and 31.32% experienced wet conditions in those same years. The detailed table can be found in an appendix section (6). This estimation's diagram is depicted in the stacked bar below.

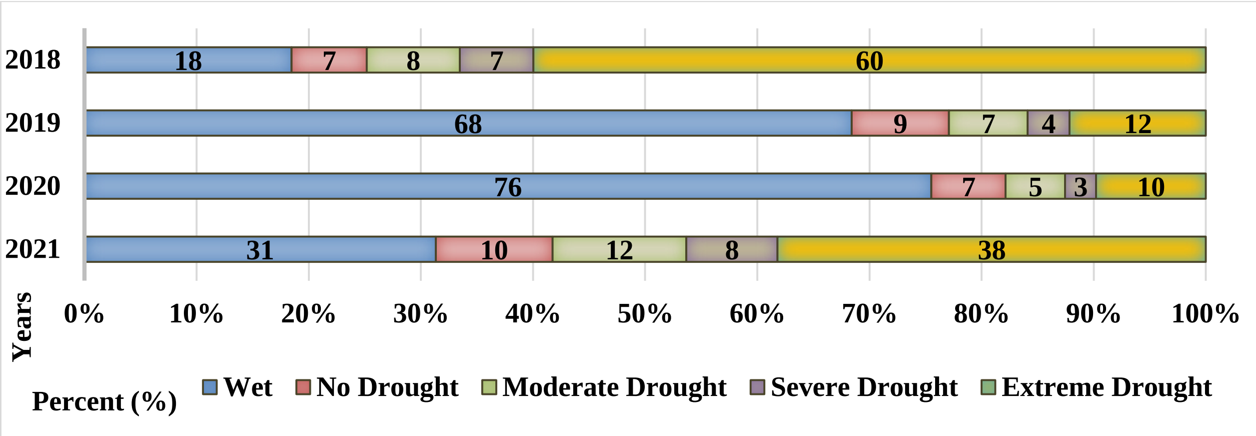

Figure 27: A stacked bar of VCI for 2018 - 2021

In this estimation, the 2021 results show that 38.19 percent of the area is in extreme drought, 8.14 percent is in severe drought, 11.94 percent is in moderate drought, 10.41 percent is not in a drought, and 31.32 percent is wet enough and not experienced any drought.

4.1.5.2. Normalized Difference Drought Index (NDDI) based Drought Estimations

NDDI values are used to identify three types of drought conditions based on NDVI and NDWI values as already pointed out in equation (*14*). The NDDI drought severity levels are No drought (<0.5), Moderate Drought (0.5-0.6), Severe Drought (0.6-1), and Extreme Drought (>1) (Angearu, Irimescu, Mihailescu, & Virsta, 2018).

Table 13: NDDI based drought approximations for Basona Werana (1989 - 2021)

NDDI Drought Severity Level	1989		2000		2010		2021	
	Ar.(km^2)	Percent	Ar.(km^2)	Percent	Ar.(km^2)	Percent	Ar.(km^2)	Percent
No Drought (<0.5)	578.54	42.81	451.09	33.38	565.18	41.82	258.32	19.12
Moderate Drought (0.5-0.6)	67.73	5.01	81.48	6.03	56.46	4.18	82.22	6.08
Severe Drought (0.6-1)	219.85	16.27	270.43	20.01	199.59	14.77	282.79	20.93
Extreme Drought (>1)	485.22	35.91	548.35	40.58	530.13	39.23	728.02	53.87

These four years are compared to the historical year 1984, as well as the previous three years (2018-2020), as shown below. It suggests that the intensity of drought has been steadily increasing over the last three decades. Extreme drought climbed from 24.4% in 1984 to 53.87% in 2021, with a corresponding rise in each decade. While severe and moderate droughts remained stable over these three decades, ‘no drought’ areas have decreased from 52.25% in 1984 to just 19.12% in 2021.

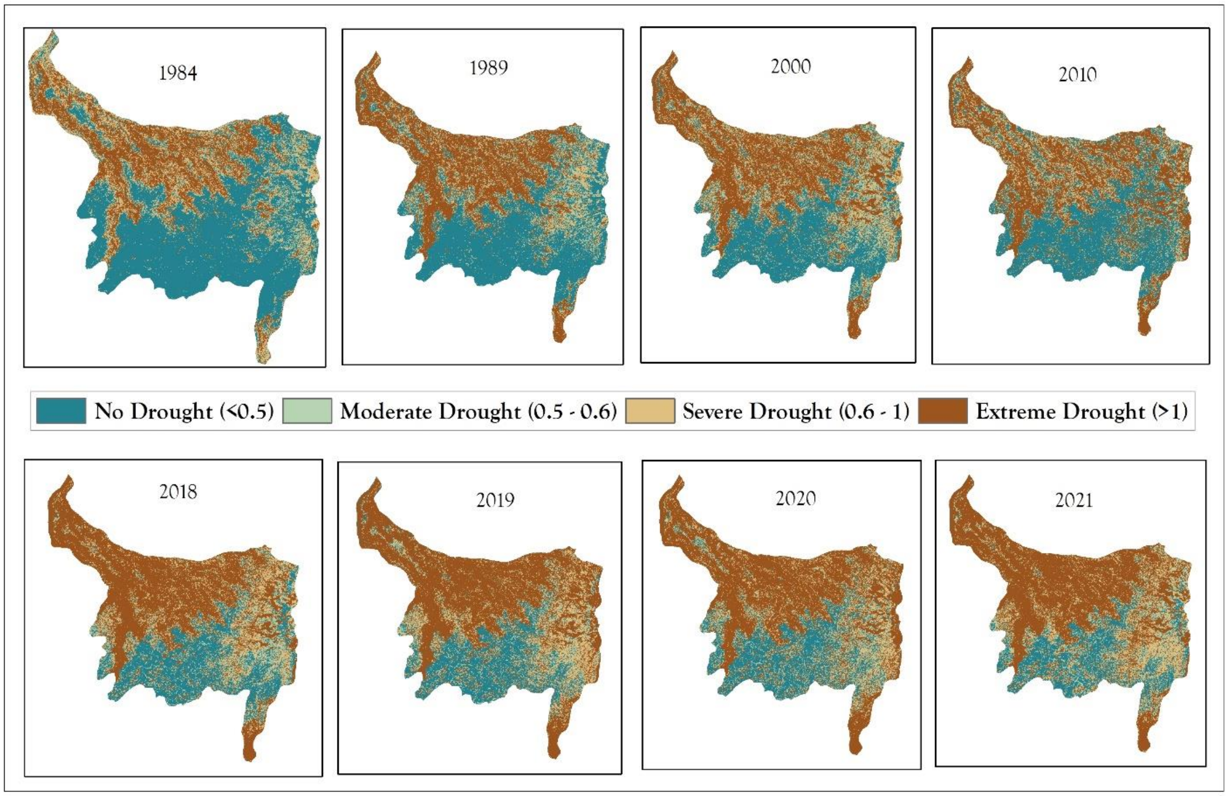

Figure 28: A Normalized Difference Drought Index (NDDI) Map for Eight Historical Years

In terms of stacked bar, it's illustrated on Figure 29: Normalized Difference Drought Index for selected years (1984 – 2021.

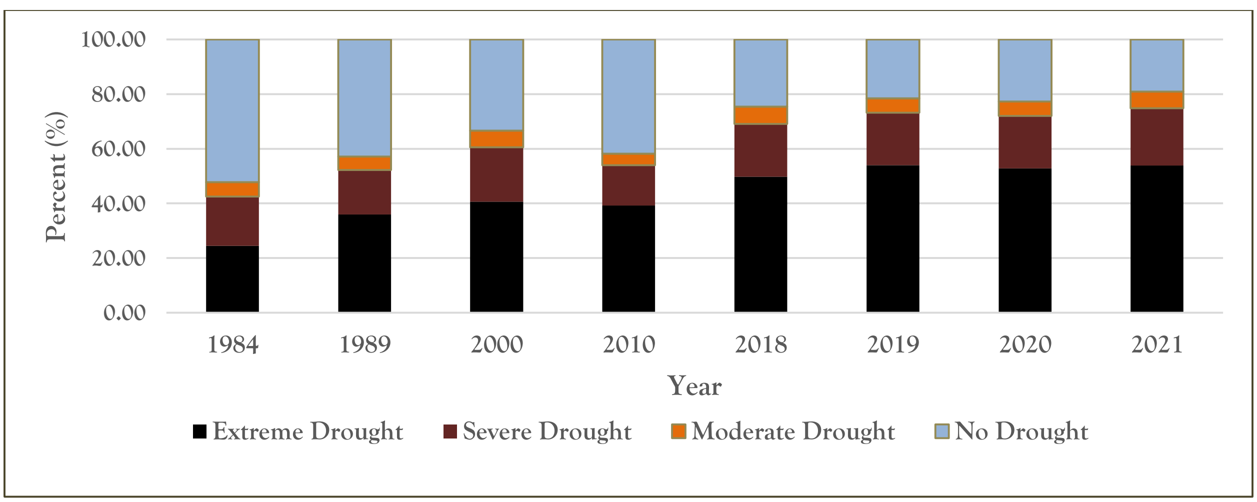

Figure 29: Normalized Difference Drought Index for selected years (1984 – 2021

While extreme drought conditions have steadily increased from 24.43% to 53.87%, severe and moderate drought levels have not shown any significant difference.

Table 14: Areas affected by drought (in percent) using NDDI values for 8 selected years

NDDI Drought Severity Level (%)	1984	1989	2000	2010	2018	2019	2020	2021
No Drought	52.25	42.81	33.38	41.82	24.63	21.58	22.68	19.12
Moderate Drought	5.25	5.01	6.03	4.18	6.28	5.24	5.33	6.08
Severe Drought	18.07	16.27	20.01	14.77	19.27	19.21	19.15	20.93
Extreme Drought	24.43	35.91	40.58	39.23	49.82	53.97	52.84	53.87

Though it's beyond the scope of the thesis to see seasonal variation, the NDDI values have been tested for the latest the year 2021. The comparison is made between January and May 2021. The NDDI of May 2021 has moderately similar values to the month used in the last assessment i.e., January. They shared areas in a proportion - no drought (14.25%), moderate drought (4.46%), severe drought (19.73%), and extreme drought (61.57%). Though the precipitation amount appeared to be 6.56 and 74.82 in January and May respectively (CHIRPS, 2021), the NDDI values seemed to shift only slightly. This indicates the unique capacity of NDDI for a particular year without a seasonal difference. So, in general, NDDI valuations for those eight years appear to be accurately estimated for each year.

4.1.5.3. Correlation of Drought Indices with Precipitation

To identify which drought index better represents the actual drought conditions, major three drought severity levels (extreme, severe, and medium) of VCI and NDDI areal coverage (percentage) values of 8 years are correlated with respective monthly and annual precipitation amounts derived from (CHIRPS, 2021). To estimate the approximate annual precipitation for 2021, the five months (January to May) average of 2021 is taken and extrapolated for annual precipitation using the recent year's 5 months and annual rainfall amounts. For the rest of the years, the amounts directly derived are applied.

Table 15: Correlation between drought severity levels of 8 years VCI and NDDI values with respective precipitation amounts

Code	Drought Severity levels and their respective precipitation values (annual or monthly)	Vegetation Condition Index (VCI)	Normalized Difference Drought Index (NDDI)
1	Extreme Drought Vs. Annual Precipitation (8 Yrs)	-0.05	0.47
2	Extreme Drought Vs. Month. Precipitation (8 Yrs)	0.13	0.41
3	Severe Drought Vs. Annual Precipitation (8 Yrs)	-0.80	0.63
4	Severe Drought Vs. Monthly Precipitation (8 Yrs)	-0.73	0.55

5	Moderate Drought Vs. Annually Precipitation (8Yrs)	-0.89	0.41
6	Moderate Drought Vs. Monthly Precipitation (8 Yrs)	-0.91	0.44

The results are plotted in the following clustered bar. The faded blue bars indicate VCI, while the faded green bars indicated NDDI correlation values with their respective year and monthly rainfall amounts. To see further details of precipitation amounts, refer to appendix (4).

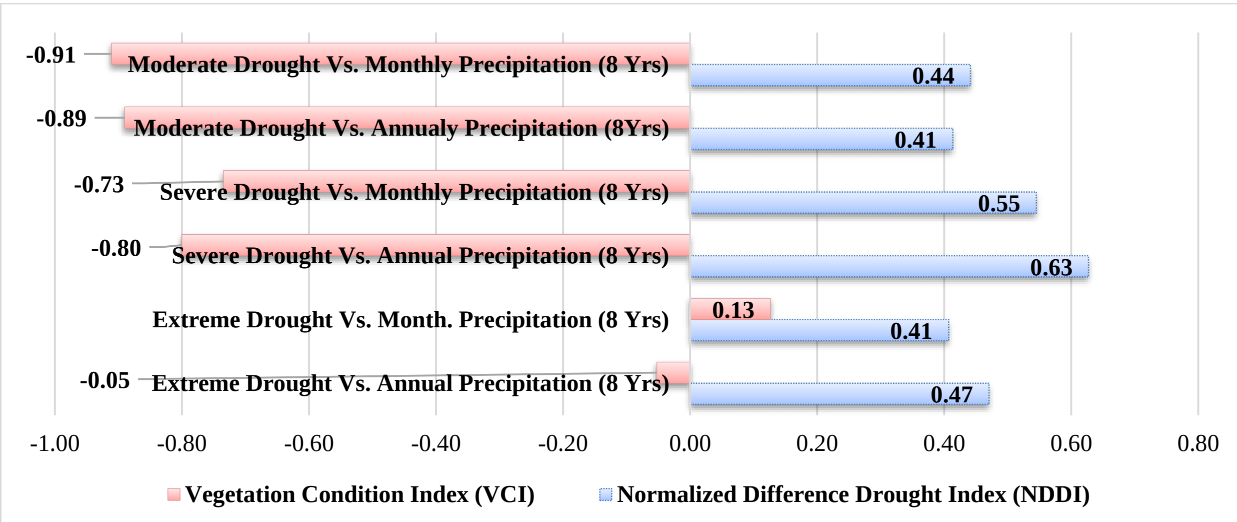

Figure 30: Correlation of VCI and NDDI severity degrees with precipitation

Drought values are expected to correlate inversely with precipitation amounts under normal conditions, and the bigger the value, the greater the association. VCI has higher correlation values than its counterpart NDDI. While the most of Vegetation Condition Index correlations are negative, all Normalized Difference Drought Index values are positively correlated with precipitation levels of respective years/months. While medium drought degree with yearly precipitation has the strongest association for VCI, its severe drought for NDDI. Extreme drought degree is the weakest associated in both VCI and NDDI for the sample years taken in Basona Werana.

To selectively inquire whether annual precipitation or monthly precipitation values better represent drought conditions in these indices, the three values are selectively summed up. When the annual precipitation value related only correlations (1, 3, and 5 in Table 15: Correlation between drought severity levels of 8 years VCI and NDDI values with respective precipitation amounts) are collectively summed, it gives values of -1.74 for VCI and 1.51 for NDDI. Similarly, the sum of monthly precipitation-related values yields -1.52 for VCI, whereas it is 1.39 for NDDI.

4.1.8. UAS Based Biomass Assessment

The UAS-based vegetation indices, as discussed in section 2.5.2. Visible Range (UAS Suited) Vegetation Indices, are confined only in the visible range (Red, Green, and Blue). The Visible Atmospheric Resistant Index (VARI) has been computed for Basona Werana using Landsat 08 in 2021, clipped for the Wayou UAS area of interest. The minimum and maximum ranges have contracted from (Min: -0.33, Max: 0.23) for the whole Basona Werana to (Min: -0.16, Max: 0.08) for the Wayou UAS block. The range of values for sentinel 2A ranges between -0.27 and 1.44.

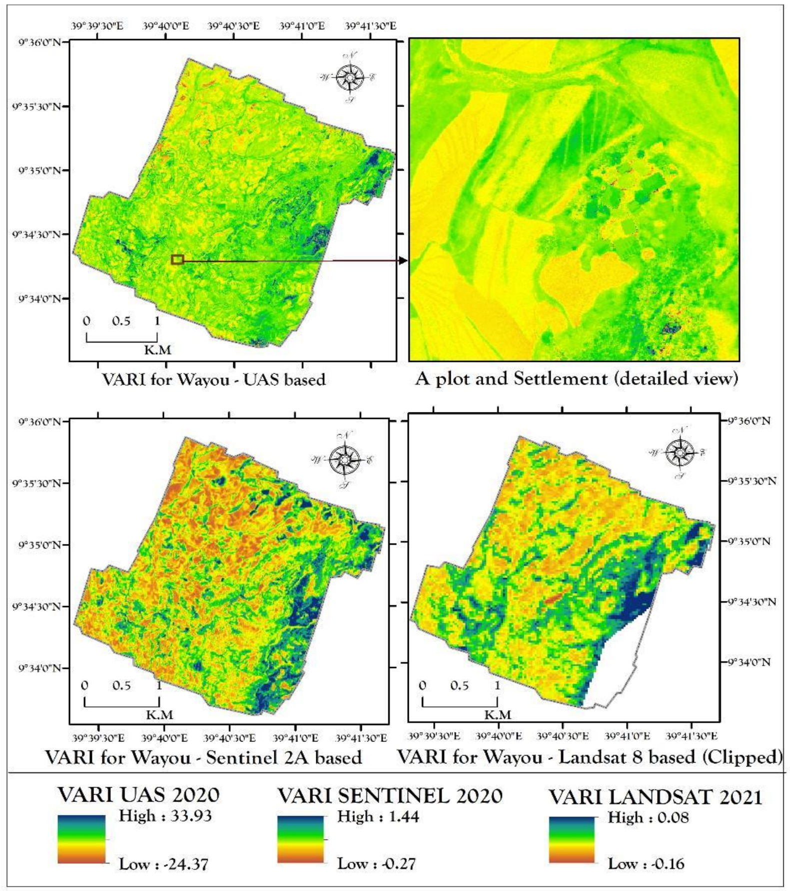

Figure 31: Visible Atmospheric Resistance Index (VARI) using UAV Imagery

The high-resolution Wayou UAS block has been also computed for VARI values. The results have few unintended pixelated values in places where there is pixel smearing (pixel stretch). Pixel stretch exists during the orthorectification process when the input digital elevation values don't fit for orthogonal projection. To reduce this unusual effect, the mosaic has been resampled 4 times to 0.48m spatial resolution. It has been recomputed for VARI and the unusual max-min index values have been considerably reduced.

4.1.9. Land Suitability Analysis

The land suitability assessment is confined to agriculture, particularly crop production. The latest (2021) classification results already indicated that the 1,005 km^2 (100454 ha) area is covered by various crop types. But, what portion of the entire land of the district is assumed to be suitable for agricultural activities is the point of analysis of this section. This question is addressed at the end of this section.

In the Ethiopian context, elevation plays a great role in modifying local temperature and rainfall. Therefore, it is also used as a basis for traditional agro-ecological classifications. Major crops such as teff (Eragrostis tef) grows between 1,800 to 2,200 m.a.s.l, wheat (Triticum spp.) grows between 1,000 to 2,300 m.a.s.l, while barley (Hordium spp.) grows between 2,000 to 3,500 m.a.s.l (Gorfu & Ahmed, 2014).

The digital elevation model obtained from (WLRC, 2014) is classified into three classes Weina Dega, dega, and wurch. Using the traditional agro-ecological zoning of Weinadega or midlands (1,500-2,300), Dega or highlands (2,300 – 3200), and wurch (3,200 – 3,700). Because Woreda's elevation is mostly suitable for agricultural production, the weight given in the weighted overlay is relatively low, only 15%. Weina Dega is given a relatively superior degree for its suitability to grow wheat, teff, barley, maize, sorghum, chickpeas, etc. While Dega grows barley and wheat wurch areas could grow barley only (Gorfu & Ahmed, 2014). For classifying Basona Werana into 5 classes, the agro-ecological zones explained earlier combined with natural breaks have been applied. The slope is another important component in assessing land suitability, which influences the water, and soil content, potential runoff, the usage of modern farming technologies, and other factors.

The biomass conditions based on vegetation indices are an important component of the suitability analysis. To consider the soil moisture conditions, and related factors Soil Adjusted Vegetation Index (SAVI) is included in the suitability analysis. A wide range of values is chosen based on (Mostafiz, Noguchi, & Ahmed, 2021) suitability assessment.

For assessing the suitability of soils that are found in Basona Werana, the list of soils available has been ranked based on their ecosystem services for food security.

Table 16: Soil Types and their ecosystem services compared

	Ecosystem Services conveyed					Major service
Soil Type	**Food**	**Climate**	**Water**	**Cultural**	**Sum**	
Nitosols	4	3	4	1	12	Food Security
Vertisols	4	2	3	1	10	Food Security
Cambisols	3	2	3	1	9	Food Security
Regosols	2	1	1	1	5	Biomass
Leptosols	1	1	2	1	5	Runoff

Adapted from Generalized Ecosystem service rating for soil types (FAO & ITPS, 2015)

The best soils including Nitosols and Vertisols exist on the western part of the Woreda followed by the overwhelming prevalence of cambisols in most parts of the Woreda. Regosols dominantly exist on the eastern portion, where the altitude is relatively higher and forest cover is better.

Normalized Difference Water Index (NDWI) in this analysis served as a proxy tool for estimating moisture stress risk. It makes use of NIR and SWIR bands to water content in vegetation and is depicted in equation (*13*). Natural break values of NDWI are used to classify into five classes and the rankings are reversed to associate high NDWI values for the most suitable classes.

River proximity is an important constraint that is considered in agricultural suitability. It determines the possibility for cropping during non-rainy seasons reducing the dependence on rain through irrigation possibilities.

Table 17: Constraints for land suitability analysis

Constraints	Criteria/Attributes	Points	Suitability Class	Influence (%)	Reference
Elevation	1,554 – 2,267	1	1st degree	10%	Gorfu & Ahmed, 2014
	2,267 – 3,024	2	2nd degree		
	3,024 – 3,215	3	3rd degree		
	3,215 – 3,468	4	4th degree		
	3,468 – 3,660	5	5th degree		
Slope	0 – 05	1	1st degree	25%	Mostafiz, 2021

	05 – 10	2	2nd degree		
	10 - 20	3	3rd degree		
	20 - 30	4	4th degree		
	>30	5	5th degree		
Soil Type	Nitosols, Vertisols	1	1st degree	15%	Mitiku, 2014 & FAO, 2015
	Cambisols	2	2nd degree		
	Regosols	4	4th degree		
	Leptosols, No soil	5	5th degree		
Soil Adjusted Vegetation Index (SAVI)	>0.4	1	1st degree	15%	Ewnetu, Simane, Teferi, & Zaitchik, 2021
	0.4 – 0.3	2	2nd degree		
	0.3 - 0.2	3	3rd degree		
	0.1 - 0.2	4	4th degree		
	<0.1	5	5th degree		
Normalized Difference Water Index (NDWI)	0.03 to 0.26	1	1st degree	25%	Tadesse, et al., 2021
	-0.00 to 0.03	2	2nd degree		
	-0.05 to -0.00	3	3rd degree		
	0.1 to -0.2	4	4th degree		
	<0.1	5	5th degree		
River Proximity	0 to 2	1	1st degree	10%	Sinshaw, et. al, 2021
	2 to 4.5	2	2nd degree		
	4.5 to 7.8	3	3rd degree		
	7.8 to 12.3	4	4th degree		
	12.3 to 18.2	5	5th degree		

For each constraint, the following percent of influence proportion is applied: elevation (10%), slope (25%), soils (15%), SAVI (15%), NDWI (25%), and River Proximity (10%). It’s been applied after several attempts with different scenarios.

Assigning the input values and integrating the listed constraints produced an output map with a definite pattern. The suitability classification classes recommended by FAO land suitability classification are adapted from the (Mostafiz, Noguchi, & Ahmed, 2021; Alemayehu, et al., 2020) and slightly modified to include 5 classes, where the last is a non-suitable land.

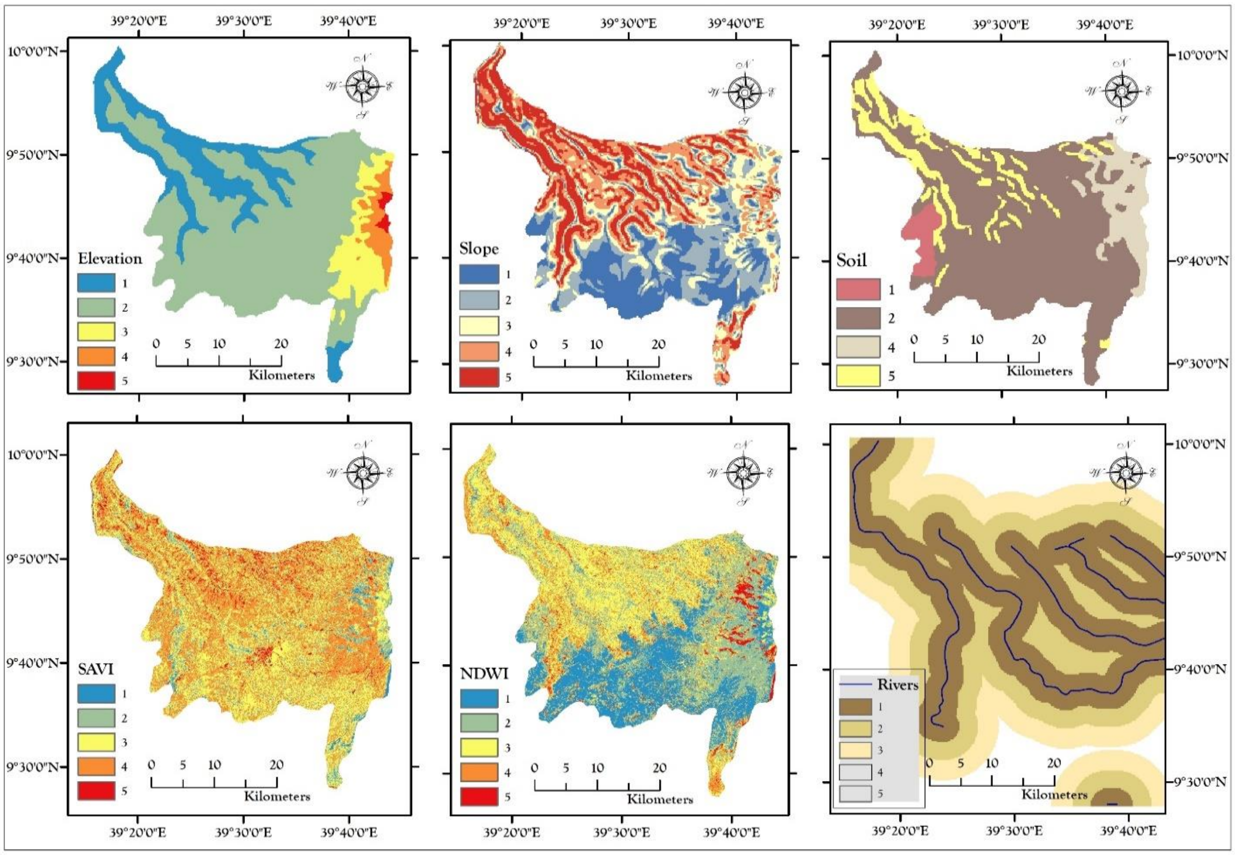

Figure 32: Map of constraints for suitability assessment

The weighted overlay analysis result indicates 72.32 km^2 area is highly suitable, 674.38 km^2 is moderately suitable, 388.12 km^2 area is marginally suitable, 181.87 km^2 is less suitable whereas 34.66 km^2 area is not suitable for farming activities. These are in a proportion of 5.35%, 49.9%, 28.72%, 13.46% and 2.56% respectively.

Table 18: Cropland Suitability Assessment results

Classification	Suitability Assessment using Weighted Overlay	
	Area (K.M^2)	Area (Percent)
Highly Suitable for Crop Pr.	72.32	5.35
Moderately Suitable for Crop Pr.	674.38	49.90

Marginally Suitable for Crop Pr.	388.12	28.72
Less Suitable for Crop Pr.	181.87	13.46
Not Suitable for Crop Pr.	34.66	2.56

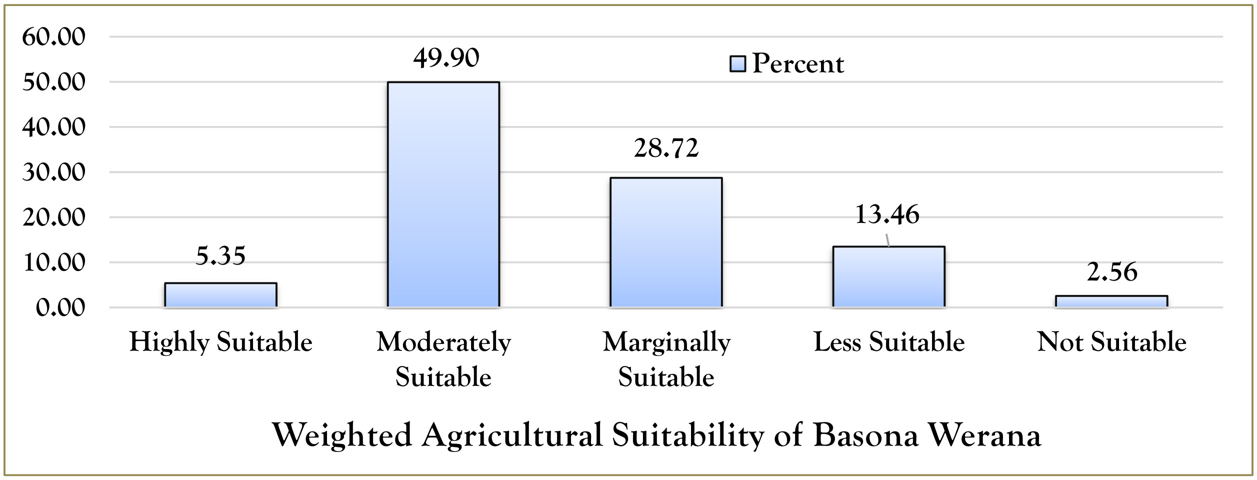

The most suitable agricultural areas are found around the central, and southern parts of the Woreda. These areas have relatively considerable plain areas more suitable for crop production, from a highland-dominated Woreda. Most of these agriculturally suitable areas are now delineated under Debre Berhan town and anticipated that the built-up areas will engulf the existing agricultural areas in the meantime.

The highest Soil Adjusted Vegetation Index (SAVI) values were found in the southern part of the Woreda, where cambisols (vertic cambisols and eutric cambisols) are abundant. On the other hand, the lowest values exist where leptosols exist. Wherever leptosols exist, the SAVI value is the lowest. So, this analysis demonstrated that cambisols are by far the soil type with the highest biomass, whereas leptosols have the lowest biomass amounts of the croplands in Basona Werana Woreda.

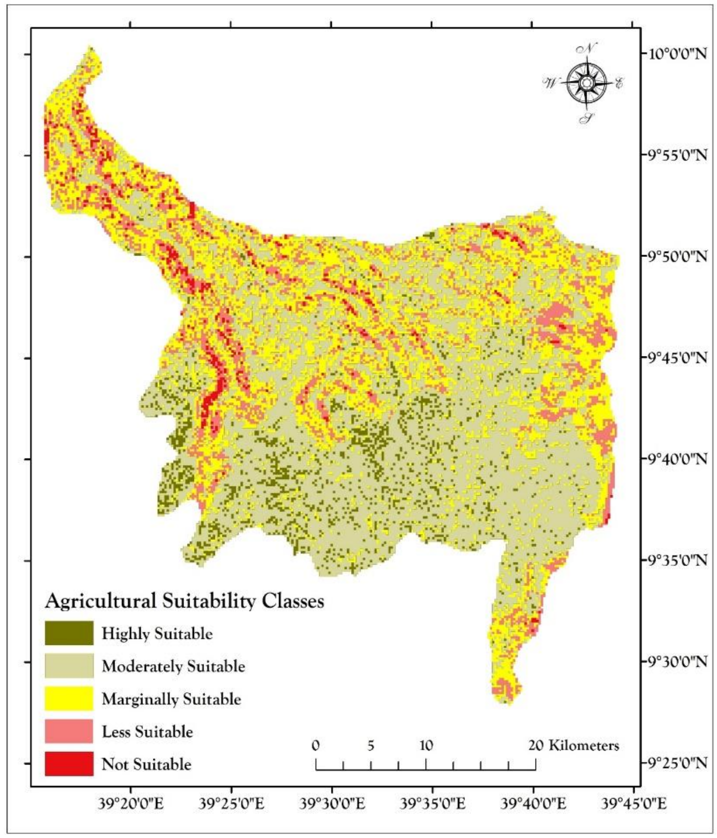

Figure 33: Agricultural Suitability Map of Basona Werana

The 300m apart equal interval point data were utilized to redistribute the suitability of the entire Woreda for individual Kebeles. With 14,558 sample points across each assigned specific Kebele name, the suitability classes were assigned using the simple GIS geoprocessing tool 'intersect'. The names of Kebeles against their respective suitability classes were tabulated in a summary table indicating their frequency distribution. The result of this table is presented in Appendix 6: Freq. Dist. of Agricultural Suitability via 300m equal interval samples. That table doesn't seem to be an accurate representation to display the relative extent of agricultural suitability across these administrative localities unless it is weighted by their respective areas or proportionate percentage distribution of each suitability class within each Kebele. For simplicity, the percentage distribution is chosen and presented in a stacked bar chart. The stacked bar is sorted based on the addition of the most suitable two classes highly suitable and moderately suitable together.

According to this analysis, Muti Cherkos Kebele distinctively has the largest highly suitable suitability class areal coverage. Considering the highly and moderately classes collectively Dibut, Kormargefiya, Angolela and DebreBerhan come in the forefront. Mati, Chembere, Gefet, Zedegor, and Metkoriya are the least agriculturally suitable areas in Basona Werana from the worst followed by the subsequent worst groups. The result also indicated that every kebele has at least some proportion of the land which lies in the moderately suitable and marginally suitable classes. While highly suitable and less suitable each covers 27 kebeles, not suitable classes covered 8 kebeles respectively.

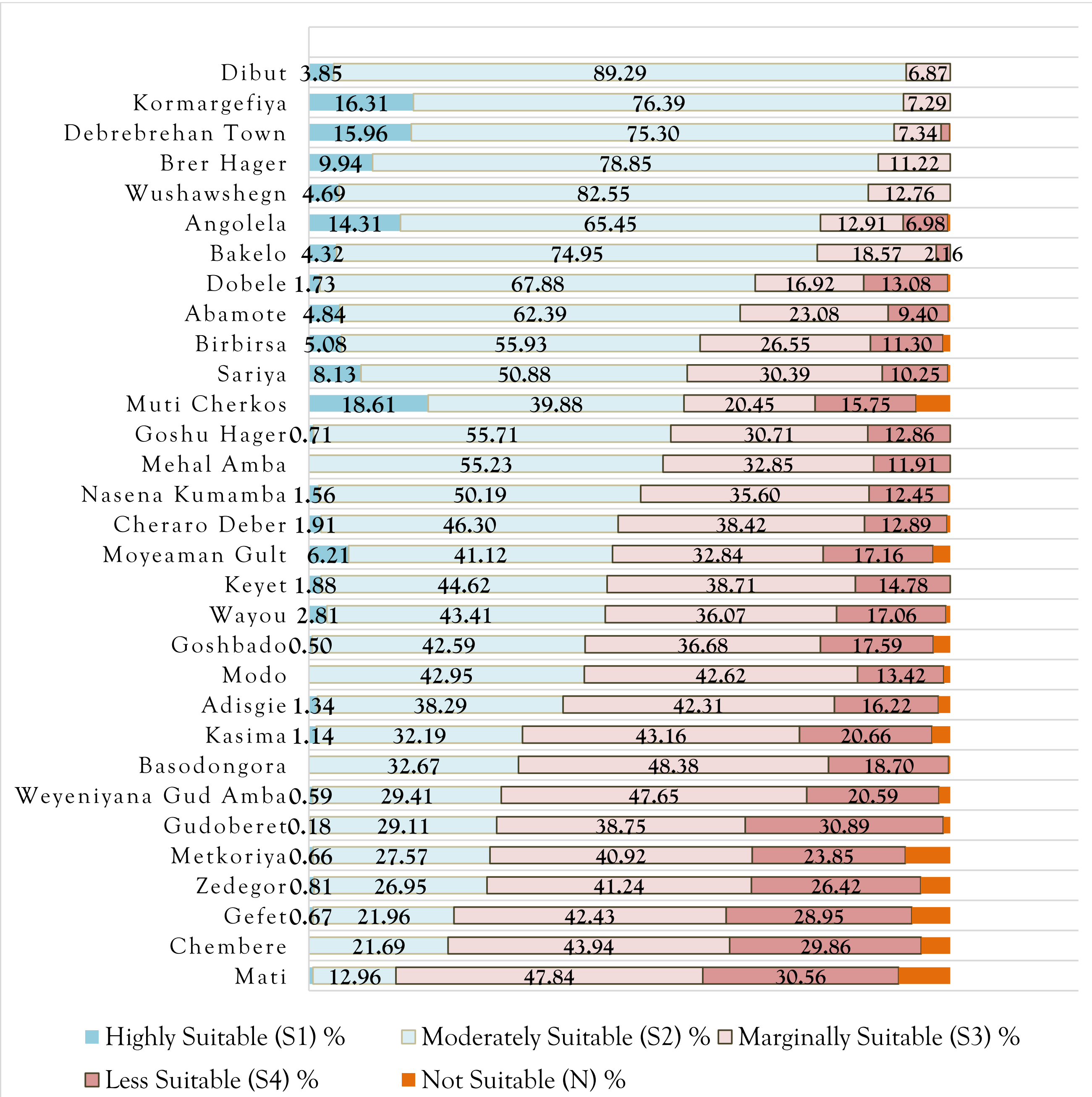

Figure 34: A stacked bar of Agricultural Suitability Rank by Kebeles

The map below is visualized based on the frequency distribution of each suitability class across the 31 kebeles normalized by the spatial extent of the respective kebeles. Generally speaking, the central and southern parts of Basona Werana are relatively more suitable for crop production, while the northwestern tip of the Woreda is relatively less suitable for agriculture.

The section concludes by attempting to answer the query of what fraction of LULC classified as croplands are considered in the various suitability classes listed above. Utilizing 'tabulate area' GIS function for LULC classes of 2021 6.14%, 56.63%, 26.62%, 9.38% and 1.23% of the total cultivated area (1004.535 km2) area are delineated as highly, marginally, moderately, less and not suitable for crop production. The result is quite close to the results estimated for the entire Woreda, as shown on Map 18. This means roughly one-third of cropland already encroaching on areas that are less or not recommended for crop yields.

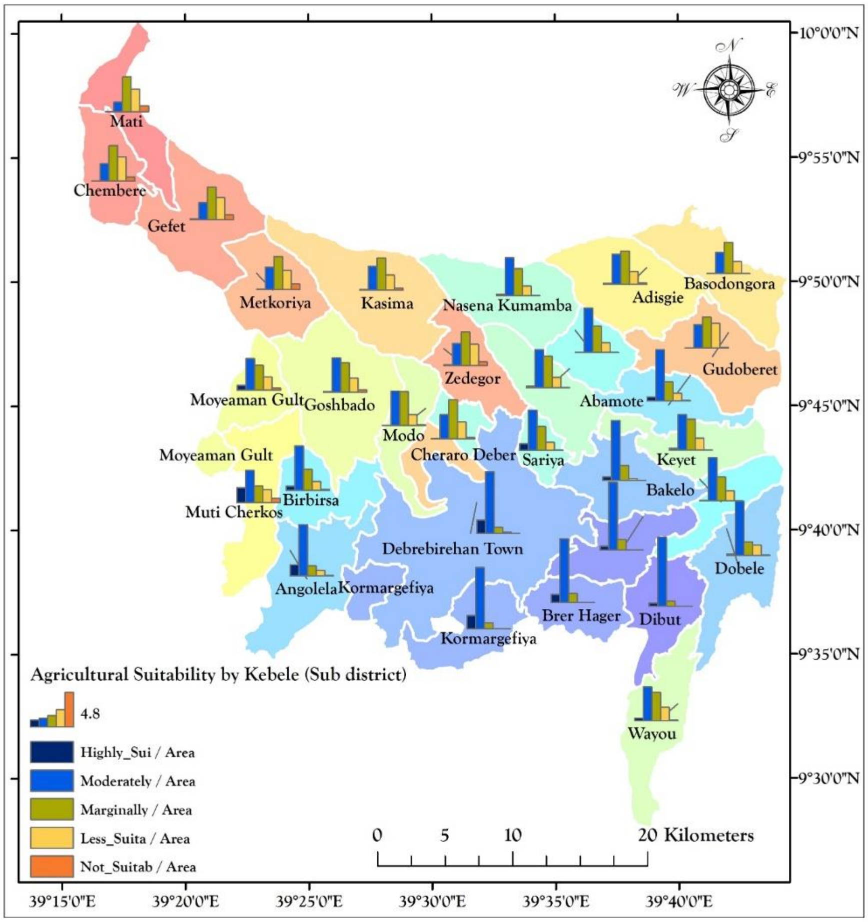

Figure 35: Agricultural suitability map across Kebeles

4.2. Discussion

4.2.1. LULC Changes

Accurate land-use and land-cover (LULC) maps derived from remote sensing data are significant for monitoring, and quantification of the environment as well as for spatiotemporal changes. It ensures sustainable development by assisting decision-makers to fully capture the dynamics of the changing environment (Bai, et al., 2017).

These findings, which are also supported by (FAO and UNEP, 2020), demonstrate that agricultural growth remains the principal cause of deforestation and forest fragmentation. The difference with FAO tropical estimates from this paper's findings is differed on - while subsistence agriculture is the most dominant factor in Basona Werana for deforestation, it accounts for only 33% for tropical deforestation in (FAO and UNEP, 2020) estimates. Others such as large-scale commercial agriculture account for 40% of tropical deforestation. It was noted by (Ayele, 2009) that 75% of the crop production in Basona Werana Woreda is subsistence-based.

The forest cover changes in Basona Werana fairly correspond to FAO estimates for the entire world. Since 1990, an estimated 420 million hectares of forest have been converted to other land use types worldwide. The rate of deforestation has slightly decreased (10 mill ha/yr.) in the years 2015 onwards than the 1990s i.e., 16 mill ha/yr. (FAO and UNEP, 2020). A similar pattern can be seen in Basona Werana, where deforestation rates peaked in the 1990s where 67.27% has been deforested and it swiftly declined to 4.11% and 3.64% in the first two decades of the twenty-first century.

Temporally speaking, the post-millennial times has shown incremental land-use/ land-cover changes from the first study period (1989-2000) at Basona Werana Woreda. This land-use change trend is comparable to the national MODIS land-use/land-cover changes calculated by (Gebreselassie, et al., 2016) for the years 2001-2009. He indicated an increment in cropland (33%), and shrublands (7%), and bare lands (12%) while substantial losses were reported from forests (26%), grasslands (11%), and water bodies (8%). Grasslands have been largely being converted to croplands in many areas to fulfill food demands for the increasing population. As trees are continuously cleared, the soil underneath tends to dry out (Wassie, 2020).

Comparing the overall land-use/land-cover change to other studies made in different parts of Ethiopia, the changes in Basona Werana are not said to be a 'dramatic' LULC change. A similar study conducted for Arsi Negele district by (Mekonnen, et al., 2018) for instance results in that agriculture, and settlement areas increased by 250%, and 618%, and forests, and woodlands decreased by 72%, and 84% over the period 1989-2016. A year later, a study conducted by

(Tolessa, et al., 2019) on the Didessa river basin revealed a loss in wetlands (97%), grasslands (76%), forests (50%), and shrublands (32%) over the years 1974 – 2014.

The average land size per household is approximately 0.4 ha, which is comparable with Arsi, Hadiya, and Gurage areas (Silva, et al., 2021). Over the past 32 years, the Woreda and its surroundings have extensively been cultivated. The trend designates that agricultural land would be increasingly subdivided into smaller plots, from the current 0.4 ha/household to a smaller parcel, where it may reach a point that can't satisfy the basic food requirements of households considering the population pressure.

Unless the Built-up, and settlement patterns, industrialization, and urbanization trends outnumber agricultural activities, croplands are by far expected to dominate the LULC as usual. Their steady increase in the next decade might surpass four-fifth of the total areal coverage of this Woreda.

The major driving force for agricultural expansion is the population increase. According to the national census of 1994, the Woreda (within a different arrangement) had a population of 112,173 people where 56,868 are men, and 55,305 are women. It reached 120,930 in the year 2007 where 61,924 are men, and 59,006 are women (CSA, 2017). If this population trend coupled with previous incremental trends in agricultural land grabs continue, approximately 1,077.33 km^2 ($4/5^{th}$) of the entire Basona Werana will be covered by croplands in 2030. In the year 2000, the world average for cropland and forests was 50% and 37% among the total habitable lands (Goldewijk, Siebert, Lightman, & Rmankutty, 2010). Comparing with Basona Werana, cropland covered 64.05% while forest covered only 5.92% demonstrating the existential threat is already stood for the proper functioning of the surrounding ecosystem.

Figure 36: Typical Settlement Patterns in Basona Werana

Poverty is among the major factors associated with these LULC changes in poor rural settings of underdeveloped countries. Forests and poor people are highly related; in fact, the world's poorest people depend on forests for various purposes. Poverty reduction, on the other hand, increases the demand for natural resources and intensifies the human desire to convert forests to cropland, pasture, and settlement. The contrary is true for rising income society, wherein reducing the dependence on natural resources, increasing the demand for recreation and environmental quality, and boosts people's motivation to conserve nature (FAO and UNEP, 2020).

The forest cover available explains the presence of available biodiversity. According to (FAO and UNEP, 2020) forests are habitats for 80% of amphibians and 75% of birds, and 68% of mammal species. So, forest preservation positively influences the preservation of the locally available species and directly implies sustainable use of the surrounding environment.

Satellite images have a shortcoming of not covering less than pixel land cover types such as roads, which are considered in built-up and settlement class. UAV imageries with high resolution could back these forms of subpixel land cover classes.

4.2.2. Drought Susceptibility

According to NDDI-based drought estimates, the 'no drought situation in 1984, Ethiopia's historical drought year, was more than half of the total area, which has now declined to less than 19.12%, indicating four-fifths of the Woreda is in some degree of drought condition. This is a big warning sign for achieving the safe, resilient, and sustainable living requirements of Woreda inhabitants, as stated in the (UN, 2015)goal 11. The sooner the issue is addressed, the better.

A plot-by-plot detailed biomass amount can be obtained from the UAS based vegetation indices, even within the visible range. The main limitation of such detailed vegetation mapping using UAVs is its lack of adequate sensitivity to vegetation bands like that of NIR part of the electromagnetic spectrum. Apart from UAVs usage in ground-truthing of satellite-based classification, its exceptional usage in drought assessment has been minimal in this study.

This study has concluded that RDVI is the most sensitive index for biomass estimation from the 6 indices matched in this study. Comparing it to the study conducted by (Barati, Rayegani, Saati, Sharif, & Narsi, 2011), 20 different vegetation indices were equated and their vegetation cover fraction. It shows that DVI and RDVI are the most sensitive indices to vegetation cover. However, this study also found a lack of adequate accuracy in arid and sparsely vegetated areas.

Both drought indicators used in this study employ NDVI values alone or combined with other indices. Some research works conducted globally and locally ascertained that commonly used vegetation indices such as NDVI have a strong correlation with rainfall amounts (Dagnachew, Kebede, Moges, & Abebe, 2020). After conducting Spatio-temporal distribution of the rainfall, land surface temperature (LST) and soil moisture variables for the whole of Ethiopia, (Liou & Mehabie, 2019) confirmed that the estimated values have matched with NDVI values.

As it’s noted by (Liou & Mehabie, 2019), the spatial distribution of drought conditions in Ethiopia is concentrated in the central and northern highlands, including North Shoa Wollo and Tigray. Pixel-based precipitation trends show a slightly increasing trend in the central highlands of the Amhara region. It is also indicated 18 years assessment, an overall 41.67% decrement in NDVI values between 2001 and 2018 is observed for the whole of Ethiopia. Almost 99% of the area in Basona Werana has shown a decrease in NDVI values compared to the previous 10-year periods.

One of the components in sustainable development is a quest to understand livelihoods, i.e., how people make a living. Poverty generally increases the degree of susceptibility to drought (Barrow, 2006). In the years 2012/13 and 2015/16 the HDI of the Amhara region was 0.455 and 0.525 respectively which is lower than Harari, Diredawa, Tigray, Gambella, and Addis Ababa (UNDP, 2018). The low Human Development Index levels of this particular region of Ethiopia have played a role in the misuse of the land, which exacerbates the recurrent droughts.

Droughts, which are highly related to rainfall amounts, have a direct implication for food security. A 10% decrease in seasonal rainfall in Ethiopia translates into a 4.4 percent decrement in food production (Ayalew, et al., 2012). With the changing climate in marginal agro-ecosystems with variable rainfall, steep slope, and with previously degraded lands the vulnerability contexts are escalated (Wassie, 2020).

The peak drought times in recent Ethiopian history according to the degree of severity are 1984, 2009, 2002. Unlike most of the southern parts of Ethiopia, notable signals for seasonal precipitation trends of either decrease or increase don't appear in the central highlands of Ethiopia. The Spring season of 1999 was dry in almost the entire Ethiopia. The summer and fall, on the other hand, were wet in the central highlands, which seemed to have normal annual precipitation like other years. Due to dry spring followed by a dry summer, 2002 was the second driest year between 1972 – 2011 for central highlands (Viste, Korecha, & Sorteberg, 2012). Unlike this assessment for the whole central highlands of Ethiopia, these years have had fairly ordinary rainfall quantities in Basona Werana, based on (CHIRPS, 2021) rainfall estimations. Rather, 2010 is the worst year in terms of severity, followed by 1989 and 2000. However, among the eight years examined, the VCI-based drought estimate places 1989 as the most drought-affected year, while the non-temporal-based NDDI estimation identifies 2021 as the most drought-affected year.

4.2.3. Land Suitability and Sustainable Development

Agriculture is a vital element to achieve Sustainable Development Goals 1 and 2 and to tackle climate change Goal 11 (Kumar, et al., 2020). Applying six essential constraints of elevation, slope, soil type, SAVI, NDWI, and river proximity half (49.9%) of the Woreda has been identified as moderately suitable for crop production, while 28.72% identified as marginally suitable. Other classes namely highly suitable, less suitable, and not suitable classes share the rest 21.38%.

The comparison of suitability classes with LULC classes revealed that built-up and settlement, bare lands, grassland, and cultivated land have the greatest mean values for cropland suitability in respective order. Forest lands comparatively shown the least suitable followed by shrub and bush, water bodies and wetlands.

According to the in-situ observation, and actual classification results, there is a high shortage of extensive grazing land (grassland). This is partly attributed to the existing harsh topography and population pressure which converts other land-use types to cropland. But, immediate changes in slopes are not limited to this, they even create harmonious land-cover patterns between cultivated areas alongside the highlands.

Figure 37: Shrub, and bush alongside agricultural areas on the northern tip of Basona Werana Woreda (GE courtesy)

The image pictured above is located at an absolute geographic location of 9°59'49.39"N, and 39°18'10.51"E. This kind of land-use pattern alongside the sloppy areas is commonplace in Basona Werana as well as most parts of the central highlands. On the flatter side, agricultural activities undertake, while the next sloppy areas are covered by the mixture of shrubs, and bushes, and sometimes small coverages of bare lands. The inconsistent sloppy, and flat areas one after the other are among the reasons for the scattered agricultural plots in such mountains.

Figure 38: Dibut Kebele terracing practices

The one shown in the picture is located at 9.6126^0 N, 39.6558^0 E located inside Dibut Kebele where soil conservation practices exist alongside the steep slopes in few instances. Among other environmental concerns, soil erosion is associated with land degradation and the occurrence of periodic droughts. These kinds of land conservation interventions are representatives of responsible land management practices which should be extended as good practices elsewhere in other Kebeles of Basona Werana as well as the central highlands. Among the notable instances, 15 million hectares of degraded land have been restored in Ethiopia and a 4 billion tree planting pledge is made by the government of Ethiopia in 2019 (FAO and UNEP, 2020). Whereas similar tree planting initiative has continued in 2020 and 2021 by 5 and 6 billion trees respectively. These utmost success stories are vital for ecosystem sustainability.

4.2.4. Remotely Sensed Data for Sustainable Development

The decreasing cost and democratization of UAVs, is causing them to be exploited more often, either unaccompanied or synergistically with satellites and other platforms. This offered another glorious moment for a better understanding of the earth's dynamics (Emilien, Thomas, & Thomas, 2021). International organizations such as WFP, UNICEF, UNDP, UNHCR, and many more are already utilizing the technology (Rosenthal, 2018).

The World Bank has identified the current and future potentials of drones to overcome the complex environments in which development work is being undertaken. Some of these are land administration, risk assessment, forestry management, urban planning, infrastructure monitoring, post-disaster assessment, medical and humanitarian aid supplies, atmospheric and environmental sensing, and crop management. These would ease time-consuming, expensive, and risky development projects implementations (World Bank, 2017).

In situations where ground-truthing of satellite-based land monitoring assessments is challenged by steep slopes, inaccessibility, political instability, or any other hampering difficulties, UAVs can be easily deployed at a relatively low cost. However, if a vast area needs to be covered, specific spots should be chosen with care. This thesis sheds light on one of the many applications of UAVs, namely how they may be used for ground-truthing satellite-based evaluations.

This research is inextricably linked to UN Sustainable Development Goals 11 and 15. The former harnesses the inclusivity, safety, resilience, and sustainability of human settlements while the latter targets sustaining terrestrial ecosystem usage and forest as well as reversing land degradation and combat desertification. Target 15.3 specifically addresses the restoration needs for areas affected by drought, flood, and desertification (UN, 2015). This thesis's land suitability assessments and identification of drought-prone zones presented in the thesis are in line with achieving these objectives.

Except for recent military and cloud-seeding initiatives, UAVs in Ethiopia are underutilized in terms of achieving sustainable development in general, and the farming sector in particular. Ethiopia largely employed aerial photography for the registration of agricultural parcels, whereas Tanzania engaged drones for the land right registration system (World Bank, 2017). Among the most sensible application areas of UAVs - agricultural survey data can easily be collected, crops can be managed fine, it can be tested for precision agriculture in various agro-ecological zones and substantiated for its exceptional potentials. The pilot test conducted by Ethiopia's Ministry of Agriculture, which provided the data for this thesis, is noteworthy.

5. CHAPTER FIVE: CONCLUSION AND RECOMMENDATION

5.1. Conclusion

Land is a resource that has to be used sustainably. Few signs of sustainable land-use management practices are noticeable in Basona Werana. Apart from outrageous land degradation trends, deforestation rates have swiftly decreased over the last 20 years compared to the period between 1990 and 2000. In these years, drought conditions seem to gradually increase from 35.91% (extreme drought) to 53.87% in 2021. In this respect, reforesting the land and applying sustainable land management practices are not luxuries for Bassona Werana.

Combined indices of vegetation and water stress, such as NDDI, can better predict current drought conditions. While general drought conditions have worsened over the last 32 years, the current year 2021 won't be the driest, conferring to the stated drought estimates. VCI on the other hand indicated among the historical years 1989, 2000, 2010, and 2021, the most recent is the wettest, while 1989 is the doughtiest.

The highly and moderately agriculturally suitable areas account for about $1/20^{th}$ and half of the total area. While approximately 16.02% of the area is either less suitable or unsuitable for crop production. The central and southern parts of the Woreda are generally suitable for agriculture, and the areas designated for urbanization particularly Debrebirhan, have been identified as highly or moderately suitable for crop production.

Prevalence of Cambisols correlated with the highest Soil Adjusted Vegetation Index values, indicating a conducive environment for overall biomass survival. Less suitable areas are characterized by the presence of relatively sloppy topography particularly susceptible to soil erosion, less productive soil types, relatively small biomass contents and higher water stress quantities, less accessibility to rivers, and associated indicators.

VCI has a better relationship with monthly and annual precipitation amounts. In terms of indicating non-temporal drought conditions for that particular year, NDDI is a good reflector of drought conditions than VCI. Landsat-based NDVI calculations have several advantages, including relatively better resolution in detecting droughts; however, it is limited during actual drought conditions, when daily or less than 14 days temporal resolution data is required, and during cloudy seasons.

A way out of drought vulnerability in Basona Werana is attained through achieving sustainable development. The key issue here ‘food security’ can only be achieved when the root causes - economic and social conditions are responded upon. Meanwhile, environmental sustainability must be considered, since it is one of the most important criteria for any development endeavor. It is also proposed in Ethiopia's national economic policies and strategies, which must be taken into account.

If the urbanization trend at Debre Berhan town is managed properly, it could serve as a growth pole for the entire Woreda. The urban demands for goods and services motivate the farmers which reside near distances to the town. The job opportunities among industries and the service sector will gradually change the agriculturally dependent inhabitants in the surrounding rural areas. The key player in facilitating this change is infrastructural developments and market linkages. The challenges in urbanization may be an encroachment of agricultural lands for other development activities.

All in all, overall economic development is by far the finest way out, considering the population growth rate and share of agricultural lands. Development shouldn’t be attained at the expense of depleting the natural resources, as most developing countries approach it. This approach to development questions the very essence of sustainability. Sustainable development, as recognized by UN 1987, encompasses the ability to meeting the needs in the present without compromising the ability to realize the needs of upcoming generations.

The use of remote sensing, photogrammetry, and GIS techniques for drought assessment, land suitability analysis, and land-cover change assessment plays an invaluable role. UAVs are currently a great resource for quick environmental monitoring, support the in-situ validation of satellite-based mapping, in the production of a very detailed vegetation index mapping, and are used for precision mapping technologies. This study is partly unique among other studies done in Ethiopia, mainly by integrating satellite and UAS systems to address few major environmental concerns of these days, which are already discussed. In this study, UAVs have proven their potential for validation of classification results and in biomass estimation. While, the superior use of UAVs over satellites, specifically for drought estimation, appeared to be nominal in this study.

First and foremost, its relatively less need for high-resolution imagery. Secondly, it lacks NIR and SWIR bands, which have proven to be exceptional components in determining advanced drought indices. As UAS technology progresses and sensor technologies become more accessible to NIR and SWIR bands with minimal weight and cost, it will supplement satellite measurements of biomass and drought.

5.2. Recommendation

To better manage the unprecedented changes in environmental variables, monitoring of LULC and drought conditions continuously is essential by local authorities. Drought monitoring could be identified by combining multi-temporal and possibly non-temporal indices to better estimate current and projected droughts. This will aid in fact-based and data-driven planning, coordination, implementation, monitoring, and evaluation of expected environmental concerns such as famine conditions.

Other critical areas to consider in this Woreda include the diversification of livelihood options and the work of improving road accessibility. The Woreda's carrying capacity is by far seems to reach its peak in terms of space. As a result, diversification of livelihood options should be one of the most pressing needs for inhabitants. High dependence on few crops is what is making people vulnerable to recurrent droughts, and the resulting famine. Infrastructural development has paramount importance for overall connectivity. The road network available in the Woreda is by far less than expected and needs additional road construction to make agricultural products more marketable.

The Ministry of Agriculture, among other bureaus of the government, tested the potential of UAVs for cadastral mapping to better support farmers in Ethiopia. These initiatives need to be sustained and replicated by other development sectors such as road and transport, water and irrigation, mining, etc. The Geospatial Information Institue of Ethiopia (GII) needs to take the foremost initiative in technically supporting the acquisition of drone-based geographic information and processing of the imageries.

Any developmental activity being underway should be environmentally sound, apart from economically feasible, and socially acceptable. The urban expansion and industrialization in Basona Werana need a closer look in this regard. For sustainably undertaking the promising developments urban, and regional planning experts along with economists, geographers, engineers, environmental experts have to assess the environmental impacts on the most vulnerable wetlands, and existing agricultural areas continually. This should be done with the cooperation of local communities, which have the constitutional right to decide on any development projects in their neighborhoods.

If government, non-governmental, and community-led afforestation, and reforestation activities are strengthened, woodlands and forests have the potential to regenerate and become a dominant land-cover type. Few instances of soil conservation, afforestation, and related environmentally beneficial initiatives need to be implemented on a broader scale over extensive areas.

For an agrarian country like Ethiopia, drought monitoring is crucial. However, when deciding which remote sensing tools and inputs to use for areas ranging from micro levels such as Kebele and Woreda to macro levels such as regions or the countrywide level, care should be taken. A higher resolution, using freely available imageries such as Landsat and Sentinel, could be more effectively applied at spatial extents smaller than the regional state level. Medium resolution inputs, such as MODIS, on the other hand, better predict drought existence at the country or regional nation level.

References

Abdullah, M., Gholoum, M., & Abbas, H. (2018). Satellite vs. UAVs remote sensing of arid ecosystems: a review within an ecological perspective. *Crimson Publishers*. doi:https://doi.org/10.31031/EAES.2018.02.000540

Al-Bakri, J., Al-Khereisat, A., Shawash, S., Qaryouti, E., Muna, & Saba. (2016). Assessment of Remote Sensing Indices for Drought Monitoring in Jordan. *University of Jordan*. doi:https://doi.org/10.9790/9622-0903015967

Alemayehu, S., Ayana, E., Dile, Y., Demissie, T., Yimam, Y., Girvetz, E., . . . Worqlul, A. (2020). Evaluating Land Suitability and Potential Climate Change Impacts on Alfalfa (Medicago sativa) Production in Ethiopia. *MDPI*. doi:https://doi.org/10.3390/atmos11101124

Angearu, C.-V., Irimescu, A., Mihailescu, D., & Virsta, A. (2018). Evaluation of Droughts and Fires in the Dobrogea Region, Using MODIS Satellite Data. *Sciendo*. doi:https://doi.org/10.2478/alife-2018-0050

Angessa, A., Lemma, B., & Yeshitela, K. (2019). Land-use and Lan-cover dynamics and their drivers in the central highlands of Ethiopia with special reference to the Lake Wanchi watershed. *Springer*.

Arkebauer, T. J. (2005). Leaf Radiative Properties and the Leaf Energy Budget. *University of Nebraska Agronomy and Horticulture Faculty Publications*.

Artiola, J., Pepper, I. L., & Brusseau, M. L. (2004). *Environmental Monitoring Characterization.* Elsevier Science & Technology Books.

Ayalew, D., Tesfaye, K., Mamo, G., Yitaferu, B., Bayu, & Wondimu. (2012). Variability of rainfall and its current trend in Amhara region, Ethiopia. *Africa Journal of Agricultural Research*. doi:https://doi.org/10.5897/AJAR11.698

Ayele, Z. E. (2009). *Smallholder Farmers' Decision Making in Farm Tree Growing in the Highlands of Ethiopia.* Oregon: Oregon State University, A dissertation.

Bai, X., Sharm, R., R. T., Wuliangha, B., Tana, G., & Kondoh, A. (2017). A detailed and High-Resolution Land Use and Land Cover Change Anaysis over the Past 16 Years in the Horqin Sandy land, Inner Mongolia. doi:https://doi.org/10.1155/2017/1316505

Barati, S., Rayegani, B., Saati, M., Sharif, A., & Narsi, M. (2011). Comparison the accuracies of different spectral indices for estimation of vegetation cover fraction in sparse vegetated areas. *Elsevier, Egyptian Journal of Remote Sensing and Space Science*.

Barrow, C. J. (2006). *Environmental Management for Sustainable Development.* New York: Taylor and Francis Group.

Belgiu, M., & Csililik, O. (2014). Sentienl-2 cropland mapping using pixel-based and object-based time-weighted dynamic time warping analysis. *Elsevier*. doi:https://doi.org/10.1016/j.rse.2017.10.005

Berihun, M., Tsunekawa, A., Haregeweyn, N., Meshesha, D., Enyew, A., Tsubo, M., . . . Yibeltal, M. (2019). Exploring land use/land cover changes, drivers and their implications in contrasting agro-ecological environments of Ethiopia. *ScienceDirect*. doi:https://doi.org/10.1016/j.landusepol.2019.104052

Bewket, W., Gessesse, B., & Bräuning, A. (2015). Why does Accuracy Assessment and Validation of Multi-resolution-based Satellite Image Classification matter? A methodological discourse. *SINET: Ethiop. J. Sci.*

Centre for humandata. (2021). Predicting Drought-Related Food Insecurity in Ethiopia. Retrieved from https://centre.humdata.org/predicting-drought-related-food-insecurity-in-ethiopia/

CHIRPS. (2021). Climate Hazards Group Infrared Precipitation with Stations (CHIRPS). Santa Barbara, California, United States. Retrieved 05 09, 2021, from http://chg.geog.ucsb.edu/data/chirps

Colomina, L., & Molina, P. (2014). Unmanned aerial systems for photogrammetry and remote sensing: a review. *ISPRS J. of Photogrammetry Remote Sensing*. doi:https://doi.org/10.1016/j.isprsjprs.2014.02.013

Costa, L., Nunes, L., & Ampatzidis, Y. (2020). A new visible band index (vNDVI) for estimating NDVI values on RGB images utilizing genetic algorithms. *Elsevier*. doi:https://doi.org/10.1016/j.compag.2020.105334

CSA. (2017). *Summary and statistical reports of the population and housing census.* Addis Ababa.

Dagnachew, M., Kebede, A., Moges, A., & Abebe, A. (2020). Effects of Climate Variability on NDVI in the Gojeb River Catchment, Ethiopia. *Hindawi*. doi:https://doi.org/10.1155/2020/8263246

Damtea, W., Kim, D., & Im, S. (2020). Spatiotemporal Analysis of Land Cover Changes in the Chemoga Basin, Ethiopia, Using Landsat and Google Earth Images. *MDPI, Sustainability*. doi:https://doi.org/10.3390/su12093607

Dervisoglu, A., Bilgilioglu, B. B., & Yagmur, N. (2020). Comparison of Pixel-Based and Object-Based Classification Methods in Determination of Wetland Coastline. *International Journal fo Environment and Geoinformatics (IJEGEO)*. doi:https://doi.org/10.30897/ijegeo.713307

Dinku, S. (2017). *Forest Degradation Monitoring and Assessment of Biomass in Harenna Buluk Woreda, Bale Zone, Ethiopia, Using Remote Sensing and GIS Techniques.* Addis Ababa: AAU, College of Natural and Computational Sciences, School of Earth Science.

EBC. (2021, 06 06). Ethiopian Forest Cover Reaches 17.2 percent. Addis Ababa, Ethiopia. Retrieved 06 10, 2021, from https://www.fb.com/100001778744540/posts/3980076048728314/?app=fbl

Emilien, A.-V., Thomas, C., & Thomas, H. (2021). UAV & Satellite synergies for optical remote sensing applications: A literature review. *ScienceDirect, 3*. doi:https://doi.org/10.1016/j.srs.2021.100019

Eng, L., Ismail, R., Hashim, W., & Baharum, A. (2019). The use of VARI, GLI and VIGreen formulas in detecting vegetation in aerial images. *International Journal of Technology*. doi:https://dx.doi.org/10.14716/ijtech.v10i7.3275

Ewnetu, A., Simane, B., Teferi, E., & Zaitchik, B. F. (2021). Mapping and Quantifying Comprehensive Land Degradation Status Using Spatial Multicriteria Evaluation Technique in the Headwaters Area of Upper Blue Nile River. *Sustainability*. doi:https://doi.org/10.3390/su13042244

FAO and UNEP. (2020). *The State of the World's Forests.* Rome. doi:https://doi.org/10.4060/ca8642en

FAO, & ITPS. (2015). *Status of the World's Soils - Main Report.* Rome.

Faridatul, I. M., & Ahmed, B. (2020). Assessing Agricultural Vulnerability to Drought in a Hetrogeneous Environment: A Remote Sensing-Based Approach. *MDPI*, 1-17. doi:https://doi.org/10.3390/rs12203363

Fern´andez-Delgado, M., Cernadas, Eva, Barro, S., Amorim, & Diani. (2014). Do we Need Hundreds of Classifiers to Solve Real World Classification Problems? *Journal of Machine Learning Research, 15*.

Fiker, H. (2020). *Climate change adaptation response and its impact on household food security the case of basona werana woreda, North Shewa Zone ANRS, Ethiopia.* Addis Ababa: AAU, College of development Studies.

Flood, N. (2017). Comparing Sentinel-2A and Landsat 7 and 8 Using Surface Reflectance over Australia. *MDPI*, 2-7. doi:https://doi.org/10.3390/rs9070659

G/Michael, H. (2021). *Land use Land cover change and its implications on Land Surface Temperature change in Addis Ababa and its Satellte Towns, Ethiopia.* Addis Ababa: AAU, College of Development Studies, Environment and Sustainable Development, MA Thesis.

Gebreselassie, S., O, K., Mirzabaev, A., Nkoya, E., Alisher, M., & Joachin, B. (2016). Economics of land degradation and improvement in Ethiopia. In *Economics of Land Degradation and Improvement – A Global Assessment for Sustainable Development* (pp. 401-439). New York. doi:http://dx.doi.org/10.1007/978-3-319-19168-3

Genemo, B. U. (2012). *Remote Sensing and GIS Based Urban Sprawl Susceptibility Analysis: A case study of Shashamane Town, West Arsi Zone, Ethiopia.* Addis Ababa: AAU, School of Earth Science, MA Thesis.

Goldewijk, K., Siebert, S., Lightman, D., & Rmankutty, N. (2010, August 04). Anthropogenic transformation of the biomes, 1700 to 2000. *Global Ecology and Biogeography, 19*(5). doi: https://doi.org/10.1111/j.1466-8238.2010.00540.x

Gorfu, D., & Ahmed, E. (2014). *Crops and Agro-ecological Zones of Ethiopia.* Addis Ababa: EIAR.

Gray, P. C., Ridge, J. T., Poulin, S. K., Seymour, A. C., Schwanetes, A. M., Swenson, J. J., & Johnston, D. W. (2018). Integrating Drone Imagery into High Resolution Satellite Remote Sensing Assessments of Estuarine Environments. *MDPI*. doi:https://doi.org/10.3390/rs10081257

Gu, Y., Brown, J., Verdin, J., & Wardlow, B. (2007). A five-year analysis of MODIS NDVI and NDWI for grassland drought assessment over the central Great Plains of the United States. *Geophysical Research Letters*. doi:https://doi.org/10.1029/2006GL029127

Hana, Y. T. (2019). *Dairy Technology Adoption and Its Impact on Household Food Security: The Case of Basona Warena Woreda, Amhara Region, Ethiopia.* Addis Ababa: AAU, College of Development Studies, MA Thesis.

Hazaymeh, K., & Hassan, Q. K. (2016, 09 29). Remote sensing of agricultural drought monitoring: A state of art review. *AIMS Environmental Science*, 1-20. doi:10.3934/ENVIRONSCI.2016.4.604

Hoque, M., Biswarjeet, P., & Ahmed, N. (2020). Assessing drought vulnerability using geospatial techniques in northwestern part of Bangladesh. *ScienceDirect*, 1-8. doi:https://doi.org/10.1016/j.scitotenv.2019.135957

ITA, UDC. (2021). *Unammed Aercraft Systems (UAS)*. Retrieved from International Trade Administration, U.S. department of commerce: https://www.trade.gov/unmanned-aircraft-systems

Jayawardhana, W., & Chathurange, V. (2020). Investigate the Sensitivity of the Satellite-Based Agricultural Drought Indices to Monitor the Drought Condition of Paddy and Introduction to Enhanced Multi-Temporal Drougth Indices. *Jornal of Remote Sensing & GIS*. doi:https://doi.org/10.35248/2469-4134.20.9.272

Jenson, J. R. (2015). *Introductory Digital Image Processing: A Remote Sensing Perspective* (4th ed.). New Jersey: Prentice Hall, Upper Saddle River.

Klarin, T. (2018). The Concept of Sustainable Development: From its Beginning to the Contemprary Issues. *Zagreb International Review of Economics & Business, 21*, 67-94. doi:https://doi.org/10.2478/zireb-2018-0005

Klisch, A., & Atzberger, C. (2016). Operational Drought Monitoring in Kenya Using MODIS NDVI Time Series. *MDPI*. doi:https://doi.org/10.3390/rs8040267

Kouchak, A., Farahmad, A., Melton, F., Teixeira, J., & Anderson, M. (2015). Remote sensing of drought: Progress, challenges and opportunities. *Review of Geophysics, AGU Publications*, 452-480. doi:https://doi.org/10.1002/2014RG000456

Kumar, K. A., Reddy, G., Masilamani, P., Turkar, S., Sandeep, & Obi. (2020). Integrated drought monitoring index: A tool to monitor agricultural drought by using time-series datasets of space-based earth observation satellites. *ScienceDirect*, 4-9. doi:https://doi.org/10.1016/j.asr.2020.10.003

Kusumo, A. N., Reckien, D., & Verplanke, J. (2019). *GIS in Sustainable Urban Planning and Management - A Global Perspective.* (M. v. Maarseveen, J. Martinez, & J. Flacke, Eds.) New York, US: Taylor & Francis Group.

Le, M. S., Chien, H., & Liou, Y.-A. (2019, 03). Normalized Difference Latent Heat Index for Remote Sensing of Land Surface. *IEEE Transactions on Geoscience and Remote Sensing*, 1423-1433.

Li, Z., Chen, J., Baltsavias, E., & Aplin, P. (Eds.). (2008). *Advances in Photogrammetry, Remote Sensing and Spatial Information Sciences; An International Society of Photogrammetry and Remote Sensing Book Series.* London, UK: Taylor & Francis Group.

Lillesand, T., Kiefer, R. W., & Chaipman, J. W. (2008). *Remote Sensing and Image Interpretation* (Vol. 6th ed). New York: Wiley.

Liou, Y.-A., & Mehabie, G. (2019). Spatio-temporal Assessment of Drought in Ethiopia and the Impact of Recent Intense Droughts. *MDPI*. doi:https://doi.org/10.3390/rs11151828

Manfreda, S., Helman, D., Su, Z., & Toth, B. (2018). On the Use of Unmanned Aerial Systems for Environmental Monitoring. *MDPI Remote Sensing*, 2-14. doi:https://doi.org/10.3390/rs10040641

Matese, A., Toscano, P., Gennaro, S. F., Genesio, L., Vaccari, F. P., Primicerio, J., . . . Gioli, B. (2015). Intercomparison of UAV, Aircraft and Satellite Remote Sensing Platforms for Precision Viticulture. *MDPI*. doi:https://doi.org/10.3390/rs70302971

McKinnon, T., & Hoff, P. (2017). *Comparing RGB-Based Vegetation Indices With NDVI For Drone Based Agricultural Sensing.* AGBX.

Mekonnen, T., Gebremedhin, N., Assefa, A.-m., & Moreda, B. (2019). *Geography of Ethiopia and the Horn; A University and Colleges Module.* MoSHE.

Meselu, Y. K. (2019). Determinants of improved faba bean seed adopted and value chain mapping: The case of Basona Werana District in Amhara Region, Ethiopia. *MSc Thesis*. Retrieved from http://hdl.handle.net/123456789/9262

Meyfroidt, P., Chowdhury, R. R., & Garrett, R. (2018). Middle-range theories of land system change. *Elsevier*.

Mostafiz, R., Noguchi, R., & Ahmed, T. (2021). Agricultural Land Suitability Assessment Using Satellite Remote Sensing-Derived Soil-Vegetation Indices. *MDPI*. doi:https://doi.org/10.3390/land10020223

Mulinge, W., Gicheru, P., Murithi, F., Maingi, P., Kihiu, E., Kirui, O., & Mirzabaev, A. (2016). Economics of Land Degradation and Improvement in Kenya. In *Economics of Land Degradation and Improvement – A Global Assessment for Sustainable Development* (pp. 471-498). doi:https://doi.org/10.1007/978-3-319-19168-3_16

Nigussie, G., Moges, M., Michael, M., & Steenhuis, T. (2019). Assessment of Suitable Land for Surface Irrigation in Ungauged Catchments: Blue Nile Basin, Ethiopia. *MDPI*. doi:https://doi.org/10.3390/w11071465

Nyssen, J., Debever, M., Gebremeskel, G., Wit, B., Hadgu, K., Vriese, S., . . . Demissie, B. (2021). Online digital archive of aerial photographs (1935-1941) of Ethiopia. doi:https://doi.org/10.1002/gdj3.115

Pahar, S. P., Paembonan, S. A., & Soma, A. S. (2021). Identification of drought level using normalized difference heat index on Maros watershed. *The 1st International Conference on Environmental Ecology of Food Security*. Orlando. doi:https://doi.org//10.1088/1755-1315/681/1/012123

Prashar, A., & Jones, H. G. (2016). Assessing drought responses using thermal infrared imaging,". In *Methods in Molecular Biology* (pp. 209-214).

Qotera.org. (2021). *የኢትዮጵያ ህዝብ ቆጠራ*. Addis Ababa.

Rojas, O., Vrieling, A., & Rembold, F. (2011). Assessing drought probability for agricultural areas in Africa with coarse resolution remote sensing imagery. *Elsevier*. doi:https::/doi.org/10.1016/j.rse.2010.09.006

Rosenthal, A. (2018, August 13). Drones for development: How UAVs are supporting the global goals. New York, United States of America. Retrieved from https://unfoundation.org/blog/post/drones-for-development-how-uavs-are-supporting-the-global-goals/

Schoonenboom, J., & Johnson, R. B. (2017). How to Construct a Mixed Methods Research Design. *Springer*, 107-130. doi:https://doi.org/10.1007/s11577-017-0454-1

Shahabfar, A., Ghulam, A., & Eitzinger, J. (2012). Drought monitoring in Iran using the perpendicular drought indices. *ScienceDirect*. doi:https://doi.org/10.1016/j.jag.2012.01.011

Sharma, R. C., Hara, K., & Hirayama. (2017). A Machine Learning and Cross-Validation Approach for the Discrimination of Vegetation Physiognomic Types Ysing Satellite Based Multispectral and Multitemporal Data. *Hindawi*. doi:https://doi.org/10.1155/2017/9806479

Silva, J., Reidsma, P., Baudron, F., Jaleta, M., Tesfaye, K., & Ittersum, M. (2021). Wheat yield gaps across smallholder farming systems in Ethiopia. *ScienceDirect*. doi:https://doi.org/10.1007/s13593-020-00654

Sinshaw, B., Belete, A., Tefera, A., Dessie, A., Bizuneh, B., Alem, H., . . . Mamaru, M. (2021). Prioritization of potential soil erosion susceptability region using fuzzy logic and Analytical Hierarchy process, Upper Blue Nile Basin, Ethiopia. *ScienceDirect*. doi:https://doi.org/10.1016/j.wen.2021.01.001

Solazzo, D., Sankey, J. B., Sankey, T. T., & Munson, S. M. (2018). Mapping and measuring aeolian sand dunes with photogrammetry and LiDAR from Unmanned aerial vehicles (UAV) and multispectral satellite imagery on the Paria Plateau, AZ, USA. *ScienceDirect*. doi:https://doi.org/10.1016/j.geomorph.2018.07.023

Suryabhagavan, K. (2017). *GIS-based climate variability and drought characterization in Ethiopia over three decades.* ScienceDirect. doi:http://dx.doi.org/10.1016/j.wace.2016.11.005

Tadesse, M., Simane, B., Abera, W., Tamene, L., Ambaw, G., Recha, J., . . . Solomon, D. (2021). The Effect of Climate-Smart Agriculture on Soil Fertility, Crop Yield, and Soil Carbon in Southern Ethiopia. *MDPI*. doi:https://doi.org/10.3390/su13084515

Taloor, A. K., Manhas, D. S., & Kothyari, G. C. (2021). Retrieval of land surface temperature, normalized difference moisture index, normalized difference water index of the Ravi basing using land Landsat data. *ScienceDirect*. doi:https://doi.org/10.1016/j.acags.2020.100051

Thomas, D., & Meeraph, H. (2020). *Drone and Tablet Piloting Report - Testing of new methods for cadastral susrveying.* Addis Ababa: MoA.

Thonfeld, F., Steinbach, S., Muro, J., & Kirimi, F. (2020). Long-Term Land Use/Land Cover Change Assessment of the Kilombero Catchment in Tanzania Using Random Forest Classification and Robust Change Vector Analysis. *MDPI*. doi:https://doi.org/10.3390/rs12071057

Tigabie, A., Legesse, A., Chanyalew, Y., Getachew, T., & Wondale, L. (2018). *Participatory agricultural production system analysis: Implication for research and development intervention in north shewa zone.* Bahirdar: Amhara Agricultural Research Institute.

Tizale, C. Y. (2007). *The Dynamics of Soil Degradation and Incentives for optimal management in the Central Highlands of Ethiopia.* Pretoria: Dissertation, University of Pretoria, Faculty of Natural and Agricultural Sciences.

UN. (2015). *Transorming our world: The 2030 Agenda for Sustainable Development.* Retrieved from Sustainable Development: sustainabledevelopment.un.org

UNDP. (2018). *Ethiopia National Human Development Report.* Addis Ababa, Ethiopia: United Nations Development Programme, UNDP, Ethiopia.

UNESC. (2007). *Africa Review Report on Drought and Desertification.* Addis Ababa: UN Economic Comission for Africa.

Vanderstoep, S. W., & Johnston, D. D. (2009). *Research Methods for Everyday Life: Blending Qualitative and Quantitative Approaches.* San Fransisco, California, Unitee States: John Wiley & Sons Inc.

Verburg, P., Paul, S., Dijst, M., & Veldkamp, A. (2004). Land use change modelling: current practice and research priorities. *GeoJournal*. doi:https://doi.org/10.1007/s10708-004-4946

Viste, E., Korecha, D., & Sorteberg, A. (2012). Recent Drought and Precipitation Tendencies in Ethiopia. *Theoretical and Applied Climatology*. doi:10.1007/s00704-012-0746-3

Wassie, s. (2020). Natural resource degradation tendencies in Ethiopia. *Springer*. doi:https://doi.org/10.1186/s40068-020-00194-1

Whitehead, K., & Hugenholtz, C. (2014). Remote sensing of the environment with small unmanned aircraft systems (UASs), part 1: A review of progress and challenges. *J. Unmanned Veh. Syst*, 70-82. doi:https://doi.org/10.1139/juvs-2014-0006

WLRC. (2014). EthioGIS-2 Data Catalog - National Geospatial Database System Ethiopia. Water and land Resource Centre.

WMO, & GWP. (2016). *Handbook of Drought Indicators and Indices.* IMDP, World Meteorological Organization.

Worku, T., Mekonnen, M., Yitaferu, B., & Cerdà, A. (2021). Conversion of crop land use to plantation land use, northwest Ethiopia. *Elsevier*. doi:https://doi.org/10.1016/j.tfp.2020.100044

World Bank. (2017, April 27). Tapping the Potential of Drones for Development. Retrieved from https://www.worldbank.org/en/topic/transport/brief/drones-for-development

Xue, J., & Su, B. (2017). Significant Remote Sensing Vegetation Indices: A Review of Developments and Applications. (C. Li, Ed.) *Hindawi Journal of Sensors*, *2017*, 2-7. doi:https://doi.org/10.1155/2017/1353691

Zhao, F., Wu, X., & Wang, S. (2020). Object-oriented Vegetation Classification Method based on UAV and Satellite Image Fusion. *Elsevier*, 1-4. doi:https://doi.org/10.1016/j.procs.2020.06.132

Zhao, L., Shi, Y., Liu, B., Hovis, C., Duan, L., & Shi, Z. (2019). Finer Classification of Crops by Fusing UAV Images and Sentinel-2A Data. *MDPI*. doi: https://doi.org/10.3390/rs11243012

Appendices

Appendix 1: Description of UAV flight at Wayou Kebele

Label of items	Values/ amounts
Image Resolution	0.8m
Forward Overlap	80
Sidelap	75
Flight planning software	UAV-CGS
Type of flight	Double Grid Flight Plan
UAV average flight altitude a.g.l	620
Mean terrain height	2870m
Area covered per image	635.94m*425.14m

Appendix 2: Confusion Matrix of 1989 classification

Class Name	For.	Cul.	Gra.	Shr.	Bul.	Bar.	Wat.	Wet.	Total	User. Acc.	Kappa
Forests	47	9	1	3	0	0	0	0	60	0.78	0
Cultivated	3	224	2	9	1	0	1	1	241	0.93	0
Grassland	1	0	7	1	0	0	1	0	10	0.70	0
Shrub & Bush	4	1	1	22	0	0	0	1	29	0.76	0
Built-up & Sett.	0	1	0	1	8	0	0	0	10	0.80	0
Bare land	0	1	1	0	0	7	1	0	10	0.70	0
Water body & Sw.	0	2	0	2	0	0	6	0	10	0.60	0
Wetlands	0	8	0	0	1	0	1	48	58	0.83	0
Total	55	246	12	38	10	7	10	50	428	0.00	0
Prod. Acc.	0.85	0.91	0.58	0.58	0.80	1.00	0.60	0.96	0.00	0.86	0
Kappa	0	0	0	0	0	0	0	0	0	0	0.782696246

Appendix 3: Confusion Matrix of 2000 classification

Class Name	For.	Cul.	Gra.	Shr.	Bul.	Bar.	Wat.	Wet.	Total	User. Acc.	Kappa
Forests	16	0	2	2	0	2	0	0	22	0.73	0
Cultivated	6	232	2	18	0	4	2	8	272	0.85	0
Grassland	0	0	18	2	0	0	0	0	20	0.90	0
Shrub & Bush	0	6	0	60	0	0	0	2	68	0.88	0
Built-up & Sett.	0	2	0	2	16	0	0	0	20	0.80	0

Bare land	0	2	0	2	0	16	0	0	20	0.80	0
Water body & Sw.	0	2	2	2	0	0	14	0	20	0.70	0
Wetlands	0	0	0	0	0	0	0	20	20	1.00	0
Total	22	244	24	88	16	22	16	30	462	0.00	0
Prod. Acc.	0.73	0.95	0.75	0.68	1.00	0.73	0.88	0.67	0.00	0.85	0
Kappa	0	0	0	0	0	0	0	0	0	0	0.77

Appendix 4: Confusion matrix of 2010 classification

Class Name	For.	Cul.	Gra.	Shr.	Bul.	Bar.	Wat.	Wet.	Total	User. Acc.	Kappa
Forests	27	1	0	1	0	0	0	0	29	0.93	0
Cultivated	1	229	1	27	5	4	2	5	274	0.84	0
Grassland	0	0	0	0	0	0	0	0	0	0.00	0
Shrub & Bush	2	22	2	53	0	0	1	2	82	0.65	0
Built-up & Sett.	0	2	0	0	5	0	0	0	7	0.71	0
Bare land	0	0	0	0	0	0	0	0	0	0.00	0
Water body & Sw.	0	0	0	0	0	0	4	0	4	1.00	0
Wetlands	0	4	0	2	0	1	1	21	29	0.72	0
Total	30	258	3	83	10	5	8	28	425	0.00	0
Prod. Acc.	0.90	0.89	0.00	0.64	0.50	0.00	0.50	0.75	0.00	0.80	0
Kappa	0	0	0	0	0	0	0	0	0	0	0.64

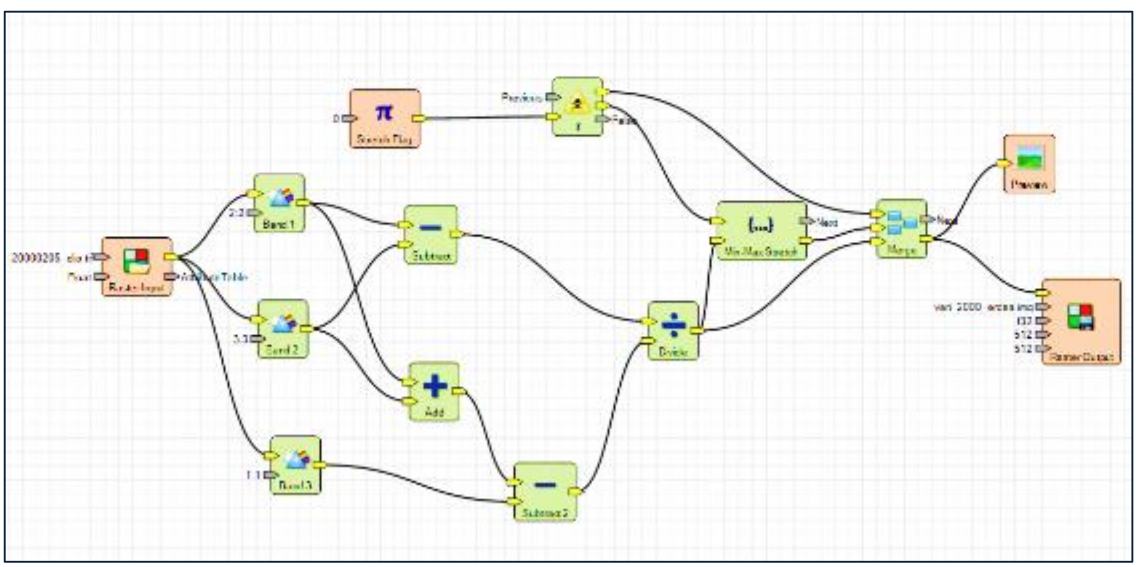

Appendix 5: VARI model [Landsat 4 to 7] Erdas Imagine®

Appendix 6: Freq. Dist. of Agricultural Suitability via 300m equal interval samples

Kebele Name	Highly Suitable	Moderately Suitable	Marginally Suitable	Less Suitable	Not Suitable
Abamote	17	219	81	33	1
Adisgie	8	229	253	97	11
Angolela	82	375	74	40	2
Bakelo	20	347	86	10	0
Basodongora	0	131	194	75	1
Birbirsa	18	198	94	40	4
Brer Hager	31	246	35	0	0
Chembere	0	77	156	106	16
Cheraro Deber	8	194	161	54	2
Debrebrehan T.	263	1241	121	22	1
Dibut	14	325	25	0	0
Dobele	9	353	88	68	2
Gefet	4	132	255	174	36
Goshbado	4	339	292	140	21
Goshu Hager	2	156	86	36	0
Gudoberet	1	163	217	173	6
Kasima	8	226	303	145	20
Keyet	7	166	144	55	0
Kormargefiya	85	398	38	0	0
Mati	2	42	155	99	26
Mehal Amba	0	153	91	33	0
Metkoriya	3	126	187	109	32
Modo	0	128	127	40	3
Moyeaman Gult	21	139	111	58	9
Muti Cherkos	91	195	100	77	26
Nasena Kumamba	8	258	183	64	1
Sariya	23	144	86	29	1
Wayou	13	201	167	79	3
Weyeniyana Gud Amba	1	50	81	35	3
Wushawshegn	18	317	49	0	0

Appendix 7: VCI calculated for 2018, 2019, 2020 and 2021 using those year's minimum and maximum

	2018		2019		2020		2021	
VCI Severity Level	Area	Percent	Area	Percent	Area	Percent	Area	Percent
Extreme Drought	810.41	59.97	164.18	12.15	132.31	9.79	516.08	38.19
Severe Drought	88.55	6.55	50.68	3.75	37.28	2.76	110.06	8.14
Moderate Drought	112.23	8.31	94.62	7.00	71.66	5.30	161.33	11.94
No Drought	90.52	6.70	117.30	8.68	89.65	6.63	140.65	10.41
Wet	249.64	18.47	924.58	68.42	1020.46	75.51	423.23	31.32

Appendix 8: The precipitation data used in correlation of VCI and NDDI in section 4.1.5.3

Year	1984	1989	2000	2010	2018	2019	2020	2021
Annual Precipitation	983.00	309.00	381.00	249.00	983.00	1248.00	1017.00	≈979.00
Monthly Precipitation	6.07	2.98	1.79	2.14	6.66	5.69	6.34	6.56